10

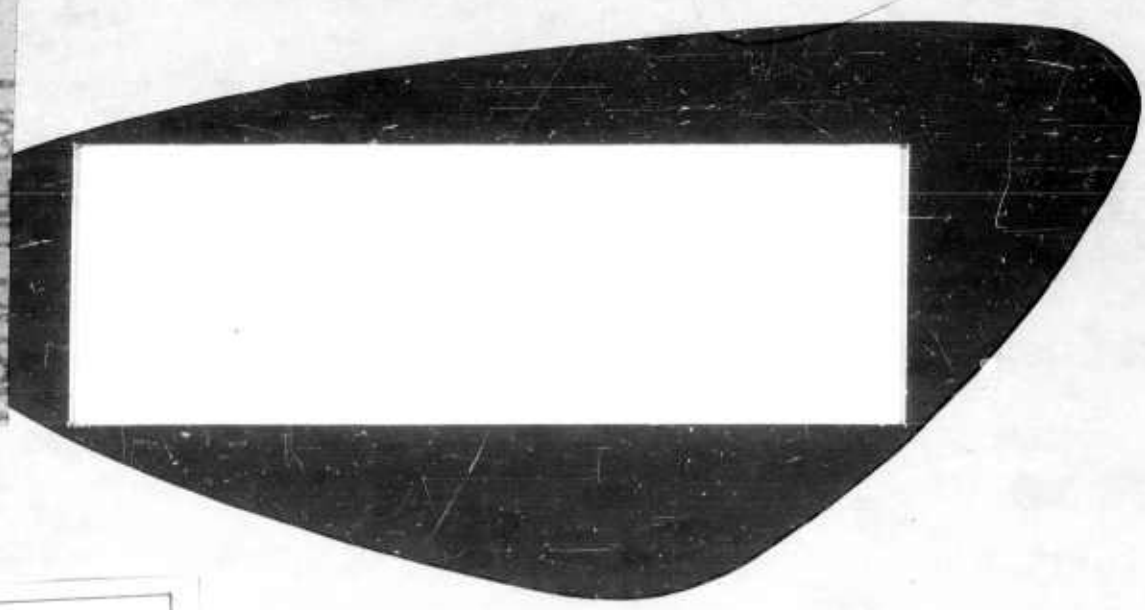





VERTOL DIVISION

BOEING AIRPLANE COMPANY

10

# THE VERTODYNE VTOL AIRCRAFT STUDY SEMI-SPAN MODEL TESTS IN HOVERING AND FORWARD FLIGHT

PRELIMINARY RELEASE

Limited Distribution

30 March 1960

# THE VERTODYNE VTOL AIRCRAFT STUDY SEMI-SPAN MODEL TESTS IN HOVERING AND FORWARD FLIGHT


**VERTOL AIRCRAFT CORPORATION**

MORTON, PENNSYLVANIA

CODE IDENT. NO. 77272




| | | |
|---|---|---|
| PREPARED BY: E. Brogan, G. Casey, B. Engel, C. Fay | REPORT NO. R-158 | NO. OF PAGES |
| CHECKED BY: A. Petach, E. Brogan | MODEL: Vertodyne Semi-Span Model | |
| APPROVED BY: W. Z. Stepniewski | CONTRACT NO. NONR 2364(00) | ITEM NO. |
| APPROVED BY | DATE | |

REVISIONS

| DATE | PAGES AFFECTED | REMARKS |
|---|---|---|
| | | |
| | | |
| | | |
| | | |

Form No. 1357B (3-56)

## ABSTRACT

The Vertodyne fan-in-wing concept has been studied in a series of static and forward speed tests. A semi-span model was tested incorporating instrumentation for measuring fan thrust, torque and wing surface pressures. Forces and moments on the model were measured at the model support. Tests were performed at the University of Detroit using the available laboratory and wing tunnel facilities. Data is presented in dimensionless form which covers the forces and moments acting on the model and the fan power required for a range of static and forward flight conditions. Wing surface pressures are presented for the same range of conditions. Significant increases in wing lift accompanied by high nose-up pitching moments were obtained in forward flight. Model static thrust per horsepower was found to decrease in ground effect. A discussion of results with conclusions and recommendations for further study is included in the report.

REV

REV

## FOREWORD

This report presents the results of wind tunnel tests of the Vertodyne VTOL configuration. They were conducted by the Vertol Aircraft Corporation of Morton, Pennsylvania, under Contract NONR2364(00), to determine the characteristics of the wing-submerged ducted fan configuration in hovering and transition to forward flight. The effect of ground proximity on hovering performance was also investigated. The model consisted of a mechanically driven ducted fan mounted in a semi-span model of NACA 64$_4$-221 Airfoil. It was tested at the University of Detroit, Detroit, Michigan, in 1958. The Office of Naval Research, Department of the Navy, administered the subject contract, which was funded by the Transportation Corps, Department of the Army.

# TABLE OF CONTENTS



REV

## I. SUMMARY

The Vertodyne Test was conducted to determine the static and transition flight characteristics of a wing-submerged ducted lift fan. Static tests were performed in the Laboratory of the University of Detroit Wind Tunnel. Tests were conducted in ground effect at various heights, and out of ground effect. Forward flight tests were conducted in the seven foot by ten foot wind tunnel of the University of Detroit.

A semi-span reflection plate type model suitable for testing in a seven foot by ten foot wind tunnel was designed. A mechanically driven ducted fan was used, with all drive components contained within the basic wing contour. Three interchangeable fan impellors, high pitch ($\emptyset_R = 55.9^o$), medium pitch ($\emptyset_R = 39.7^o$), low pitch ($\emptyset_R = 25.0^o$) provided variation in fan thrust.

The test set-up was provided with instrumentation which measured forces and moments on the model support and thrust and torque on the fan shroud. Wing surface pressure pickups provided data for a study of surface pressure distributions.

The results of the Vertodyne Test are presented in this report. Data is presented in nondimensional coefficient form to facilitate its application to future studies and designs and to permit its comparison with other investigations. Basic knowledge of the flight characteristics of the Vertodyne configuration has been gained which helps to indicate the direction in which further research should be conducted.

The most significant results of the Vertodyne study are:

1. The determination of the basic forward flight parameters covering lift, drag, pitching moment and fan power.

2. The determination of the static out-of-ground-effect thrust and power characteristics, and the changes occuring in-ground effect.

3. The presentation of surface pressure surveys to illustrate the wing surface flow characteristics, and to show the origin of the forces and moments acting on the wing.

REV

## II. LIST OF FIGURES



REV

REV

REV

## III. LIST OF SYMBOLS

$C$ Wing Chord Length, Feet

$c$ Chordwise Force, Positive Toward Trailing Edge, Pounds

$C_D$ Forward Flight Drag Coefficient; $C_D = \frac{D}{\frac{1}{2}\rho V^2 S}$

$C_D'$ Forward Flight Drag Coefficient Due to Fan Thrust;

$$C_D' = \frac{T \sin \alpha}{\frac{1}{2}\rho V^2 S}$$

$C_L$ Forward Flight Lift Coefficient; $C_L = \frac{L}{\frac{1}{2}\rho V^2 S}$

$C_L'$ Forward Flight Lift Coeffidient Due to Fan Thrust;

$$C_L' = \frac{T \cos \alpha}{\frac{1}{2}\rho V^2 S}$$

$C_M$ Forward Flight Pitching Moment Coefficient; $C_M = \frac{M}{\frac{1}{2}\rho V^2 S C}$

$C_P$ Fan Power Coefficient; $C_P = \frac{P}{\rho \pi r^2 (V_T)^3}$

$C_T$ Static Thrust Coefficient; $C_T = \frac{T}{\rho \pi r^2 (V_T)^2}$

$D$ Drag Force, Pounds

$d$ Fan Diameter, Feet

$f$ Total Force on a Fan Shroud Flexure, Pounds

$h$ Fan or Model Height Above Ground; Feet

$HP$ Fan Shaft Horsepower

$L$ Wing Lift; Pounds

$M$ Wing Pitching Moment; Foot-pounds

$P$ Fan Power; Foot-Pounds per Second

REV

| | |
|---|---|
| $\Delta P$ | Wing Surface Pressure Above Atmospheric, Inches of Water |
| q | Free Stream Dynamic Pressure; Inches of Water |
| Q | Fan Torque, Pounds Feet |
| r | Radius From Fan Axis to Torque Flexure, Inches |
| R | Fan Inlet Bellmouth Radius; Feet |
| s | Spanwise Force, Inboard Direction Positive; Pounds |
| S | Semi-Span Wing Area, Square Feet |
| t | Moments on Fan Shroud Flexures, Positive Counterclockwise, Foot Pounds |
| T | Fan Axial Thrust, Pounds |
| $T_\infty$ | Fan Axial Thrust Out of Ground Effect, Pounds |
| V | Free Stream Velocity, Miles per Hour |
| $V_O$ | Free Stream Velocity, Feet per Second |
| $V_T$ | Fan Blade Tip Speed, Feet per Second |
| $\alpha$ | Wing Angle of Attack, Degrees |
| $\delta_{fw}$ | Flap Angle, Degrees |
| $\phi_R$ | Fan Blade Root Incidence Angle; Degrees |
| $\mu$ | Tip Speed to Forward Speed Ratio; $V_T/V_O$ |
| $\rho$ | Mass Density of Air; Slugs per Cubic Foot |

Cautionary Note: Fan shroud pressure data has been presented in two basic forms for static and forward flight conditions. Refer to Figure 16 for explanation of azimuth angles used.

REV

## IV. INTRODUCTION

The Vertodyne concept has been proposed as a possible means of obtaining VTOL flight characteristics within an airframe possessing high speed forward flight capability. A wing-submerged ducted lift fan is used to provide lift in hover and in transition flight. When adequate forward speed has been attained the lift fan can be stopped and the duct openings in the wing closed allowing flight as a conventional fixed wing aircraft.

Power for the wing-submerged fan can be obtained in several ways. A mechanical drive from an engine located within the wing or fuselage presents one of the most feasible means for present day applications. Several other drive configurations have been proposed using a remotely located gas generator supplying a power turbine coupled to the lift fan. For forward flight the flow from the gas generator can be diverted aft to provide jet thrust.

Vertol Aircraft Corporation has conducted extensive analytical investigations in this field, both privately and in connection with government contracts. The Vertodyne configuration is one of the most promising concepts for transport and observation-liaison type VTOL aircraft. Reference 1, reporting the results of a VTOL aircraft comparative study performed under contract to the Office of Naval Research, indicates the Vertodyne concept to be promising for the 400 MPH cruise regime.

The basic fan-in-wing concept has been evaluated by several agencies and presented in references 3 to 13 inclusive. Favorable results are reported in these studies. Of particular interest is the basic propulsion system study conducted by General Electric (Ref. 2), under sponsorship of the U. S. Army Transportation Research and Engineering Command. The results obtained in these studies show substantially good agreement with the Vertodyne results.

The Vertodyne program was initiated to explore the flight problems in the transition range. Transition is defined as the low speed forward flight range in which the basic lift of the wing must be augmented by the thrust and induced lift created by the fan. The problems of ducted fan design had been treated analytically and experimentally by numerous investigators. However, the problems associated with the fan-in-wing combination had received only limited experimental investigation, as reported in References 3 to 6, inclusive. At the time Vertol Aircraft Corporation began studies in preparation for the subject contract, the possibility of establishing an analytical approach to the Vertodyne problem appeared remote. An extensive wind tunnel program was proposed to establish basic empirical informa-

REV

tion for definition and solution of the transition problems. In addition an investigation of the hovering characteristics both in and out of ground effect was proposed. Conflicting results had been presented in reference data, therefore a study of the static condition was felt to be worthwhile.

To carry out the Vertodyne test program a semi-span reflection plate type model suitable for testing in a seven foot by ten foot wind tunnel was designed. The ducted fan and its drive system were designed for a fan disc loading range of zero to 200 pounds per square foot.

The basic model was designed as the right half of a wing of an aspect ratio of 3.27. A straight constant chord section containing the fan was used with a tapered tip panel. The wing used an NACA $64_4$-221 airfoil section. The fan was mechanically driven with all components contained within the basic wing contour. Three interchangeable fan impellors of various pitch angles allowed operation at various thrust ranges. NACA series 65 compressor blading was used. The wing was provided with a twenty-five per cent chord flap at the trailing edge. Fan exit elbows of $20^{\circ}$ and $40^{\circ}$ bend angle, although not suitable for practical applications, were tested in order to obtain a basis for comparison for more practical systems leading to the use of the fan for forward propulsion.

During the wind tunnel tests force and moment data were obtained from the tunnel balance system. Direct force measurements were made on the model in the static tests. The fan shroud was attached to the wing by strain gaged flexures which allowed measurement of fan thrust and torque. In addition to the force and moment measuring devices the wing was provided with extensive surface pressure instrumentation to allow study of surface pressure distribution.

REV

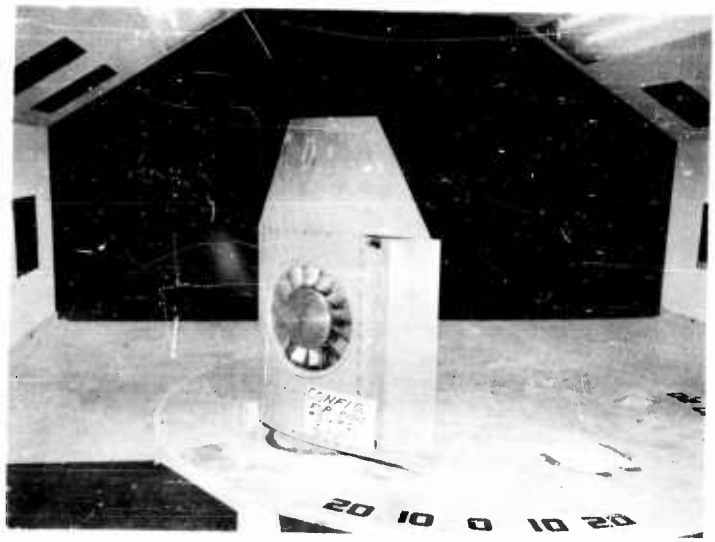


FIGURE 1

VERTODYNE MODEL, TOP VIEW, LOOKING UPSTREAM

FIGURE 2

VERTODYNE MODEL, BOTTOM VIEW, LOOKING DOWNSTREAM

## V. DESCRIPTION OF MODEL AND INSTRUMENTATION

### BASIC MODEL

The Vertodyne model arrangement consists of the right half of a wing with an aspect ratio of 3.27, composed of a rectangular center section and tapered outer panel, both of NACA $64_4$-221 airfoil section. The ducted fan is contained within the center section. Three fans, each with a different fixed incidence angle, in combination with fan rotational speed, provide variations in fan thrust. NACA Series 65 compressor blading was used in the 52% solidity single stage fan rotor. Variable incidence angle blading was not employed because of the high cost involved, instead three separate fan impellors with root pitch angles of 25.0°, 39.7° and 55.9° were used. No stator was provided because of the axial depth limitation imposed by the thickness of the wing. The same blading, including twist distribution, was provided for each of the three fans, with the design point, a disc loading of two hundred pounds per square foot, to be met by the fan with the highest incidence angle. Physical dimensions are presented in the following table and Figure 3.

| | |
|---|---|
| Diameter of fan | 12" |
| Hub radius | 3.6" |
| Outside radius | 6.0" |
| Number of blades | 13 |
| Fan speed | 10,000 RPM |
| Maximum disc loading | 200 lb./ft.$^2$ |
| Semi-Span Area (Incl.Disk) | 5.5 Ft.$^2$ |
| Fan Disk Area | .785 Ft.$^2$ |

### FAN BLADE DATA

| Station % Radius | Radius (in.) | Airfoil NACA | Pitch (deg) | Chord (in.) | Twist Distribution (deg) |
|---|---|---|---|---|---|
| 60.0 | 3.60 | 65-(15)10 | 55.9 | 1.885 | 0 |
| 73.3 | 4.40 | 65-(9.3)10 | 46.5 | 1.885 | -9.4 |
| 86.7 | 5.20 | 65-(6.7)10 | 42.0 | 1.885 | -13.9 |
| 100.0 | 6.00 | 65-(5.5)10 | 38.3 | 1.885 | -17.6 |

### FAN BLADE ANGLE ROOT SETTING

REV

| - lb/ft.$^2$ | ∅ at 60% Radius |
|---|---|
| 0 | 12.5° |
| 55 | 25.0° (Low Pitch Fan) |
| 125 | 39.7° (Medium Pitch Fan) |
| 200 | 55.9° (High Pitch Fan) |

The dimensions of the Vertodyne Model are shown in Figure 3

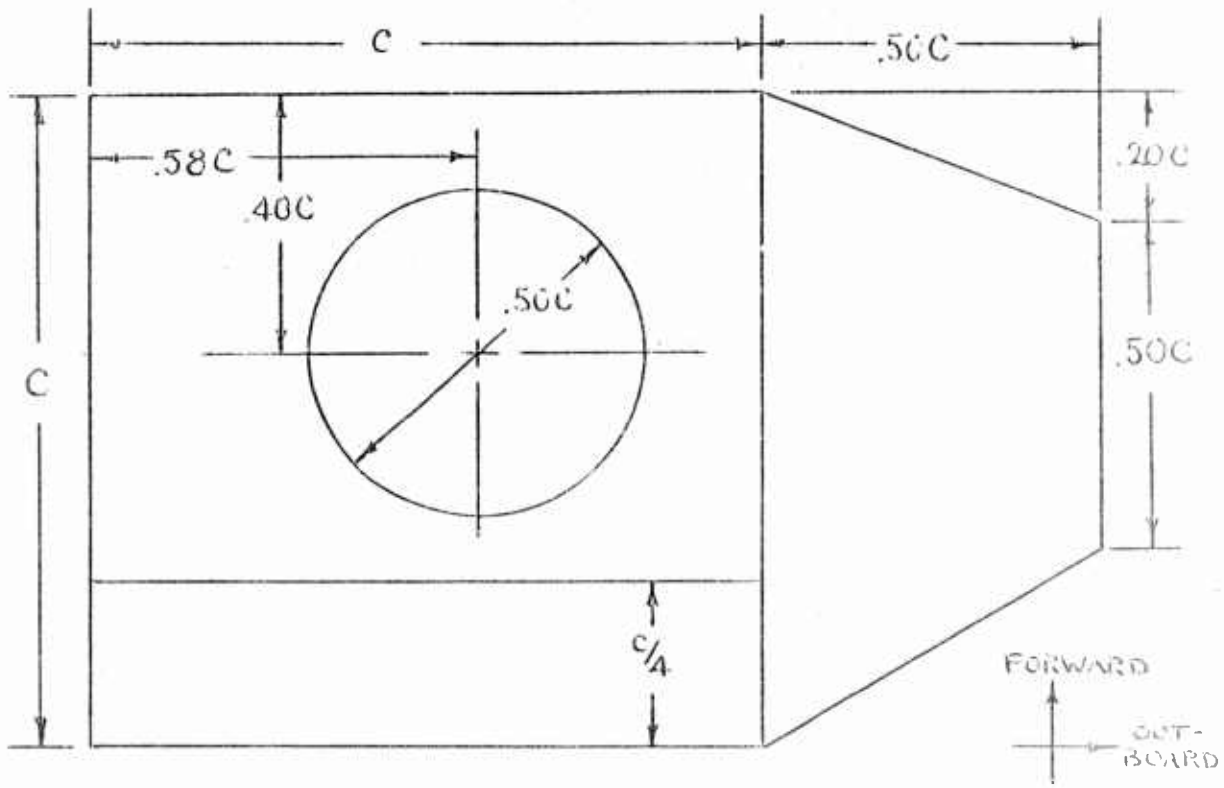


C = 2 feet

Vertodyne Model Plan View Dimensions

FIGURE 3

VERTODYNE MODEL TEST

SECTION THROUGH WING AT FAN CENTER LINE

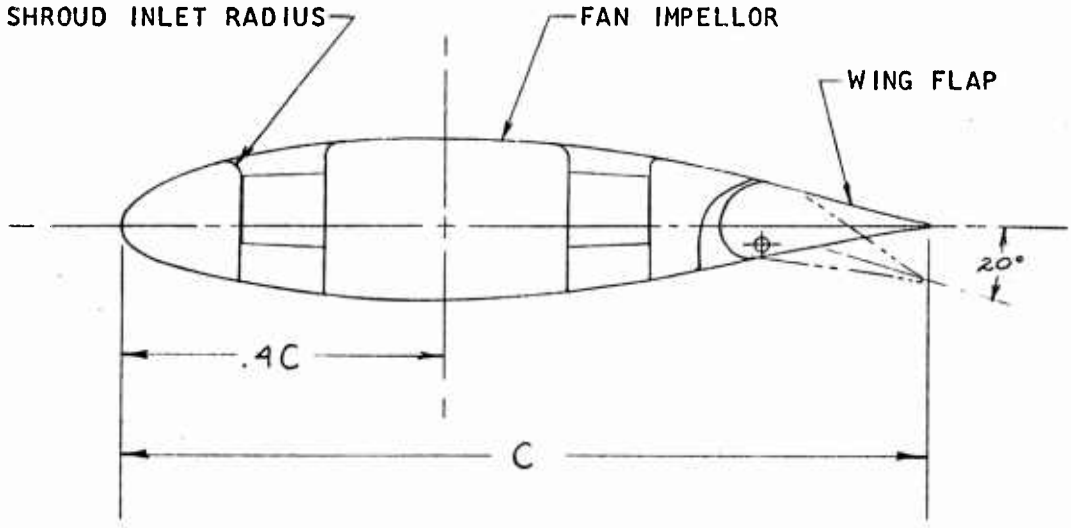


NACA $64_4$-221 AIRFOIL

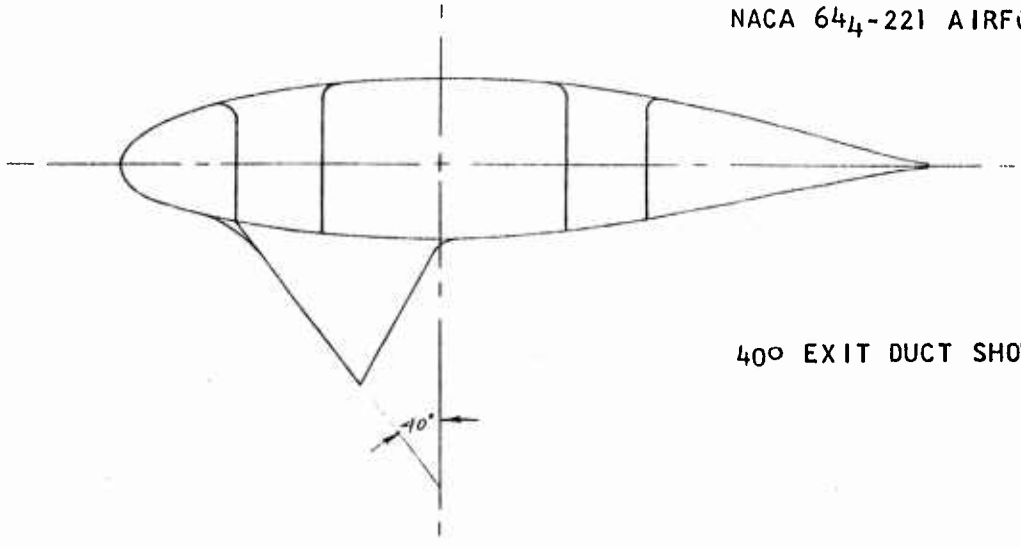


40° EXIT DUCT SHOWN

REV

FIGURE 4

## MODEL DRIVE SYSTEM

The model was powered by a 3 phase, 4 pole variable frequency electric motor, developing approximately 40 HP at 10,000 rpm. The motor was obtained on a loan basis from David Taylor Model Basin. The motor was in turn powered by the variable frequency motor-generator set of the University of Detroit Wind Tunnel facility.

A Berkely 7350 Universal EPUT Meter was used to indicate the rotational speed of the model motor. This electronic counter has an accuracy in this particular application of $\pm$ 30 rpm.

There are three iron - constantan thermocouples in the model motor which were connected to three temperature indicators. These thermocouples indicated the temperature at the hottest points of the motor coils. The motor was cooled by water which passed through a water jacket surrounding the motor. Water was pumped from a water main to the motor jacket by a Worthington turbine pump at pressures varying from 40 psi with the low pitch fan to 80 psi with the high pitch fan. The water jacket was drained directly to a sink.

The motor to fan drive passed through a $90^{o}$ angle drive transmission located behind the fan hub and within the wing contour. This was accomplished by a set of spiral bevel gears having a ratio of 1:1. The gears were supported in anti-friction bearings and were totally enclosed in a steel case. The gears and bearings were lubricated and cooled by both oil spray under pressure and splash lubrication. The oil was fed to the spray nozzles at 30 psi by a feed pump, which was supplied by a tank filled with ten gallons of MIL 1065 oil. The oil in the gear box was removed by a sump pump which then returned it to the oil tank. Both oil pumps were Tuthill internal gear type. Oil temperature was measured in a temperature well located in the line between the sump pump and the oil tank.

## ANGLE OF ATTACK SYSTEM

The angle of attack of the model was varied by an Airborne Accessories electric-linear actuator. A slide wire null balance bridge circuit was used as an angle of attack indicator. The model was locked in place by a Hannifin hydraulic (oil) cylinder and pressure was applied by a Blackhawk hand hydraulic pump.

## MODEL DATA SYSTEM

Pressure pick-ups were installed in the shroud and ring assembly, wing leading edge, wing tip, upper and lower wing surfaces, and wing flap. These pickups consisted of stainless steel tubes imbedded in the model. Tempaflex tubing was used to connect the

REV

VERTODYNE MODEL TEST

DIAGRAM OF FORCES AND MOMENTS RECORDED
DURING WIND TUNNEL TESTS

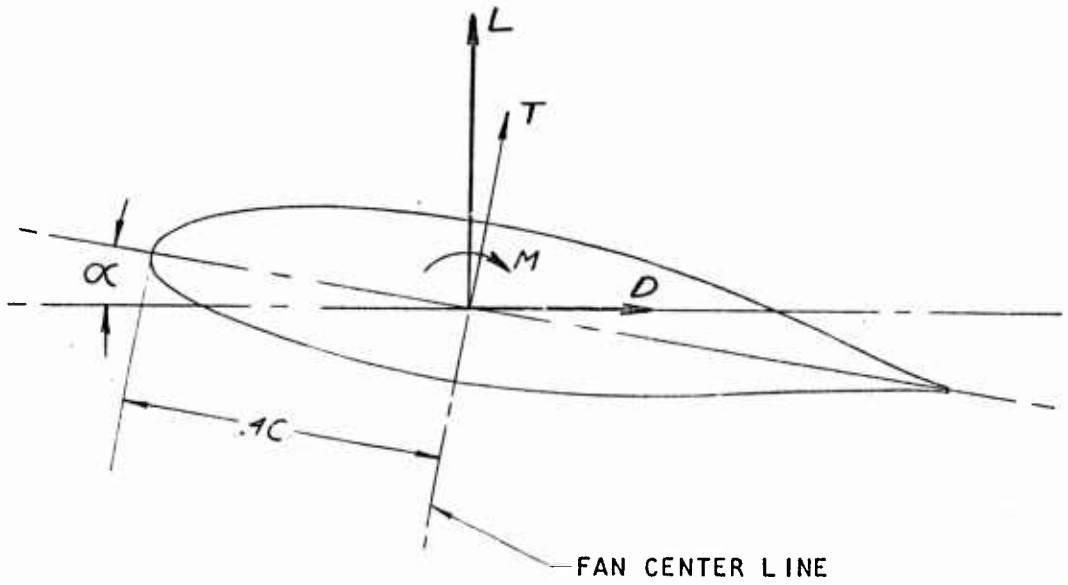


FIGURE 5

REV

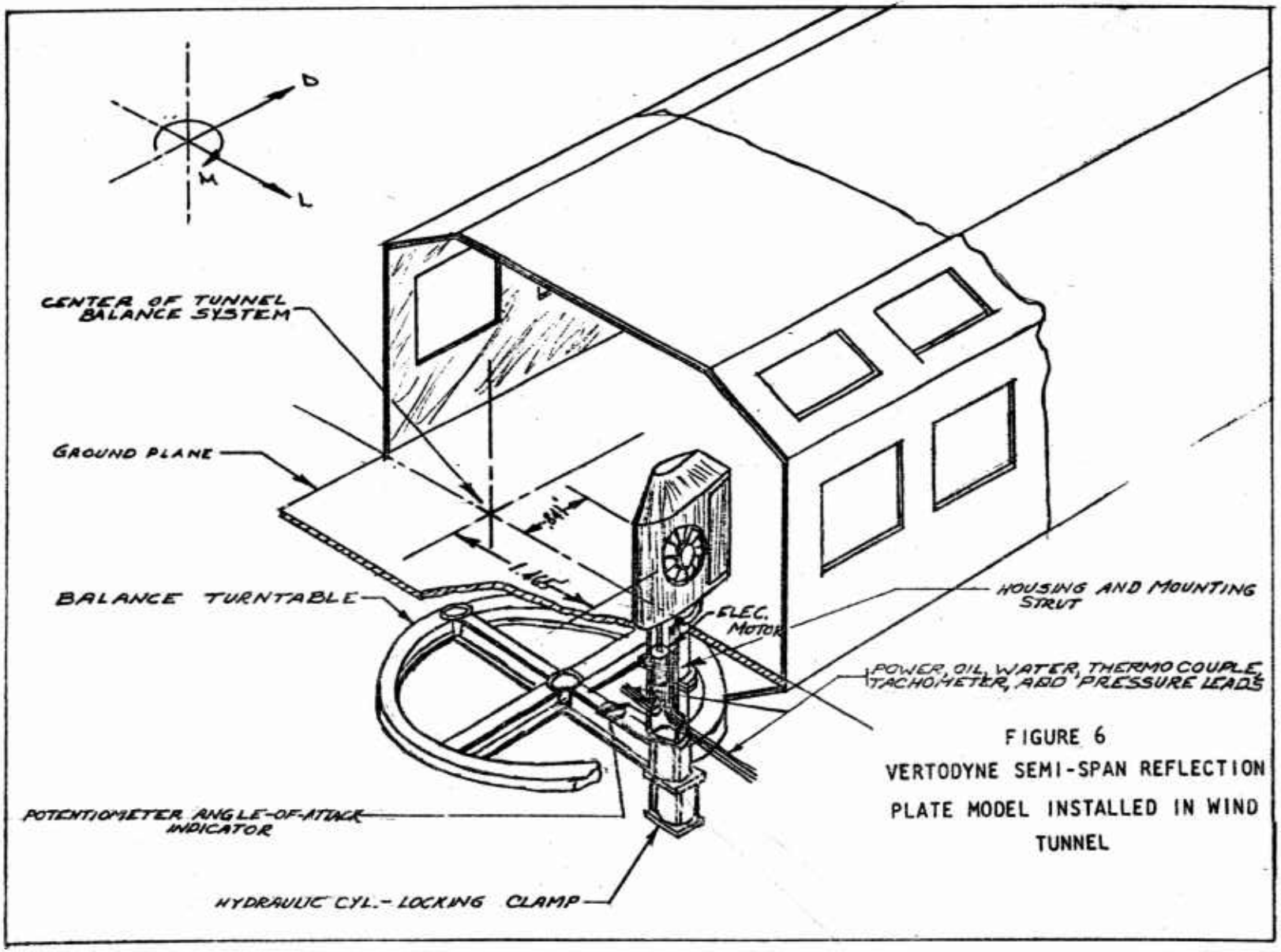


FIGURE 6
VERTODYNE SEMI-SPAN REFLECTION PLATE MODEL INSTALLED IN WIND TUNNEL

pressure pick-ups to a 100 tube manometer bank. Figures 10 and 11 show pressure pick-up installations. Figure 12 shows the fan components mounted in the fan shroud.

GENERAL INSTALLATION

Figures 6, 7, and 8 illustrate the arrangements of the model, power, lubrication, cooling, control and instrumentation systems for the wind tunnel tests.

GROUND PLANE

The ground plane used in the ground proximity tests consisted of a four foot square piece of plywood supported in a steel framework. The framework was constructed so that the center of the ground place coincided with the center of the ducted fan. The ground plane could be moved so as to be any desired distance from the model, to a minimum of 0.3 fan diameter (3.6 inches). Figure 9 shows the ground plane installation.

LIFT MEASURING DEVICE FOR STATIC TESTS

The model was mounted on a table which in turn was mounted on a set of steel casters. The casters rested on steel plates in order to reduce frictional drag due to the roughness of the Laboratory concrete floor. A Chatillon spring scale (one hundred pounds capacity) was attached to the table to register total model lift, as shown in Figure 9. This setup was calibrated with dead weights and found to be accurate to within one-half pound up to one hundred pound thrust.

POWER MEASUREMENTS

The power used by the model motor was determined from a fan torque strain gage system and fan RPM. A wattmeter and motor calibration were used to substantiate the power determined from torque and RPM.

VERTODYNE BALANCE SYSTEM

The balance system used in the Vertodyne Model was designed primarily to measure fan lift and fan torque. A total of eight strain gaged flexures were used, four in each system. Each flexure was designed to measure axial load with a minimum of sensitivity to other loads.

To measure torque, the fan, transmission, and fan shroud assembly were supported by four strain gaged flexures. These flexures were arranged with their sensitive axis tangential to the fan periphery in the plane perpendicular to the fan's rotational axis. The strain gaged flexures were attached to a rigid intermediate ring around the shroud assembly. Figure 14 shows the

REV

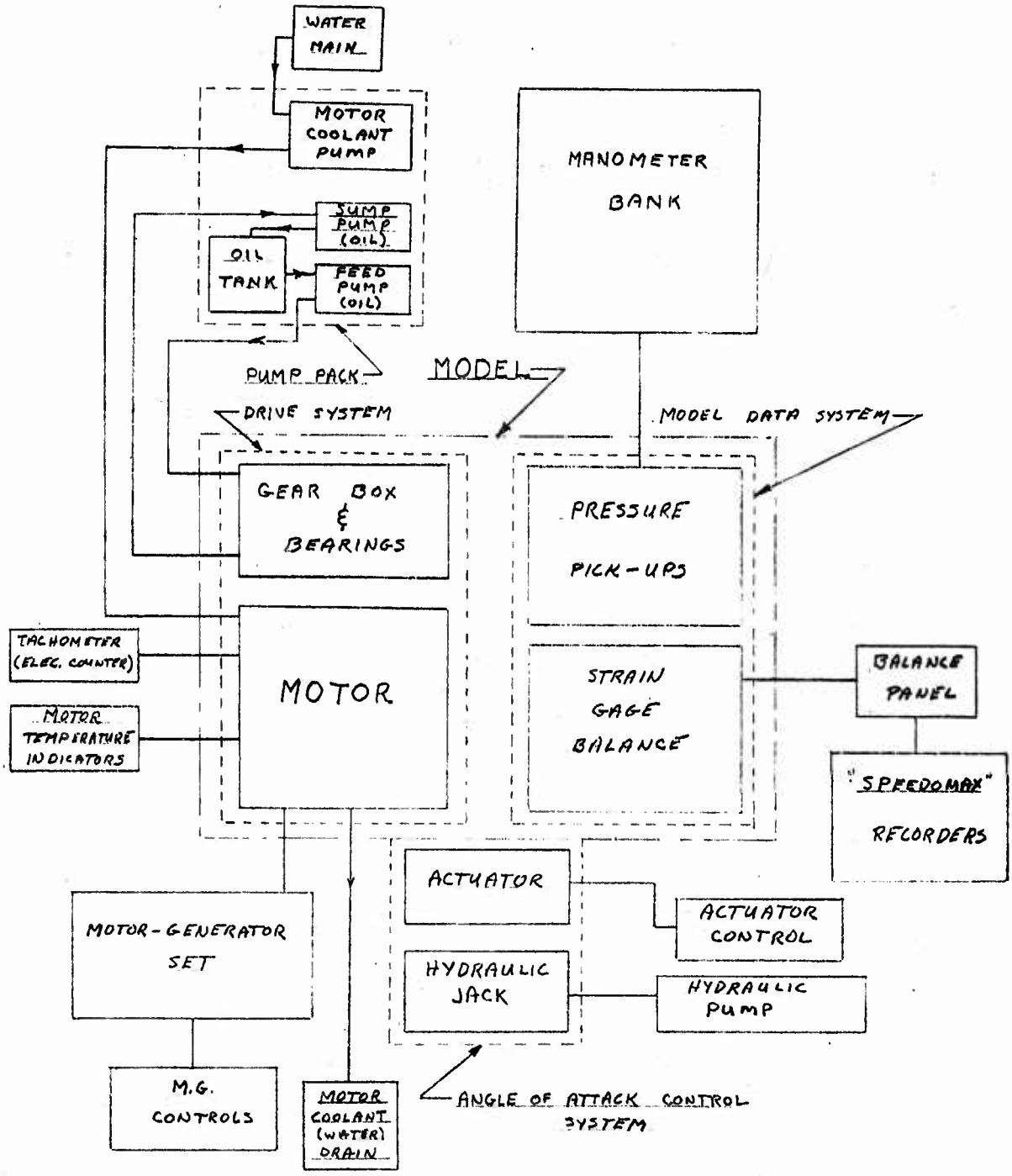


FIGURE 7
SCHEMATIC DIAGRAM OF VERTODYNE MODEL INSTALLATION AND INSTRUMENTATION

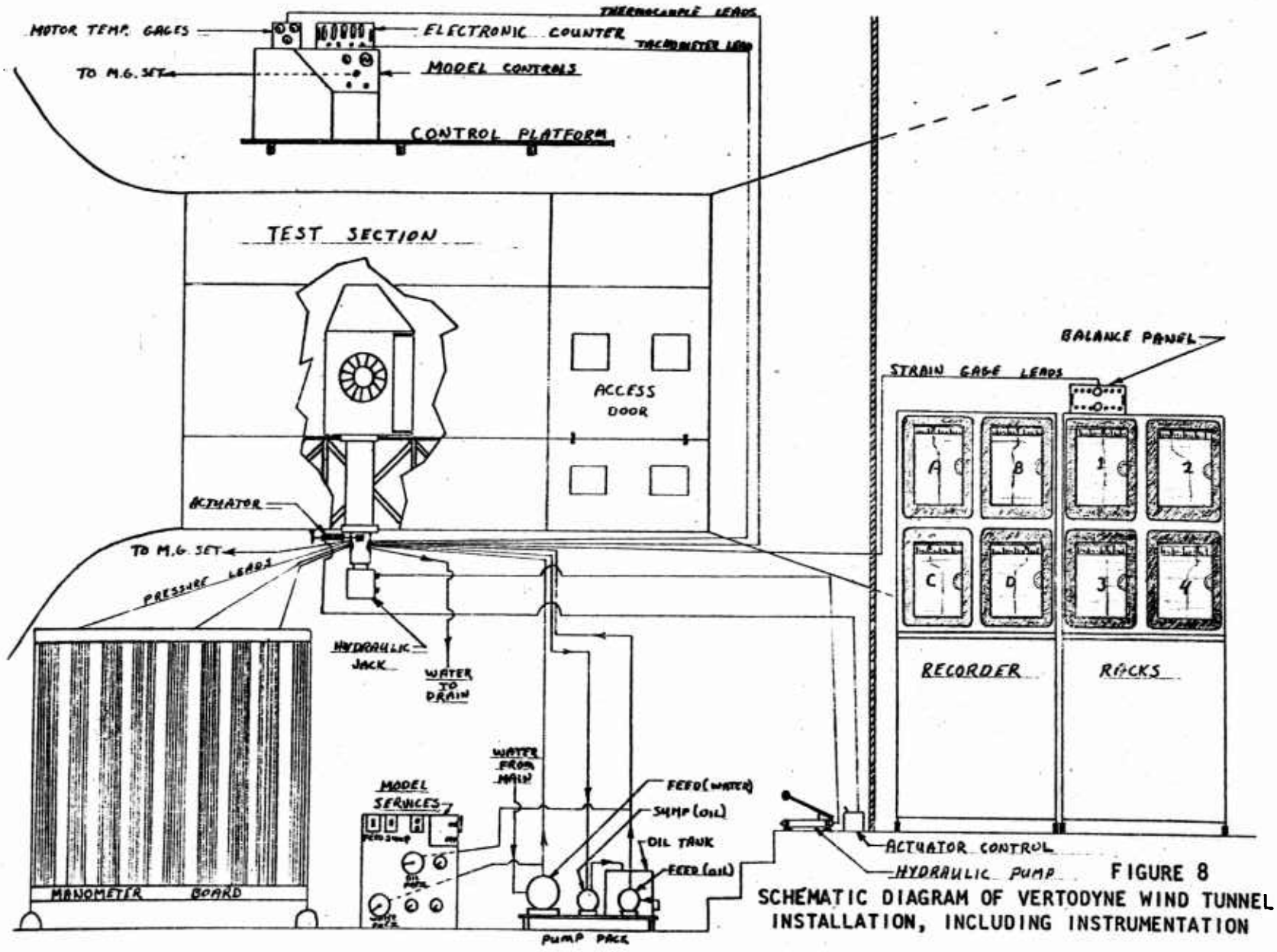


FIGURE 8

SCHEMATIC DIAGRAM OF VERTODYNE WIND TUNNEL INSTALLATION, INCLUDING INSTRUMENTATION

location of the strain gaged flexures, and the forces acting on the torque flexures.

To measure lift, the intermediate ring was supported by the other four strain gaged flexures. These strain gaged flexures were arranged with their sensitive axis parallel to the fan thrust axis. In this case the strain gaged flexures were attached to the wing main structure.

In both the lift and torque systems the four flexures were arranged at 90 degree intervals about the fan.

Each of the eight strain gaged flexures contained a 4-arm bending bridge utilizing Baldwin SR-4 strain gages, type AB-7, with a gage resistance of approximately 120 ohms. All eight bridges were powered by a common gage power battery. Balancing was accomplished by using a B & F Instruments Company Type 12-200 Balance Panel. This balance panel also supplied a short calibration of each bridge for periodic checks of circuit sensitivity. Each bridge output was individually recorded on one of eight Leeds & Northrup Speedomax Recorders of the Strip Chart Type.

Lift was determined as the sum of the average strain gage readings at flexures A, B, C & D, see Figure 14. Torque was obtained as a sum of the average strain gage readings at flexures 1, 2, 3, & 4, and pitching moment was computed from the reaction values at flexures A & B compared to the values at C & D. The torque absorbed by the fan is less than the torque delivered to the gear box by the motor by the amount of the transmission torque loss. This loss is usually between one-half and one per cent of the transmitted torque per gear mesh. Therefore, the fan torque may be expected to be slightly less than the indicated torque by the amount of this gear loss.

By writing equations summing the forces which act on the four flexures, it may be seen that chordwise and spanwise forces fall out, so that the average of the torque measured by each of the flexures is the fan torque plus the transmission loss torque. It should be remembered that the fan shroud, where the flexures are situated, offers the only torque restraint. The torque is transmitted from the transmission through the support struts to the shroud ring.

Knowing the magnitude of the forces in each flexure (1 to 4 inclusive), chordwise and spanwise components, as well as the torque value, can be obtained:

REV

**FIGURE 9**
**SKETCH OF VERTODYNE STATIC TEST INSTALLATION**

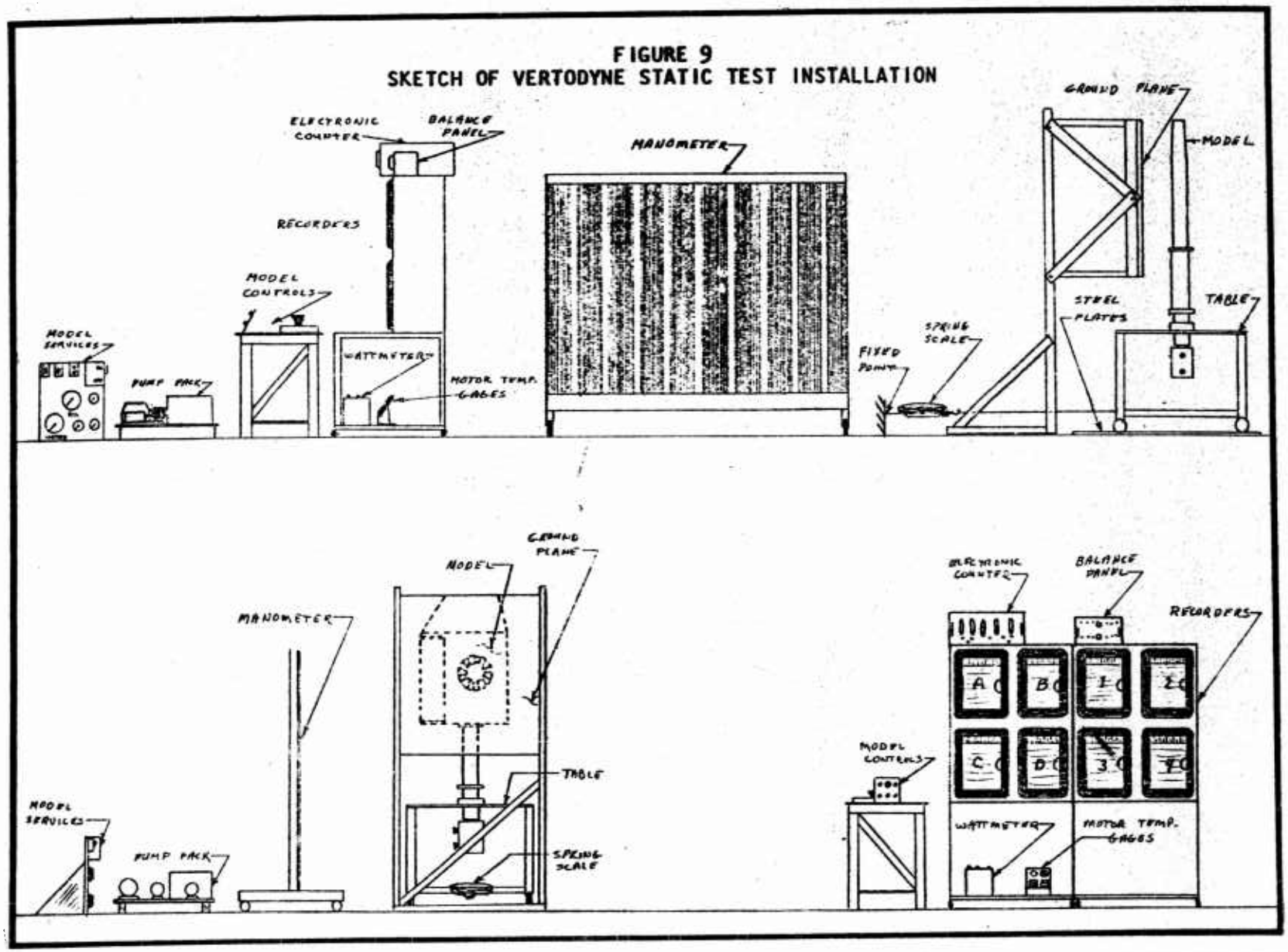

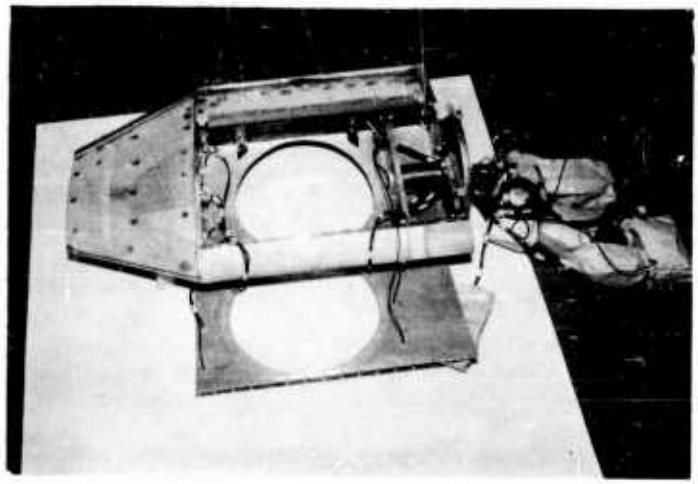

FIGURE 10

VERTODYNE MODEL WING OPENED, SHOWING WING PRESSURE PICKUPS

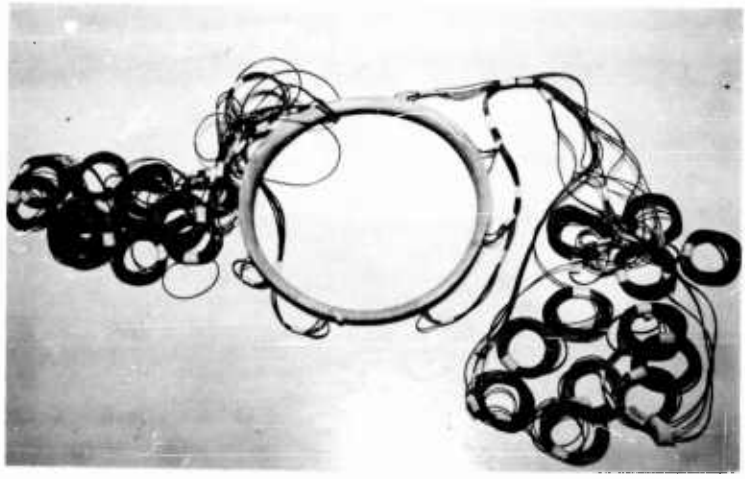

FIGURE 11

FAN INLET SHROUD WITH PRESSURE PICKUPS

$$c = \Sigma c_k$$

$$= .707f_1 + .707f_2 - .707f_3 - .707f_4$$

$$s = \Sigma s_k$$

$$= .707f_1 - .707f_2 - .707f_3 + .707f_4$$

$$Q = \Sigma t_k r$$

$$= (f_1 + f_2 + f_3 + f_4)\ r$$

where c = Chordwise forces, positive toward trailing edge,

s = Spanwise forces, positive in inboard sense,

t = Torque forces, positive counter-clockwise

Q = Torque

f = Total force on a given flexure, denoted by subscripts

r = Radius from center of rotation to flexure

Since static load calibrations of pure torque application were performed, a valid determination of torque is obtained by entering the respective static calibration curve with the test trace deflection value for each flexure and averaging the indicated total torque from each calibration, at a given operating condition. One fallacy can exist with this system, due to physical limitations of the flexure design. That is interaction between the lift and torque forces. This question was eliminated by obtaining interaction results during the static calibrations and correcting for them. It was found that torque did not affect the lift or thrust gages but that thrust did result in interaction in the torque gages.

REV

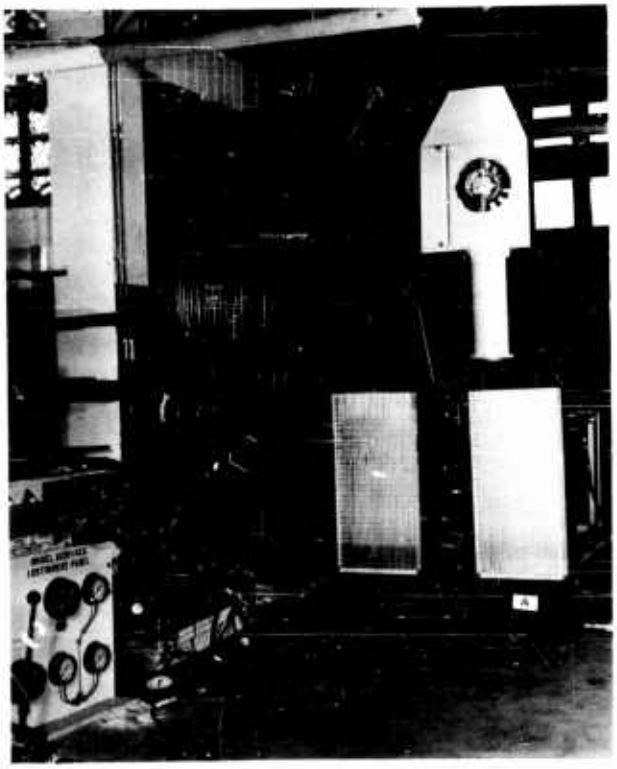

FIGURE 12

STATIC TEST INSTALLATION

FAN SHROUD INLET RADIUS DATA

| AZIMUTH POSITION | INLET RADIUS, INCHES | R/d, PERCENT |
|---|---|---|
| 0° (Leading Edge) | 0.37 | 3.1 |
| 30° | 0.54 | 4.5 |
| 60° | 0.72 | 6.0 |
| 90° | 0.72 | 6.0 |
| 120° | 0.72 | 6.0 |
| 150° | 0.32 | 2.7 |
| 180° (Trailing Edge) | 0.18 | 1.5 |
| Fan Rotor Hub | 0.50 | 4.2 |

NOTE: Reference 8 showns a minimum 6% R/d to maintain shrouded propeller static thrust efficiency.

FIGURE 13

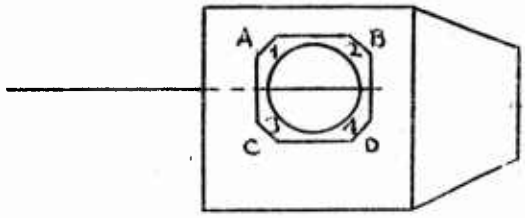


SKETCH OF LIFT AND TORQUE
FLEXURES INSTALLATION

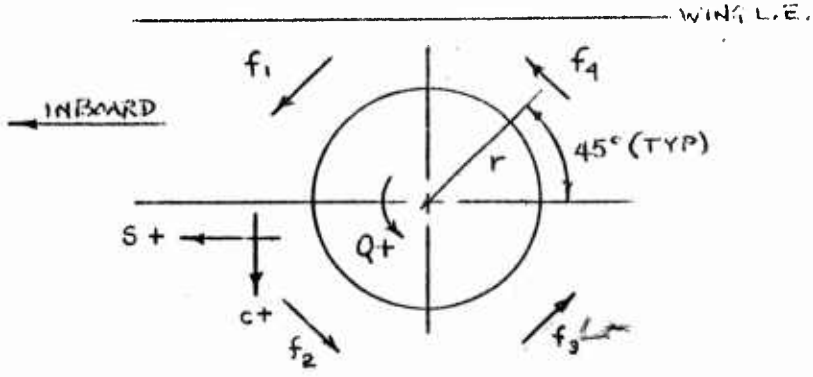


FORCES ACTING ON

TORQUE FLEXURES

FIGURE 14

SKETCH SHOWING LOCATIONS

OF PRESSURE TAPS ON WING SURFACES

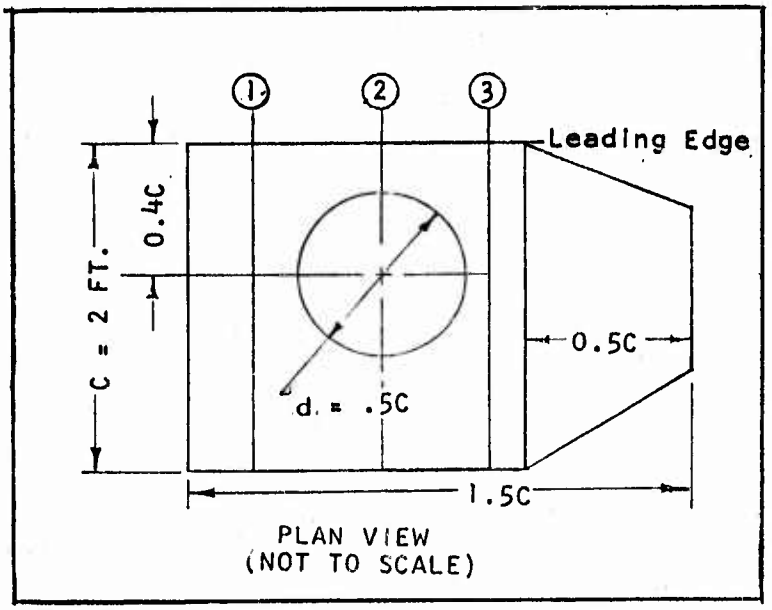


WING STATIONS OF CHORDWISE PRESSURE STATIONS:

INBOARD PRESSURE STATION (1) 0.25C

FAN CENTER PRESSURE STATION (2) 0.58C

OUTBOARD PRESSURE STATION (3) 0.97C

CHORDWISE LOCATIONS OF PRESSURE PICKUPS IN PERCENT OF CHORD LENGTH

| INBOARD | FAN CENTER | OUTBOARD |
|---|---|---|
| 2.5 | 1.25 | 2.5 |
| 5.0 | 2.5 | 5.0 |
| 9.8 | 5.0 | 9.8 |
| 20.2 | 9.8 | 20.2 |
| 40.0 | 71.0 | 40.0 |
| 60.3 | 78.0 | 60.3 |
| 78.0 | 90.0 | 78.0 |
| | 95.0 | |

FIGURE 15

SKETCH SHOWING LOCATIONS
OF PRESSURE TAPS ON FAN SHROUD SURFACE

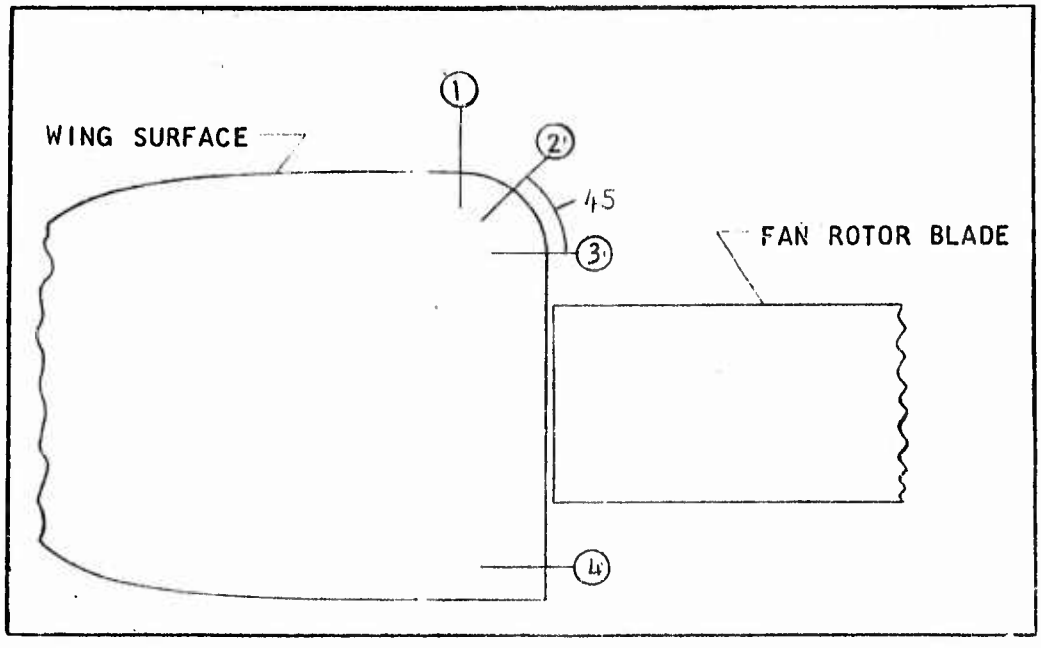


VIEW THROUGH FAN ANNULUS (NOT TO SCALE)

FAN SHROUD FLOW-WISE PRESSURE STATIONS

① At Tangency Line Of Upper Wing Surface and Inlet Radius

② 45° Through Inlet Radius

③ At Tangency Line of Inlet Radius and Shroud Diameter

④ 0.25 Inch Upstream of Annulus Exit

Peripheral Azimuth Locations of Pressure Pickups
(0° At Leading Edge, Clockwise From Above)

0°, 22.5°, 67.5°, 112.5°, 157.5°, 202.5°, 247.5°, 292.5°, 337.5°

Cautionary Note: Static Test Data are Presented as In Azimuth Description Above, but Forward Flight Data are Presented According to Conventional Helicopter Rotor Azimuth Locations, i.e., 0° at Trailing Edge, Positive in Direction of Rotation.

FIGURE 16

## VI. TEST PROGRAM AND PROCEDURE

The model test program consisted of a static test phase and a forward flight phase. The forward flight phase was conducted in the University of Detroit seven foot by ten foot subsonic wind tunnel during February, March, and April, 1958. The static test phase was conducted out of the tunnel in the University of Detroit Aeronautical Laboratory in August 1958. However, some static fan performance was investigated in the tunnel by operating each fan, with rotor blade root incidence angles of 25.0°, 39.7° and 55.9°, at various rotational speeds.

The model performance in forward flight was investigated by using two of the three fan rotors at the design rotational speed of 10,000 rpm and the third, ($\phi_R$=55.9°) at 9060 rpm because of excessive motor heat at higher powers. Wing angle of attack, air speed, wing flap position, and fan exit duct turning angle were also varied to study the model performance. The low pitch fan, with a root incidence angle of 25°, was destroyed in the wind tunnel because of a faulty installation. Fortunately, a sufficient investigation of the low pitch fan configuration had been conducted prior to this mishap to determine the most forward location on the model apparent center of pressure associated with airspeed variation.

During the model static ground effect tests, it was intended that, as in the forward flight tests, each of the three fans be tested. However, the replacement fan for the one destroyed in the wind tunnel was itself destroyed at the fan manufacturer's test facility during acceptance tests prior to delivery. This incident occurred two work days before the scheduled start of the static test phase. The other equipment had already been delivered to the University of Detroit and the test facility scheduled, so it was decided to proceed with testing. As an alternative to using the low pitch fan, the medium pitch fan was operated (in addition to its design speed of 10,000 rpm) at 6,000 rpm, to approximate the disc loading of the low pitch fan. Therefore, the fan configurations tested in the ground proximity test were:

1. Medium pitch fan, root incidence angle 39.7°, @ 6,000 rpm
2. Medium pitch fan, root incidence angle 39.7°, @ 10,000 rpm
3. High Pitch fan, root incidence angle 55.9°, @ 9,060 rpm

REV

## VII. PRESENTATION OF DATA

The results of the subject testing are presented graphically in Figures 17 to 55 following Section XI. The data has been divided into two main groups as follows:

1. Force, moment and fan power data
2. Wing surface pressure data

These groupings are further divided to cover the performance of the fan and the model in static and forward flight conditions.

An attempt has been made to present the Vertodyne data in convenient non-dimensional form to allow comparison with studies made by other groups. An investigation of the presentations used in published reports was conducted to find the most desirable form consistent with these requirements.

Static data is presented in terms of $C_T$ (thrust coefficient) and $C_P$ (power coefficient) which are related to fan tip speed. These factors are plotted versus fan blade pitch angle.

Model performance in forward flight is presented in conventional wing coefficients $C_L$ (lift), $C_D$ (drag), and $C_M$ (pitching moment) which are related to forward speed. These factors are plotted versus $\mu^2 = (V_T/V_0)^2$.

References to the fan alone in this report refer to fan characteristics observed while being operated within the wing. The measurements of fan thrust and power which were obtained include the effects of flow over the wing on the fan. The fan was not tested out of the wing.

The wing surface pressure data has been presented as $\triangle P$ or $\triangle P/q$ plotted against chordwise station. Data is included for static and forward flight.

The data received from the University of Detroit which covers wind tunnel operation of the model has been included in Appendix B. The effect of the flap and of the exit ducts is shown by these curves. The coefficients and symbols used are defined within the appendix.

REV

## VIII. DISCUSSION OF RESULTS

The discussion of results deviates slightly from the order used in the presentation of data. To allow better visualization of the characteristics of the wing and fan combination, the force, moment, and power data is considered with the pressure data. Divisions are made between the static and the forward flight data.

### A. Static Performance

#### 1. Static Performance Out of Ground Effect

Static tests of the Vertodyne model were conducted out of the wind tunnel in the University of Detroit Aeronautical Laboratory. Force, moment, and power data were taken for the fan and the total model and are presented in Figures 17 to 20. Surface pressure data was recorded for these runs and is presented in Figures 32 to 39.

Tests were conducted with the high and medium pitch fans. A low pitch fan was not available for the static tests.

Comparative thrust coefficient versus blade pitch angle curves are presented for the fan and for the fan-and-wing. The increased thrust due to the wing can readily be seen. A power coefficient curve is also presented plotted versus blade pitch angle, see Figure 19.

Figure 17 shows total model thrust per horsepower versus disc loading for the two fans tested. A comparison is made with the theoretical curves for a ducted propeller and for an ideal free propeller. The calculated download due to the fan support struts has been added to the high pitch fan thrust values to determine a corrected curve. The corrected high pitch fan curve shows some agreement with the theoretical values. The greater deviation at higher disc loadings is assumed to be due to non-optimum inlet conditions.

The inlet shroud did not have a uniform inlet radius around its periphery. The radius used near the trailing edge was necessarily smaller than the value which would normally be considered adequate. This was brought about by the requirement of completely containing the fan and its transmission within the wing. An adequate radius was used on the forward and side portions of the inlet.

A series of in-tunnel static runs were made in conjunction with the forward speed tests. These in-tunnel runs show approximately 15% lower total model thrust compared to out-of-tunnel runs. The difference in thrust is attributed to

REV

tunnel wall effects. For the purposes of this report this data has not been included.

Fan pitching moments were obtained from data from the four shroud thrust measuring points. Longitudinal center of pressure location was obtained from the pitching moments and total fan thrust. The center of pressure of the fan assembly was found to lie forward of the fan axis for all static conditions, thus indicating greater induced lift developed over the forward portion of the inlet lip, see Figure 20.

Extensive wing surface and shroud pressure data was obtained during the static runs. Chordwise distributions of wing surface pressures for the high and medium pitch fans were determined and are presented in Figures 32 to 34 and 36 to 38. Fan shroud pressures around the fan circumference are presented in Figures 35 and 39.

Negative pressures were observed on the upper surface of the wing when operated out of ground effect. This effect is due to the high velocity inlet air passing over the upper surface of the wing. The induced lift which is created explains the higher thrust obtained for the total model over that obtained for the fan alone. The major portion of this induced lift acted on the wing; however, a small portion acted on the shroud and was measured as fan thrust.

2. Static Performance in Ground Effect

Static tests in ground effect were also conducted out of the wind tunnel in conjunction with the out of ground effect tests. Force, moment, and power data was taken for the fan and the total model. Surface pressure data was recorded.

Runs were made with the high pitch and medium pitch fans. A low pitch fan was not available for these tests; therefore to obtain the same disc loading the medium pitch fan was also run at 60% of its design speed. It is believed that, in this way, conditions corresponding to the operation of the low pitch fan were sufficiently approximated for a study of ground effect at lower disc loadings.

Figure 22 shows the increase of thrust in ground effect versus model height above ground. Curves are presented for the total model and for the fan. The increase of power in ground effect can be deduced from Figure 21. The decreasing thrust per horsepower (shown in Figure 21) for the total model which was observed in ground effect can be partially explained by a study of the wing surface pressures. Moving into ground effect a marked

REV

decrease in magnitude of the upper surface negative pressures was noted in Figures 32 and 36. This was accompanied by a build-up of negative pressures on the lower surface forward of 20% of the chord. The thrust reducing effect of these surface pressures is apparently offset by the build-up of pressures on the fan disc and hub area. This phenomenon is indicated by the reduced magnitude of the negative pressures observed at fan shroud exit station (4) Figure 16. The net effect of these pressure changes is an increase in total model thrust in ground effect for a constant fan rotational speed.

The decreasing negative pressures on the upper surface are assumed to be due to a changing inlet flow pattern created by the exiting air which is deflected by the ground plane. The lower surface negative pressures are believed to be due to vortex flow set up by the exiting air.

The static tests were run with the model in an open room without a reflecting plane on the inboard section of the wing. The pressures recorded for the inboard underside of the wing might be altered in an actual application using a fuselage.

B. Forward Flight Performance

Forward flight tests of the Vertodyne model were run in the University of Detroit wind tunnel. Force, moment, and power data were taken for the fan and for the total model. Surface pressures were also recorded.

Tests were run with the high, medium, and low pitch fans. The low pitch fan failed while being tested thus limiting the available data for that blade angle.

Total model forward flight performance curves show the increase of $C_L$, $C_D$, and $C_M$ with increasing $\mu^2$. The effect of blade pitch angle can be seen by comparison of the curves on each figure. The effect of the fan can readily be seen from the substantial lift available at negative angles of attack.

The direct contribution of the fan thrust to lift and drag is shown in Figures 29 and 30. A basic wing curve is presented in Appendix B to allow comparison with the fan-in-wing data. The increase of model lift per horsepower at higher forward speeds is shown in Figure 31.

Center of pressure location was obtained from the model pitching moment and lift data. The curves which are presented, Figures 27 and 28, show extreme forward travel of the center of pressure at all angles of attack with reduced $\mu^2$ values. The

REV

location of the center of pressure lies well beyond the wing leading edge for much of the negative angle of attack data.

The surface pressure data illustrates the effect of the fan on upper surface leading edge negative pressures. Large magnitude negative pressure peaks are recorded in this region at lower forward speeds and positive angles of attack, see Figures 43 to 46. A reduction in magnitude of the peak is noted at higher speeds. It can be seen from the curves that the stagnation point shifts upward around the leading edge with increasing forward speed. The effect of forward speed tends to overcome the effect of inlet suction. The flow pattern around the leading edge becomes smoother at higher forward speeds thus reducing the sharp pressure peak noted at the lower forward speeds.

The increasing lift and pitching moment at increasing angle of attack are reflected in the surface pressure data, see Figures 43 to 46. The positive angle of attack pressure curves lie substantially above the zero degree angle of attack curves. The large magnitude of the nose-up pitching moment can be anticipated in these curves. Most of the lift augmentation due to the fan is due to induced lift on the upper surface of the wing forward of the inlet.

The test runs made with the wing flap deflected yielded increased lift to drag ratios as was expected. No unusual effects were observed; consequently the data obtained is presented in its original form as presented by the University of Detroit, in Appendix B. Pressure data is presented in Figures 48, 49 and 55.

The exit ducts which were tested were intended to deflect the exit air aft and provide net forward thrust. The ducts were unsuccessful. Slight drag reduction was obtained in some cases while in others drag was increased. The data obtained is presented in its original form in Appendix B.

REV

## IX. CONCLUSIONS

1. Forward flight characteristics indicate a significant increase in lift due to the fan at negative as well as positive angles of attack.

2. Large magnitude nose up pitching moments were recorded for the model in forward flight, caused by high induced lift on the wing leading edge.

3. Total model static thrust is greater than the thrust of the fan alone due to induced lift on the wing upper surface.

4. Model static thrust obtained for a constant fan rotational speed increases in ground effect.

5. Model static thrust per horsepower decreases in ground effect.

6. In static operation, wing upper surface negative pressures act on the area within 0.3 fan diameters of the fan duct.

7. Model lift per horsepower increases with increasing forward speed.

8. The exit ducts which were used were ineffective in turning the fan exit air aft, and did not produce a significant reduction in drag.

REV

## X. RECOMMENDATIONS

1. A large quantity of data dealing with the fan-in-wing concept has become available in the past few months. Wind tunnel tests of wing submerged ducted fans are reported in References 10 to 13 . Also of great interest is the series of wind tunnel tests currently being conducted on the Vanguard aircraft in the full scale Ames wind tunnel.

   In view of the availability of this experimental material it is recommended that an investigation be made to determine whether correlation is possible with a simple theory based on the momentum concept.

2. Further advancements in the fan-in-wing field are possible using the existing Vertodyne hardware and building on the knowledge gained from the earlier studies. Improvements in hovering and transition performance would be the primary aim of these later tests.

   It is felt that use of the "Jet Wall" concept has particular merit as a means of deflecting the fan slipstream. "Jet Wall" effects used in conjunction with expansion of the primary slipstream can be investigated following minor modifications to the Vertodyne model.

3. Using the information obtained from the advanced model tests a parametric study should be conducted to determine the feasibility of designing and building a full scale Vertodyne aircraft. The study should direct attention to the use of existing engines and versions available in the near future.

REV

## XI. REFERENCES

1. Vertol Aircraft Corporation, Final Summary Report Comparative Study VTOL Aircraft, Report No. R-85.

2. General Electric Company Flight Propulsion Laboratory Department, Preliminary Study Data, Convertible Propulsion Systems for VTOL Aircraft, June 1958.

3. Hickey, D. H. Preliminary Investigation of the Characteristics of a Two-Dimensional Wing and Propeller with the Propeller Plane of Rotation in the Wing-Chord Plane. NACA RM A S7F03, August 1957.

4. Fay, C. B. Characteristics of a Shrouded Rotor in a Cross Flow, Massachusetts Institute of Technology, M S. Thesis, June 1957.

5. Wardlow, R. L. and Templin, R. J., Preliminary Wind Tunnel Tests of a Lifting Fan in a Two-Dimensional Aerofoil, National Aeronautical Establishment (Canada) Report IR-207, September 1957.

6. Han, N. D. and Moser, H. H., Preliminary Investigation of a Ducted Fan in Lifting Forward Flight, Massachusetts Institute of Technology, June 1958.

7. von Glahn, U., Exploratory Study of Ground Proximity Effects on Thrust of Annular and Circular Nozzles, NACA TN 3982, April 1957.

8. Taylor, R. T., Experimental Investigation of the Effects of Some Shroud Design Variables on the Static Thrust Characteristics of a Small Scale Shrouded Propeller Submerged in a Wing, January 1958.

9. Vertol Aircraft Corporation, Proposal for Vertodyne Wind Tunnel Program Extension, Report No. PR-240, March 1958.

10. Switzer, J. R., VTOL Wing-Fan Model Tests, General Electric Company, Flight Propulsion Laboratory, Report No. R58AGT953, 1959.

11. Hickey, D. H. and Ellis, D. R., Wind Tunnel Tests of a Semi-span Wing with a Fan Rotating in the Plane of the Wing, NASA TN-D-88, October 1959.

REV

12. Moser, H. H. and Livingston, C. L., Experimental and Analytic Study of the Ducted Fan and Fan-In-Wing in Hovering and Forward Flight, Massachusetts Institute of Technology, ASTIA Document No. 213316, January 1959.

13. Wardlaw, R. L. and McEachern, N. V., A Wing-Submerged Lifting Fan: Wind Tunnel Investigations and Analysis of Transition Performance, National Aeronautical Establishment (Canada) Report LR-243 April 1959.

REV

# FORCE, MOMENT AND FAN POWER DATA

REV

VERTODYNE MODEL TEST
TOTAL MODEL STATIC THRUST PER HORSEPOWER
VS.
DISC LOADING

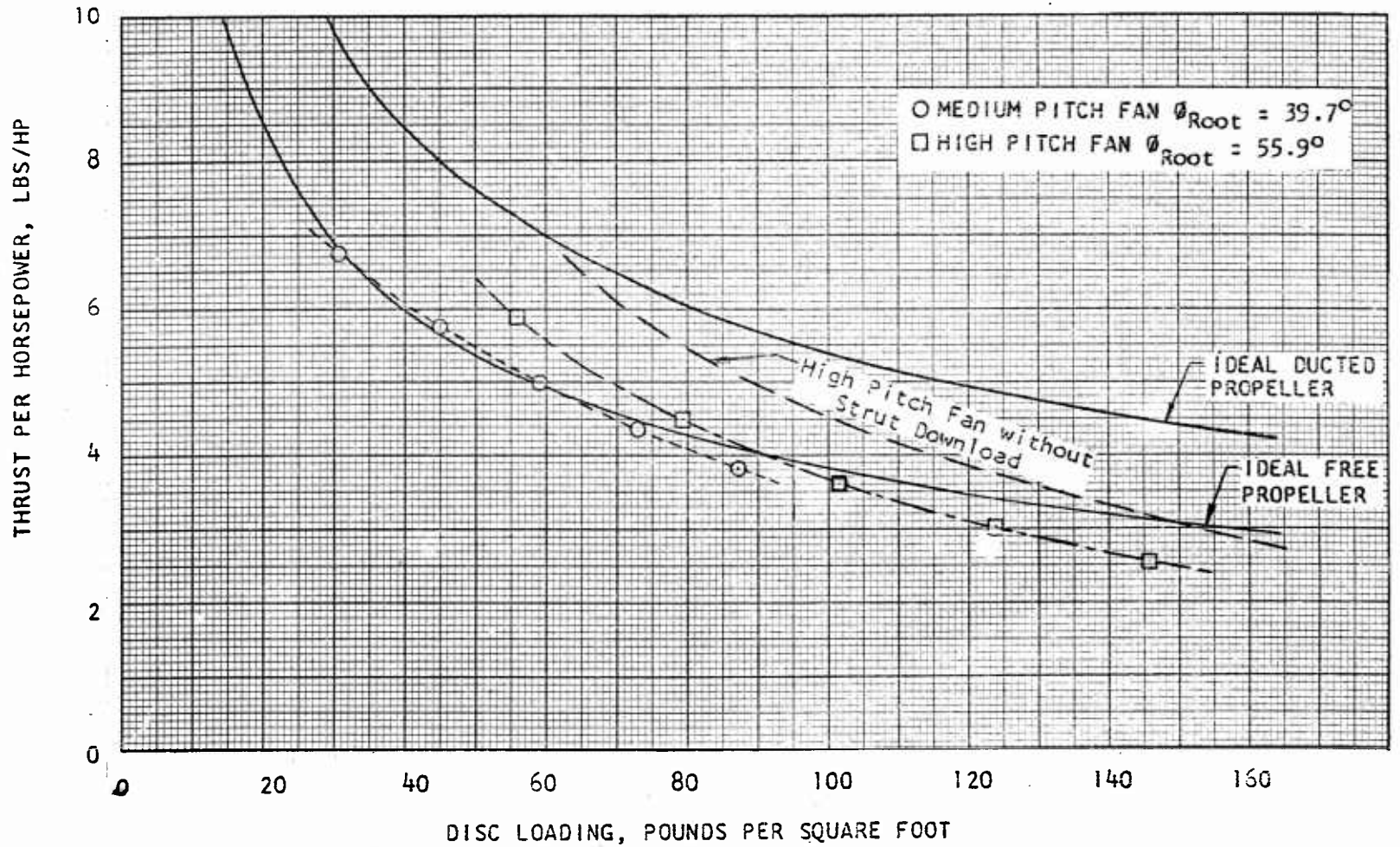


FIGURE 17

VERTODYNE MODEL TEST
FAN STATIC THRUST PER HORSEPOWER VS. RPM
FOR FANS WITH THREE DIFFERENT
BLADE ROOT INCIDENCE ANGLES
FAN ALONE

$V_o = 0$ $\frac{h}{D} = .00$ $\sigma_{Air} = 1.00$ $\delta_{Wing} = 0^o$

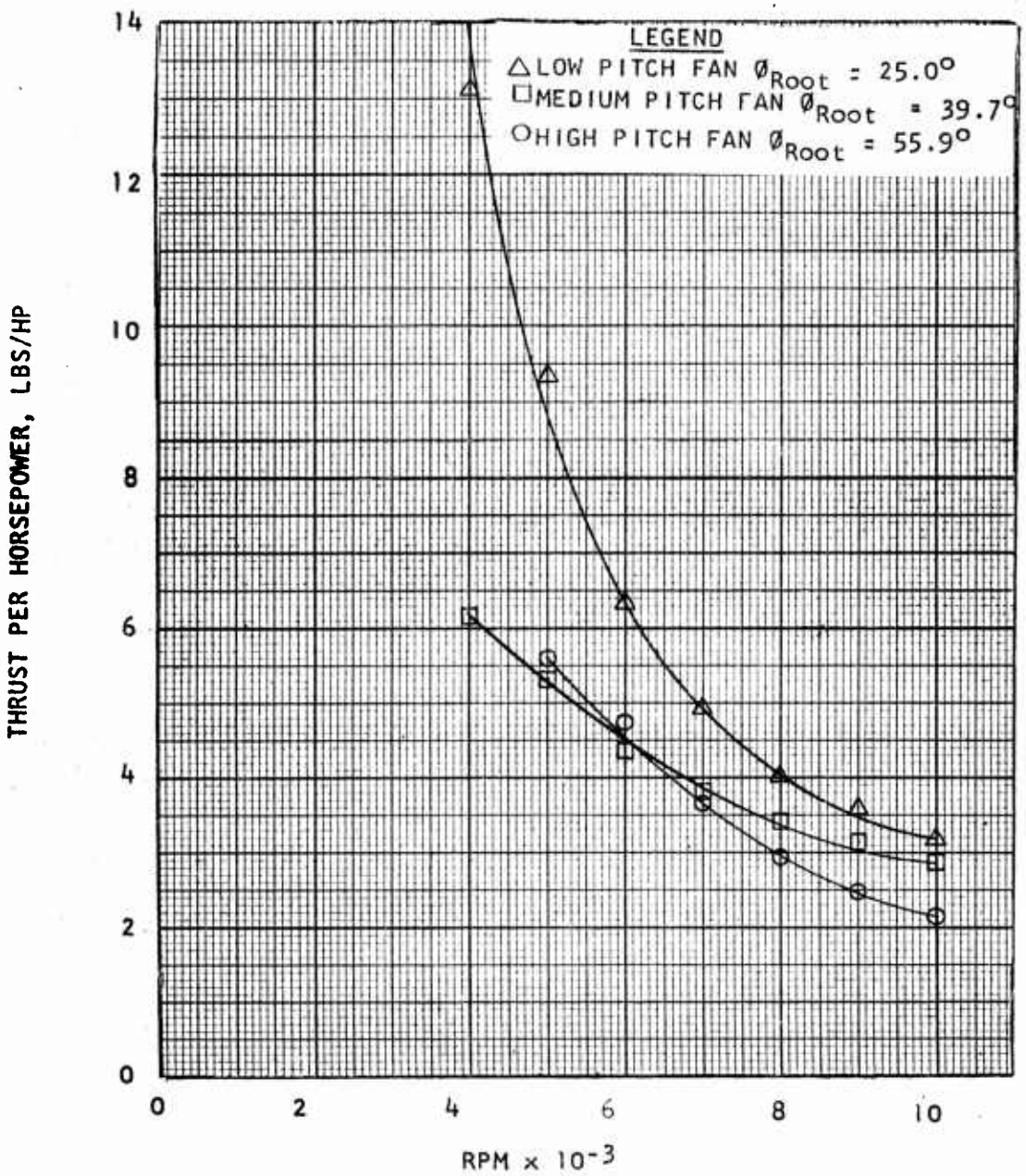


FIGURE 18

VERTODYNE MODEL TEST
STATIC OPERATION
OUT OF GROUND EFFECT

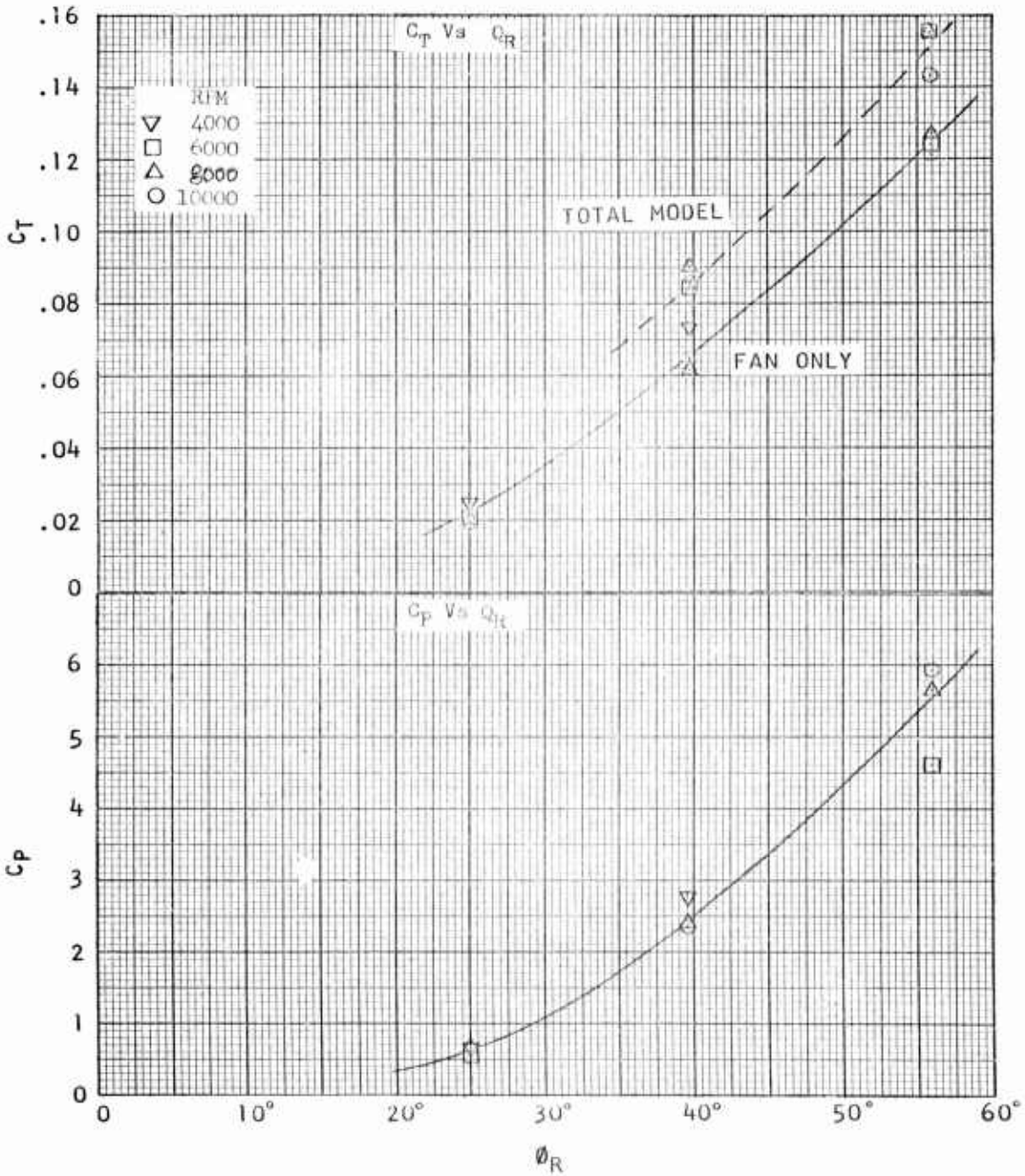


FIGURE 19

VERTODYNE MODEL TEST
STATIC FAN OPERATION
FORWARD CENTER OF PRESSURE LOCATION
VS. FAN RPM AT THREE
BLADE ROOT INCIDENCE ANGLES
FAN ALONE $\frac{h}{D}$ = 00

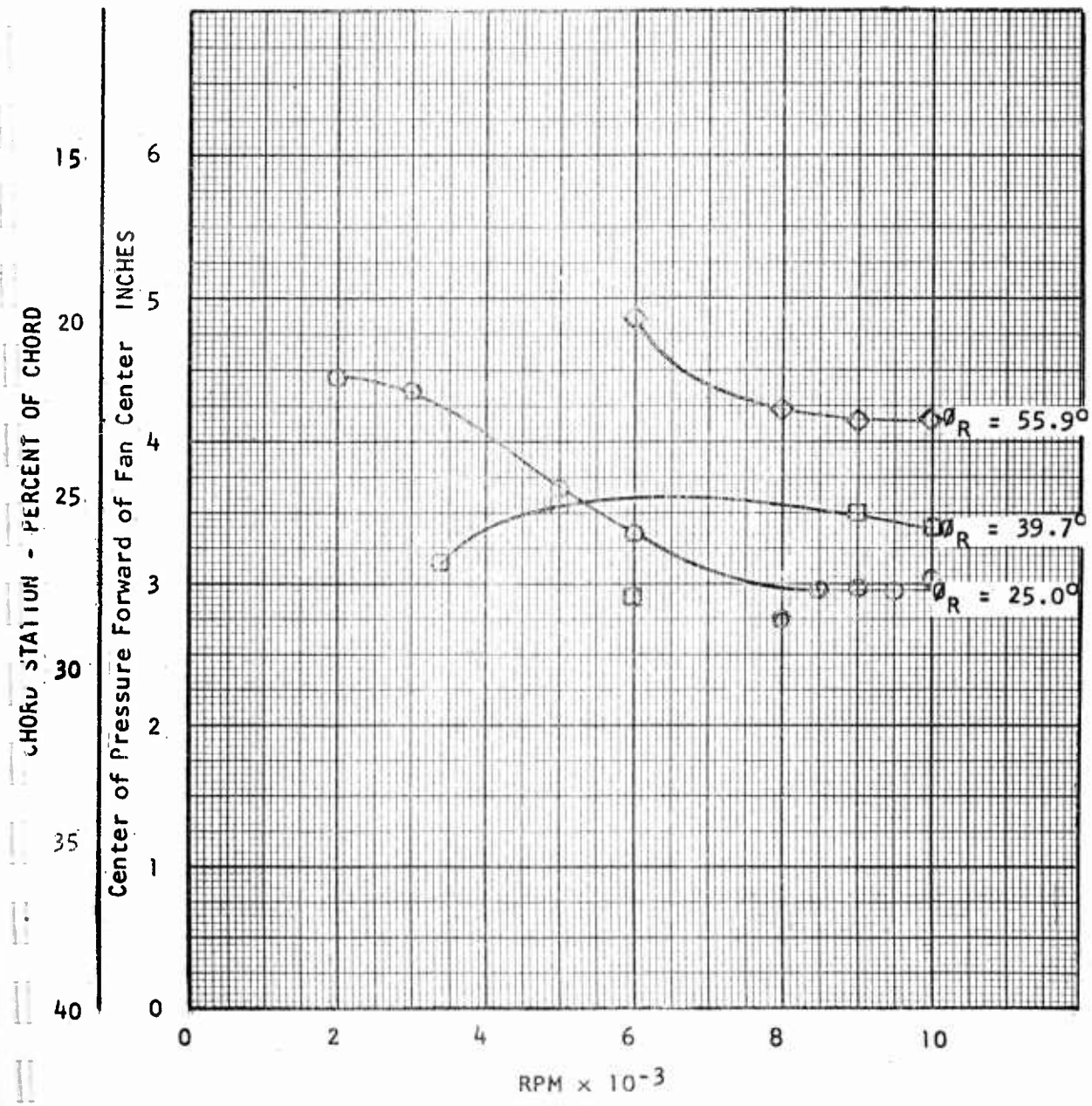


FIGURE 20

VERTODYNE MODEL TEST
STATIC OPERATION
IN GROUND EFFECT

$T/HP$ VS $h/d$

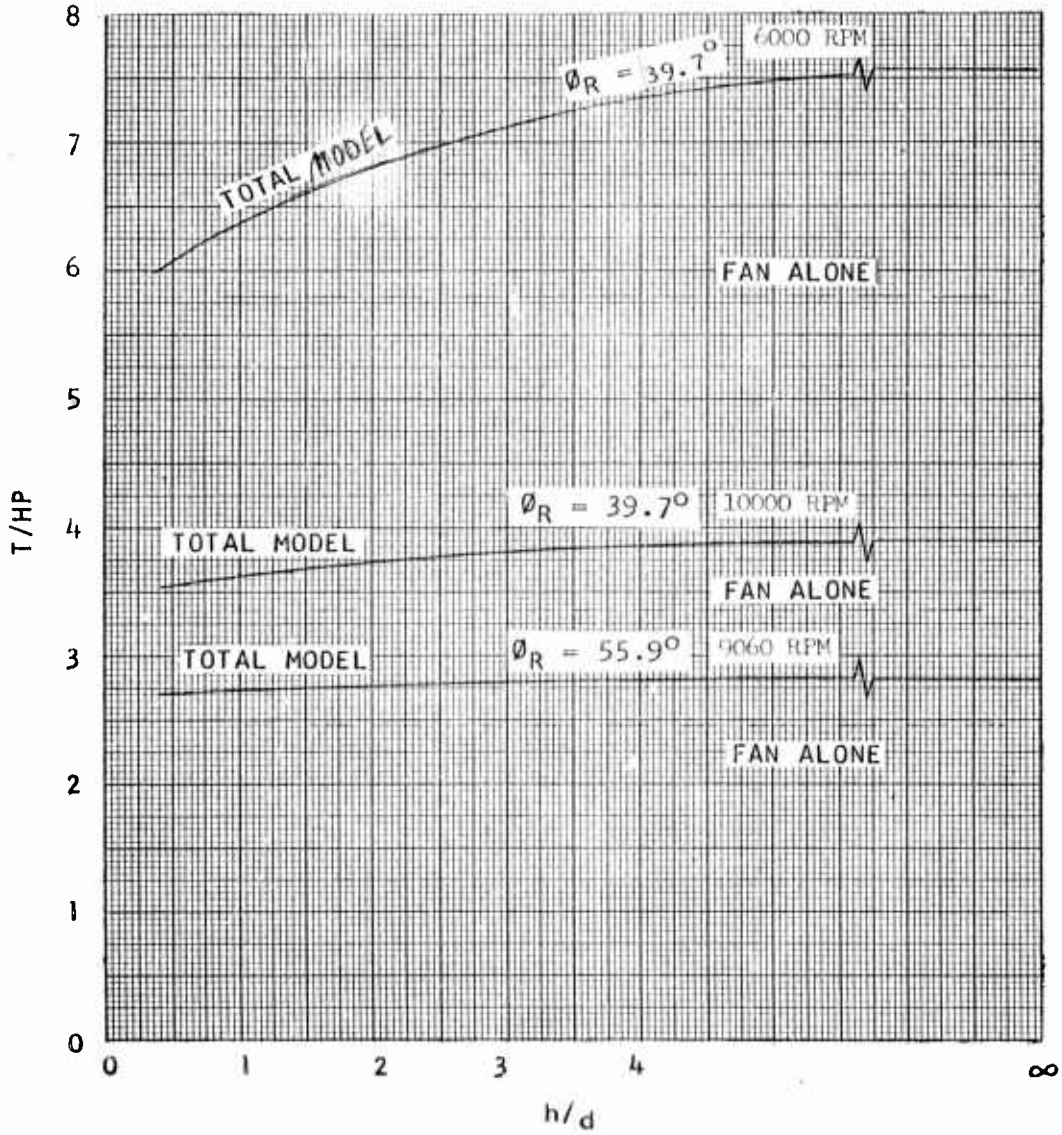


FIGURE 21

VERTODYNE MODEL TEST
STATIC OPERATION
IN GROUND EFFECT
FAN AND MODEL THRUST
$T/T_{\infty}$ VS $h/d$

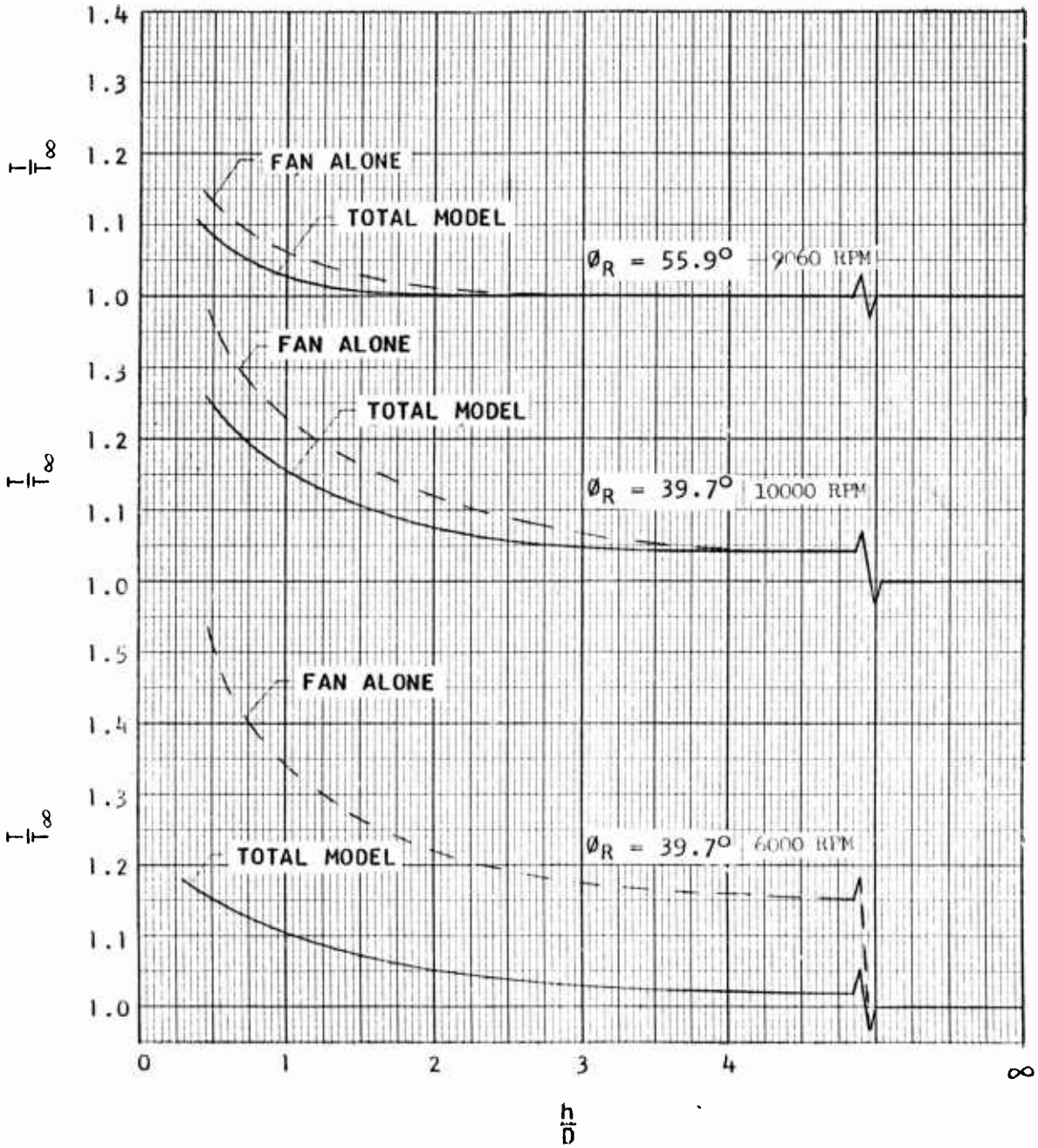


FIGURE 22

VERTODYNE MODEL TEST
FORWARD FLIGHT
WING LIFT COEFFICIENTS
$C_L$ VS $\mu^2$
FOR THREE FAN BLADE ANGLES

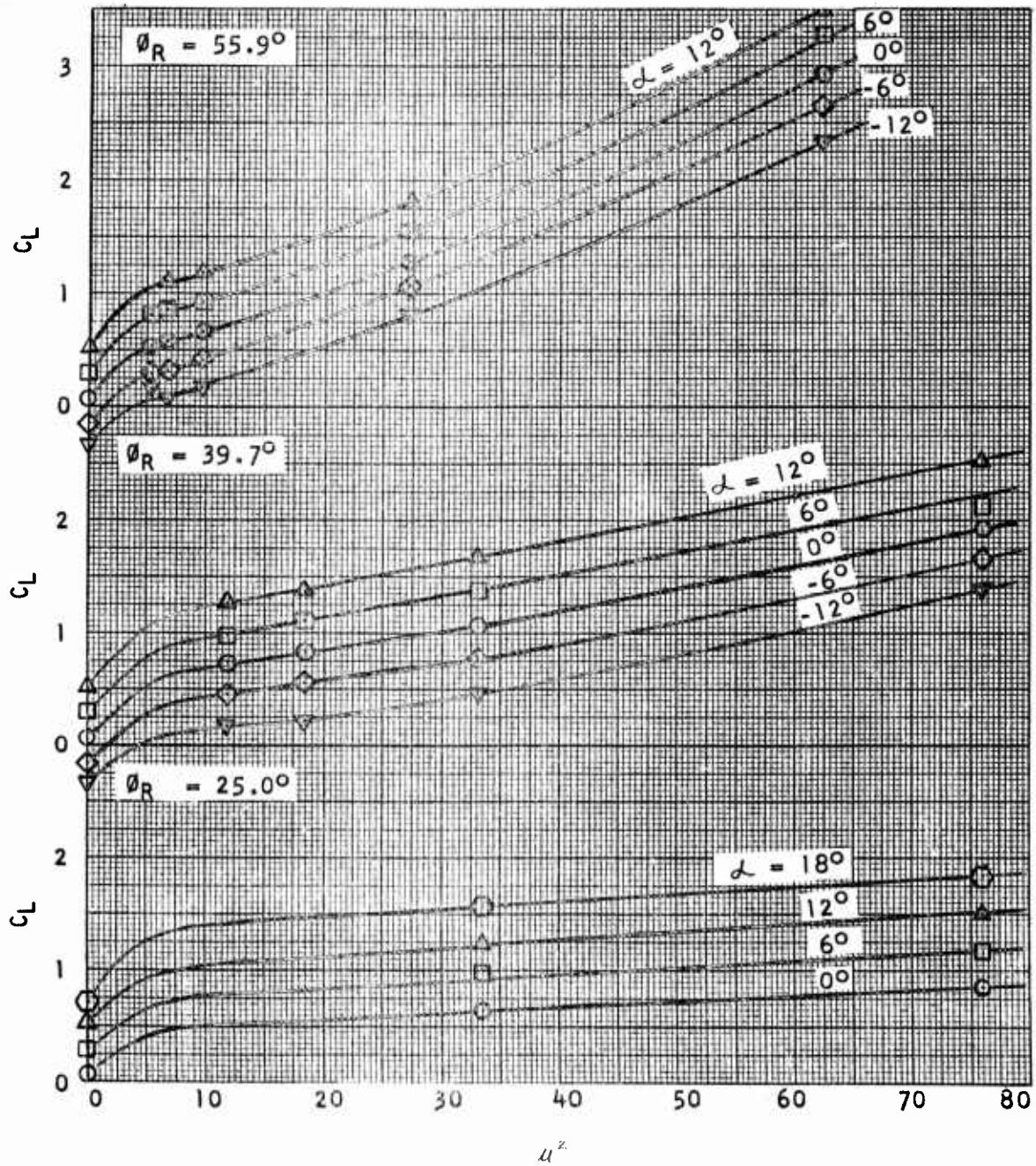


FIGURE 23

VERTODYNE MODEL TEST
FORWARD FLIGHT
WING DRAG COEFFICIENTS
$C_D$ VS $\mu^2$
FOR THREE FAN BLADE ANGLES

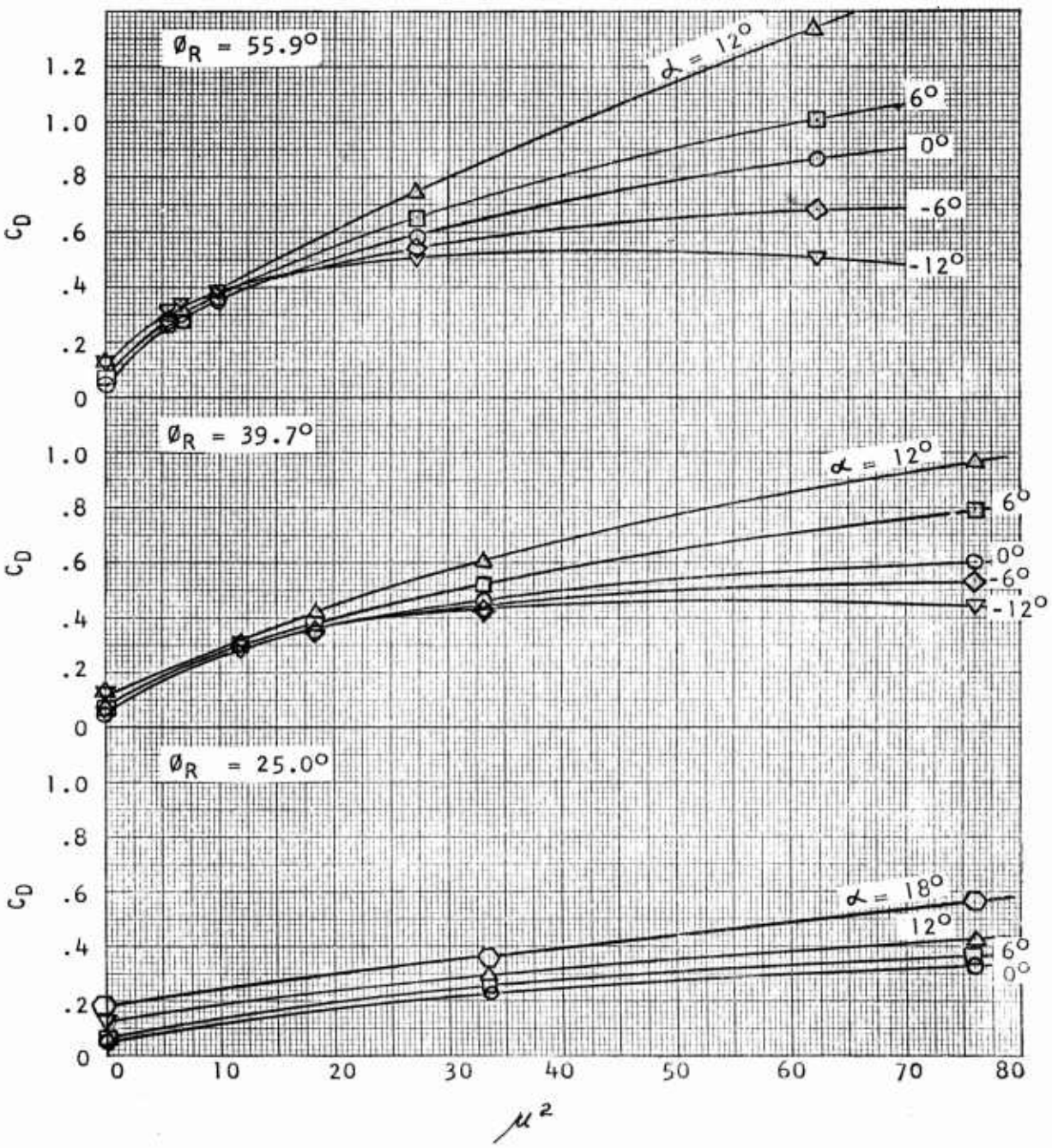


FIGURE 24

VERTODYNE MODEL TEST
FORWARD FLIGHT
WING DRAG COEFFICIENTS
$C_M$ VS $\alpha^2$
FOR THREE FAN BLADE ANGLES

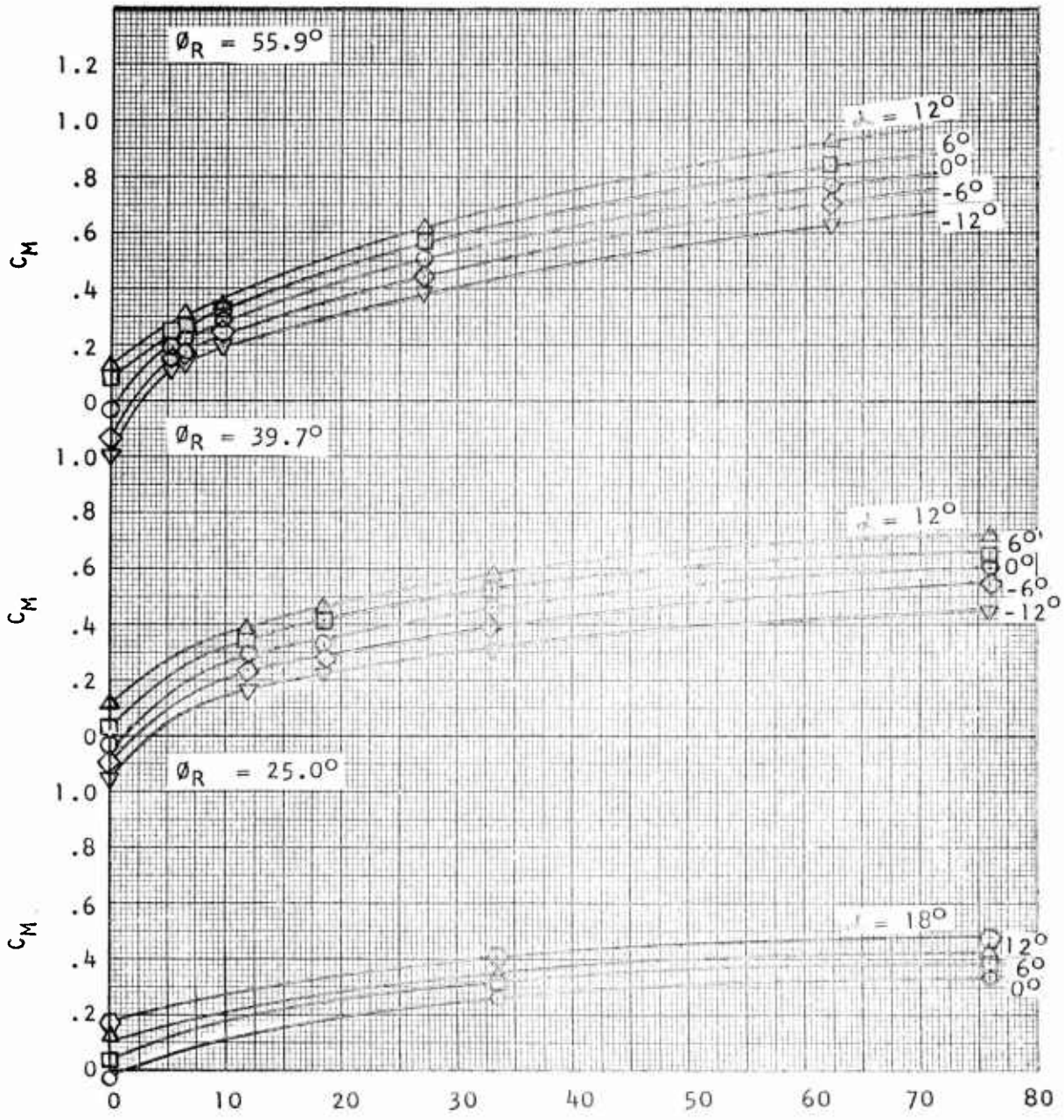


FIGURE 25

VERTODYNE MODEL TEST
FORWARD FLIGHT
FAN POWER COEFFICIENTS
$C_P$ VS $\mu^2$
MEDIUM PITCH FAN $\phi_R = 39.7°$

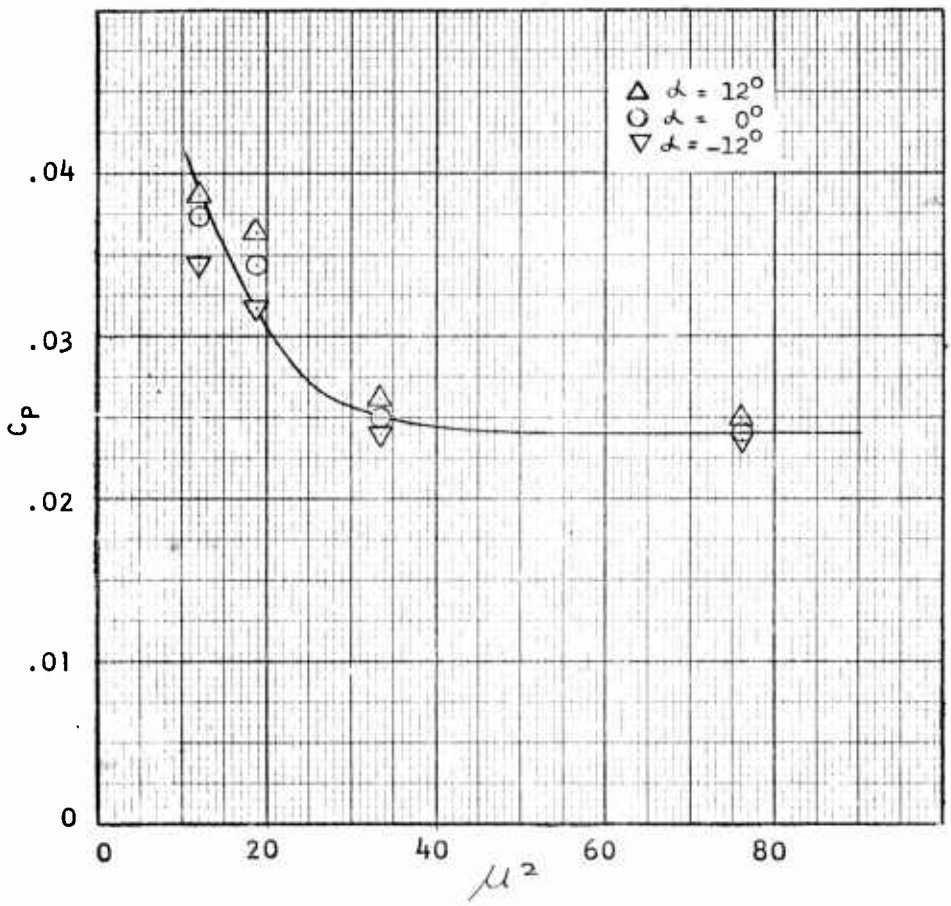


FIGURE 26

VERTODYNE MODEL TEST
FORWARD FLIGHT
LOCATION OF WING CENTER OF PRESSURE
HIGH PITCH FAN $\phi_R = 55.9°$

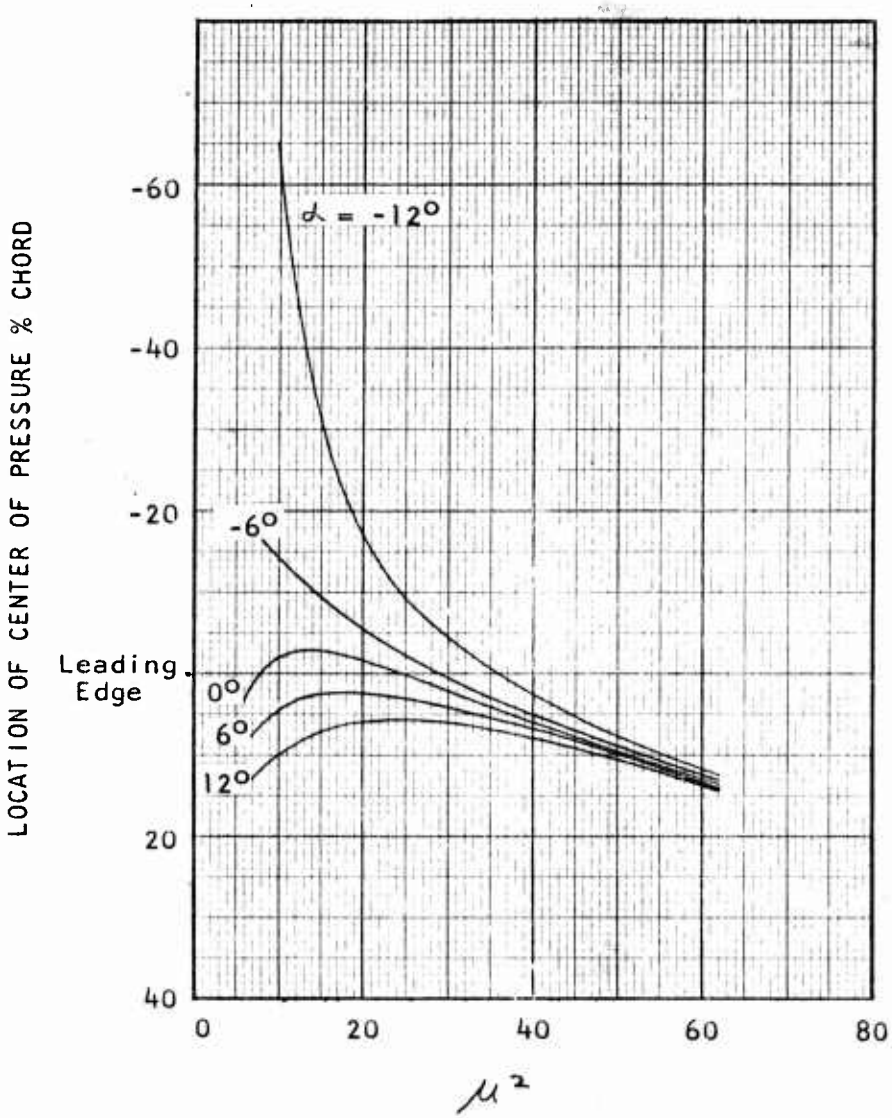


FIGURE 27

VERTODYNE MODEL TEST
FORWARD FLIGHT
LOCATION OF WING CENTER OF PRESSURE
MEDIUM PITCH FAN $R = 39.7^{o}$

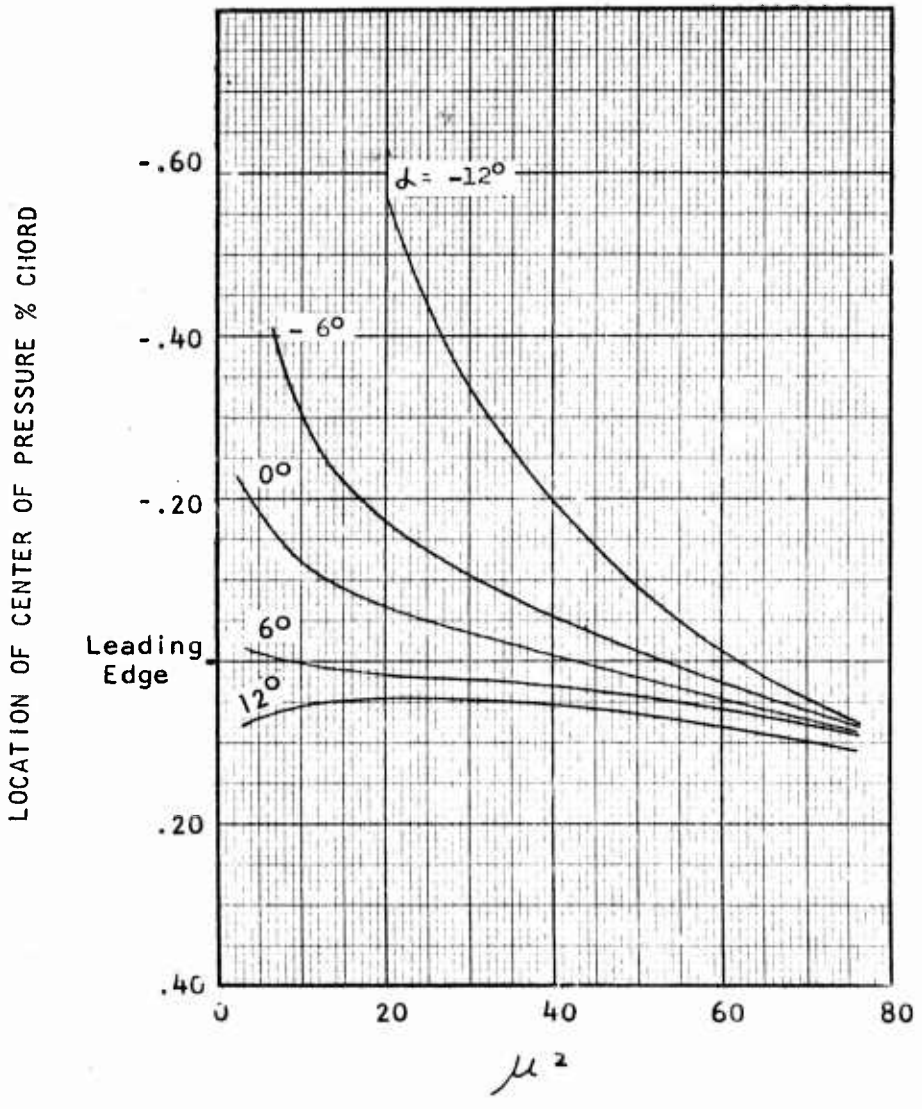


FIGURE 28

VERTODYNE MODEL TEST
FORWARD FLIGHT
LIFT COMPONENT OF FAN THRUST
$C_L$ VS $\mu^2$
FOR THREE FAN BLADE ANGLES

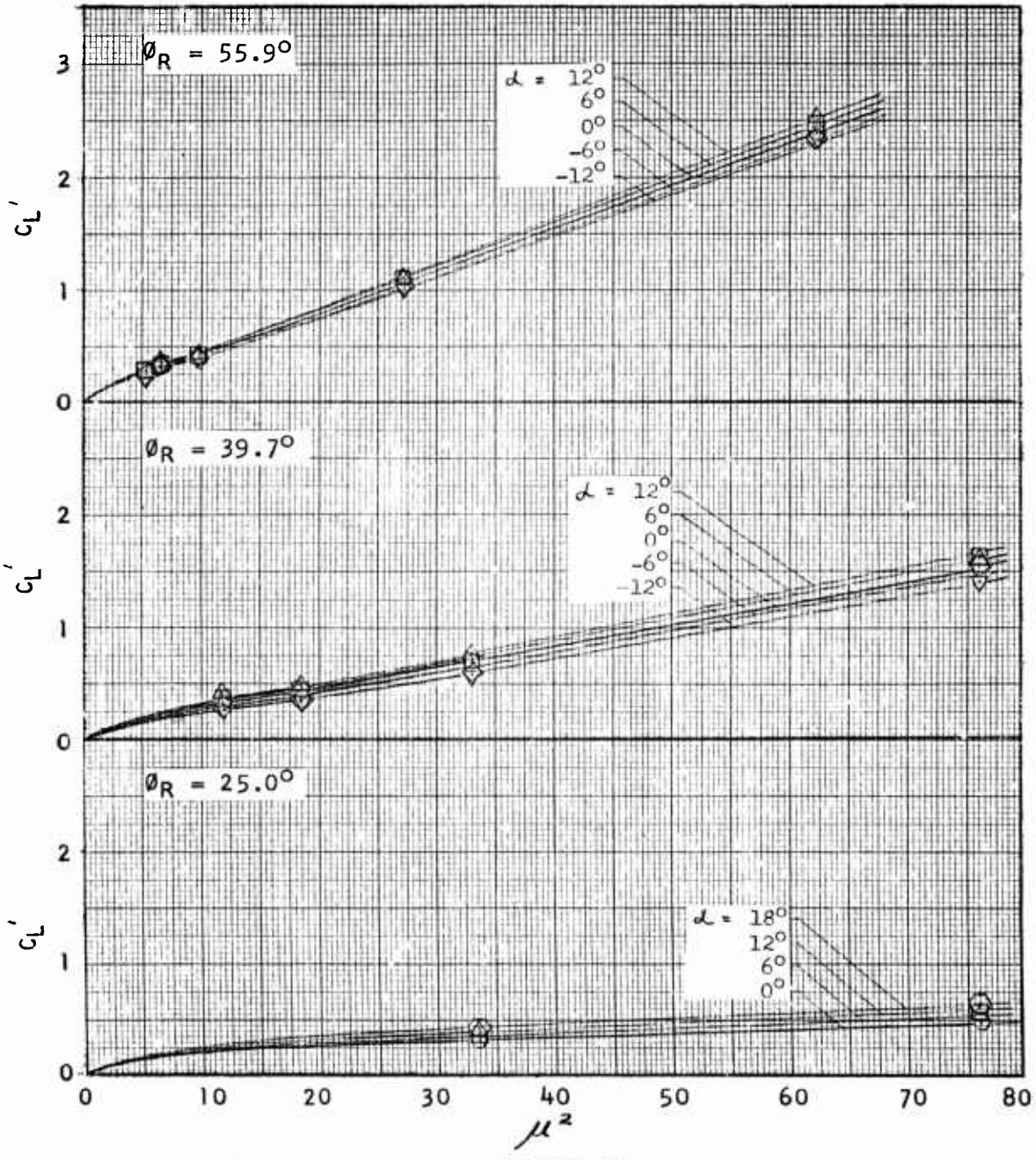


FIGURE 29

VERTODYNE MODEL TEST
FORWARD FLIGHT
DRAG COMPONENT OF FAN THRUST
$C_D$ VS $\mu^2$
FOR THREE FAN BLADE ANGLES

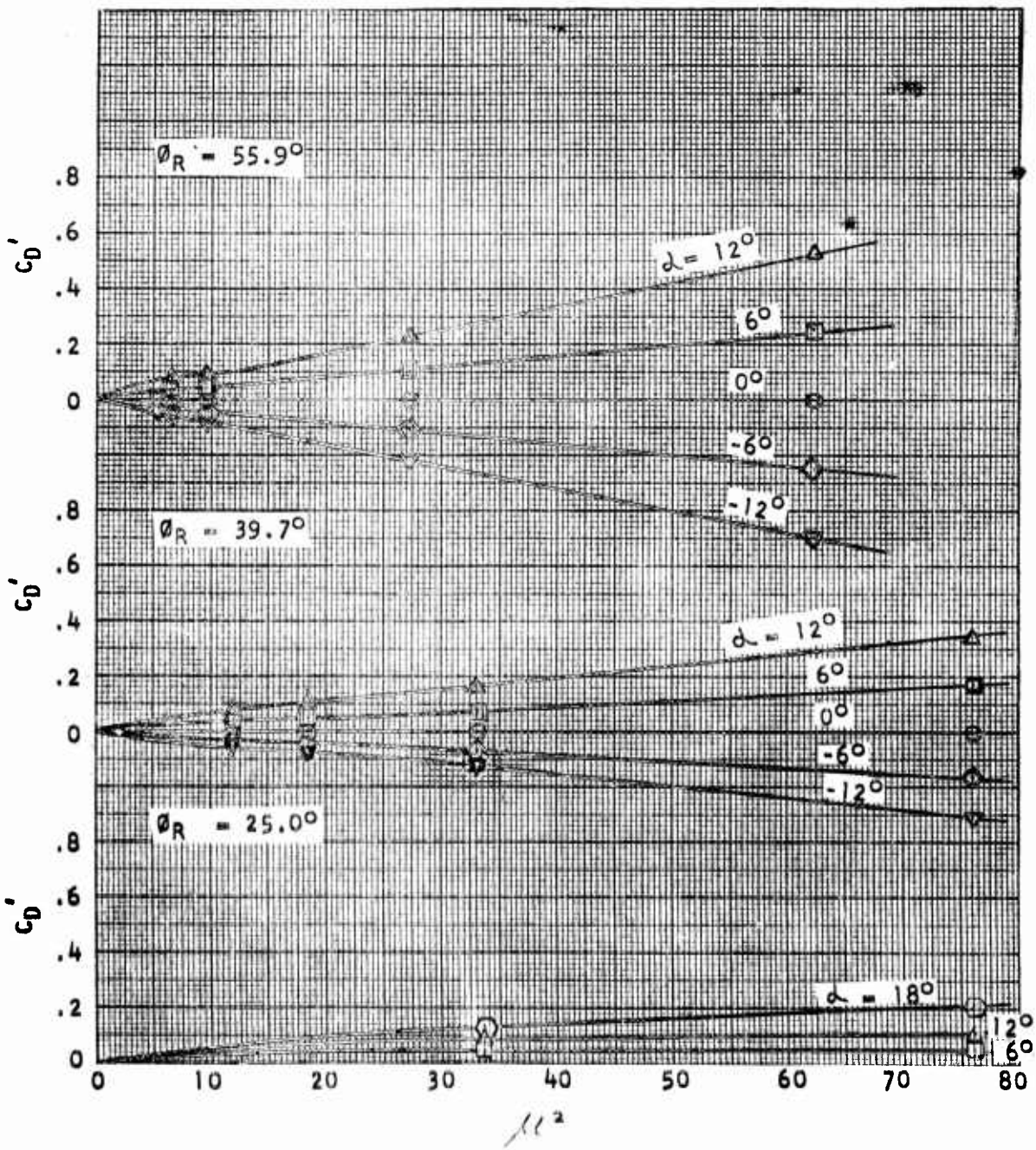


FIGURE 30

VERTODYNE SEMI-SPAN MODEL

WIND TUNNEL TESTS

FORWARD FLIGHT

MEDIUM PITCH FAN 10,000 RPM

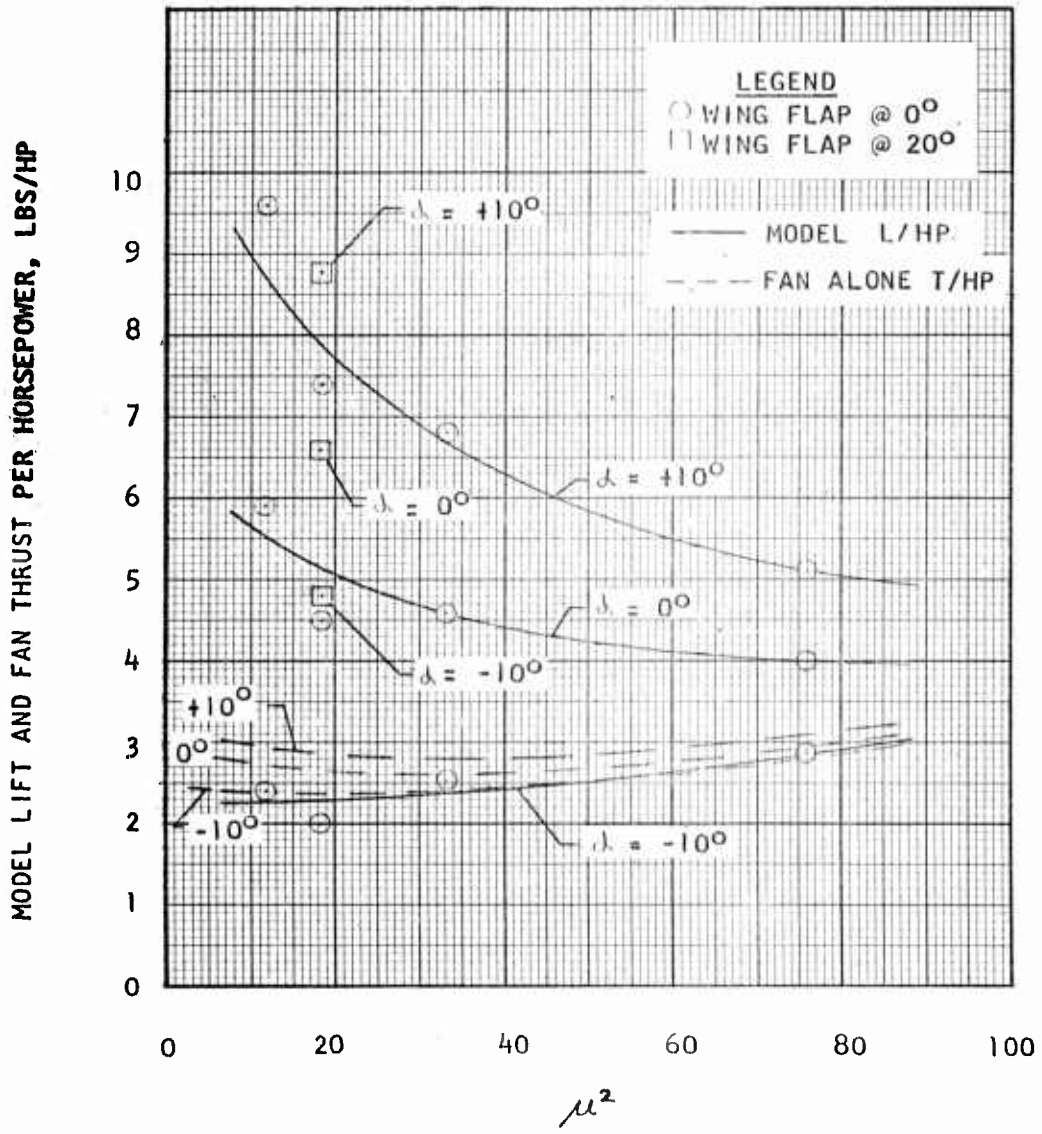


FIGURE 31

WING SURFACE PRESSURE DATA

REV

VERTODYNE MODEL TEST
WING SURFACE PRESSURES AS
A FUNCTION OF GROUND HEIGHT
MODEL STATIC ~ V = 0
INBOARD PRESSURE STATION

HIGH PITCH FAN 9060 RPM Ø root = 55.9°

PRESSURES NOT INDICATED ARE ZERO
PRESSURES ARE IN RELATION TO AMBIENT STATIC PRESSURE

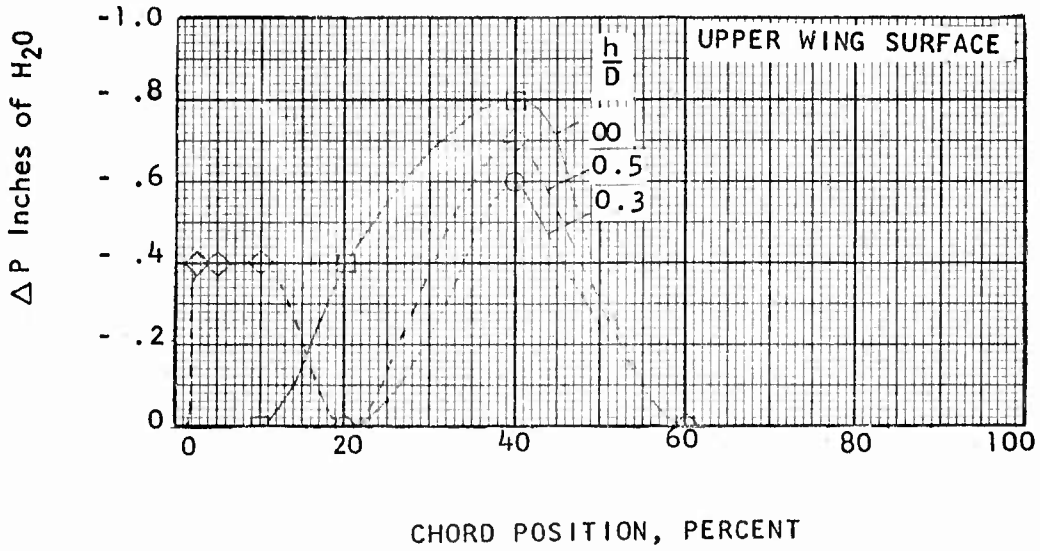


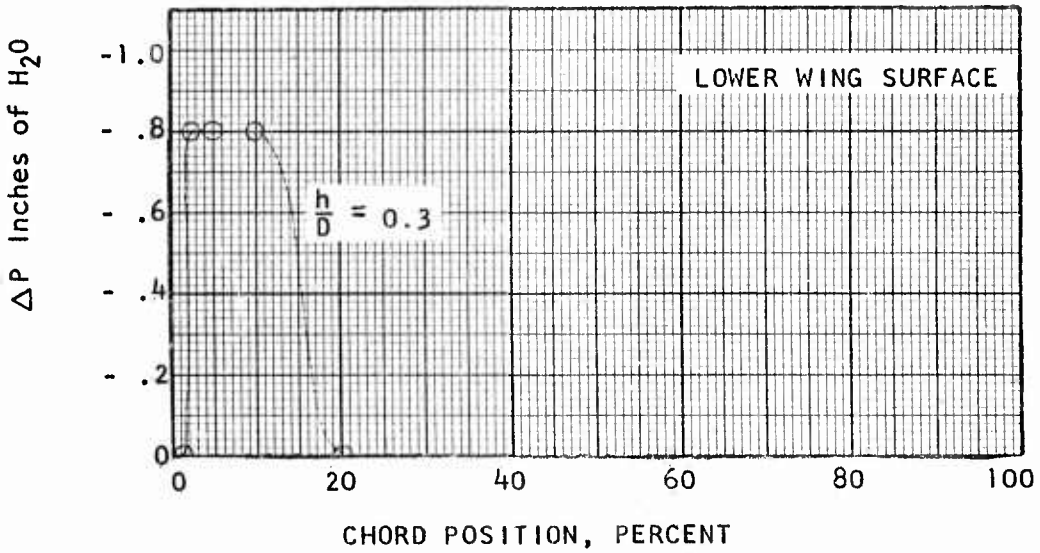


FIGURE 32

VERTODYNE MODEL TEST
WING SURFACE PRESSURES AS
A FUNCTION OF GROUND HEIGHT
MODEL STATIC $V_\infty$ = 0
FAN CENTERLINE PRESSURE STATION
HIGH PITCH FAN 9060 RPM Ø root = 55.9°

PRESSURES NOT INDICATED ARE ZERO
PRESSURES ARE IN RELATION TO AMBIENT STATIC PRESSURE

LEGEND

——————— $\frac{h}{D} = \infty$

– – – – – – – $\frac{h}{D} = 0.3$

UPPER WING SURFACE
ALL LOWER SURFACE PRESSURES ARE ZERO

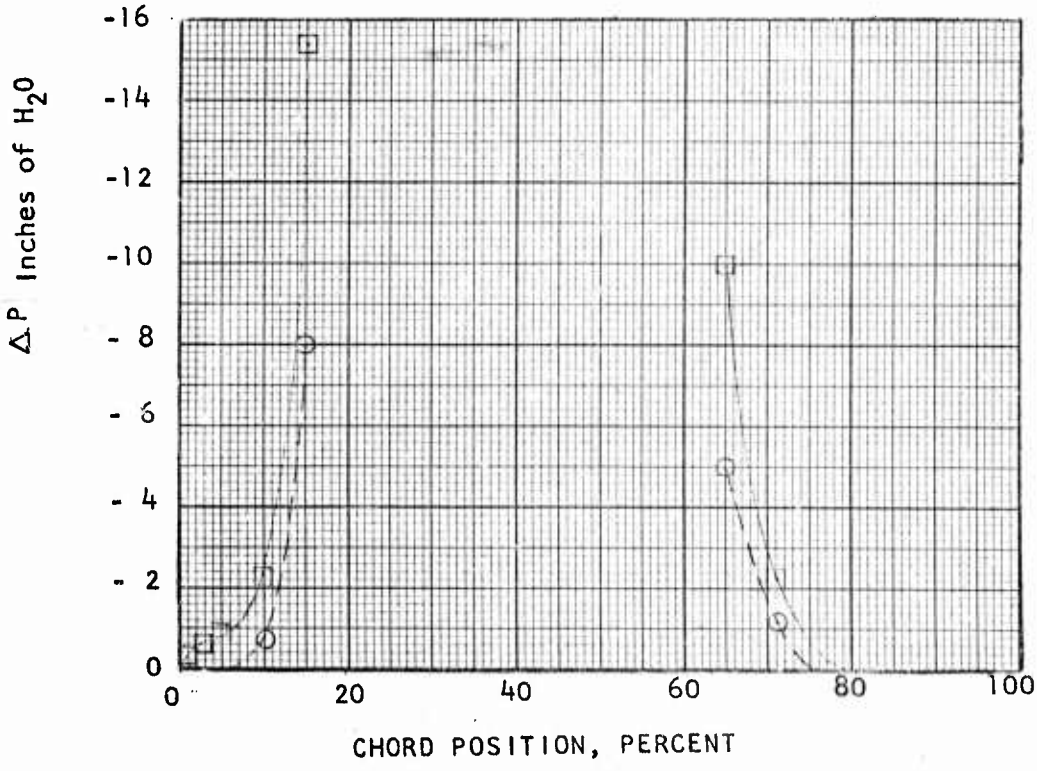


FIGURE 33

VERTODYNE MODEL TEST
WING SURFACE PRESSURES AS
A FUNCTION OF GROUND HEIGHT
MODEL STATIC ~ $V_j$ = 0
OUTBOARD PRESSURE STATION
HIGH PITCH FAN 9060 RPM Ø root = 55.9°

PRESSURES NOT INDICATED ARE ZERO
PRESSURES ARE IN RELATION TO AMBIENT STATIC PRESSURE

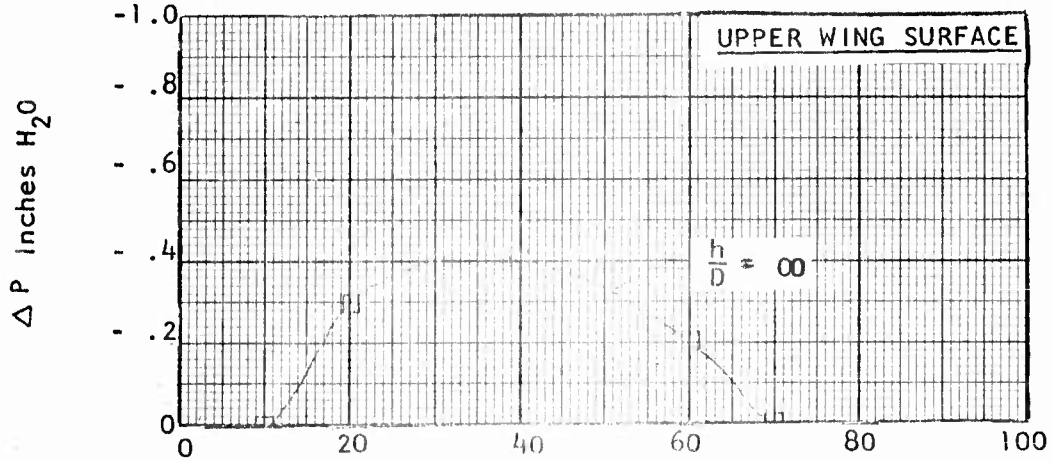


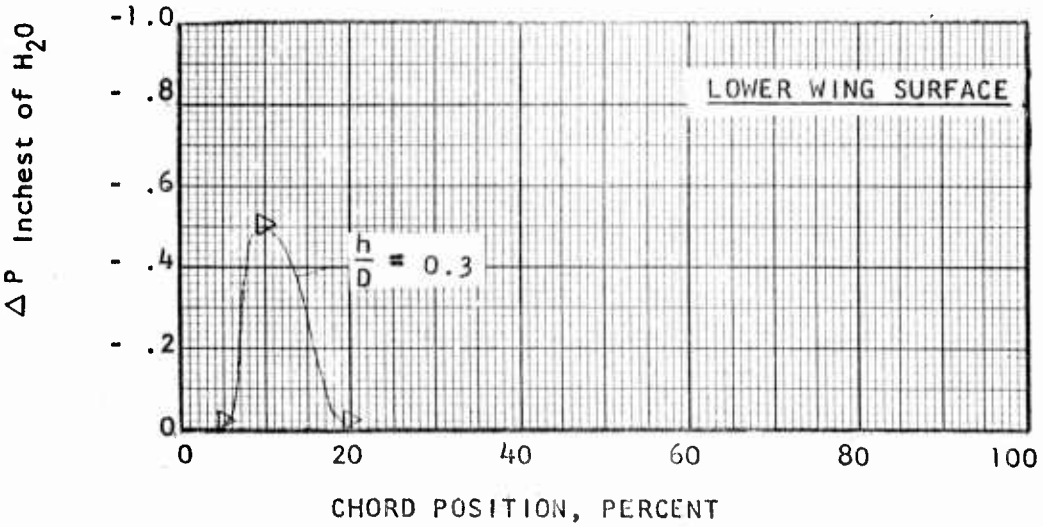


FIGURE 34

VERTODYNE MODEL TEST
FAN SHROUD PRESSURE AS
A FUNCTION OF GROUND HEIGHT
MODEL STATIC-V = 0
HIGH PITCH FAN 9060 RPM Ø root = 55.9°
FAN ROTATION COUNTERCLOCKWISE FROM ABOVE

LEGEND
□ $\frac{h}{D} = \infty$
▷ $\frac{h}{D} = 0.3$

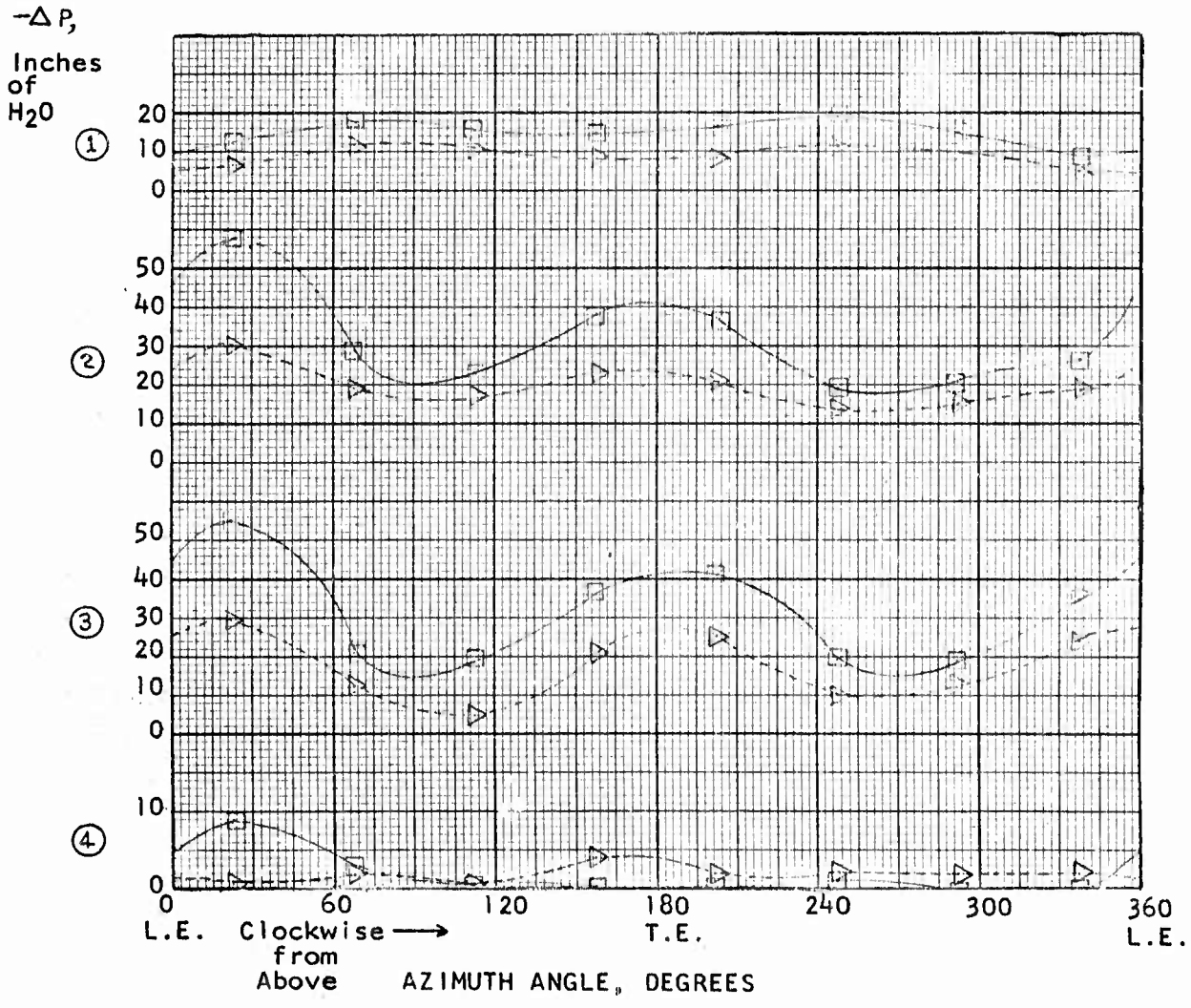


FIGURE 35

VERTODYNE MODEL TEST
WING SURFACE PRESSURES AS
A FUNCTION OF GROUND HEIGHT
MODEL STATIC ~ V = 0
INBOARD PRESSURE STATION
MEDIUM PITCH FAN 10000 RPM Ø root = 39.7°

PRESSURES NOT INDICATED ARE ZERO
PRESSURES ARE IN RELATION TO AMBIENT STATIC PRESSURE

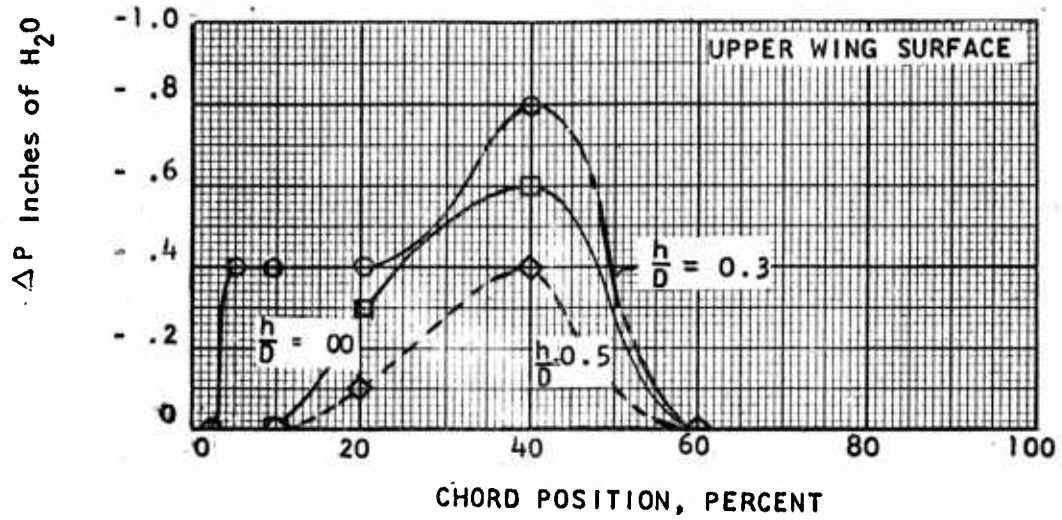


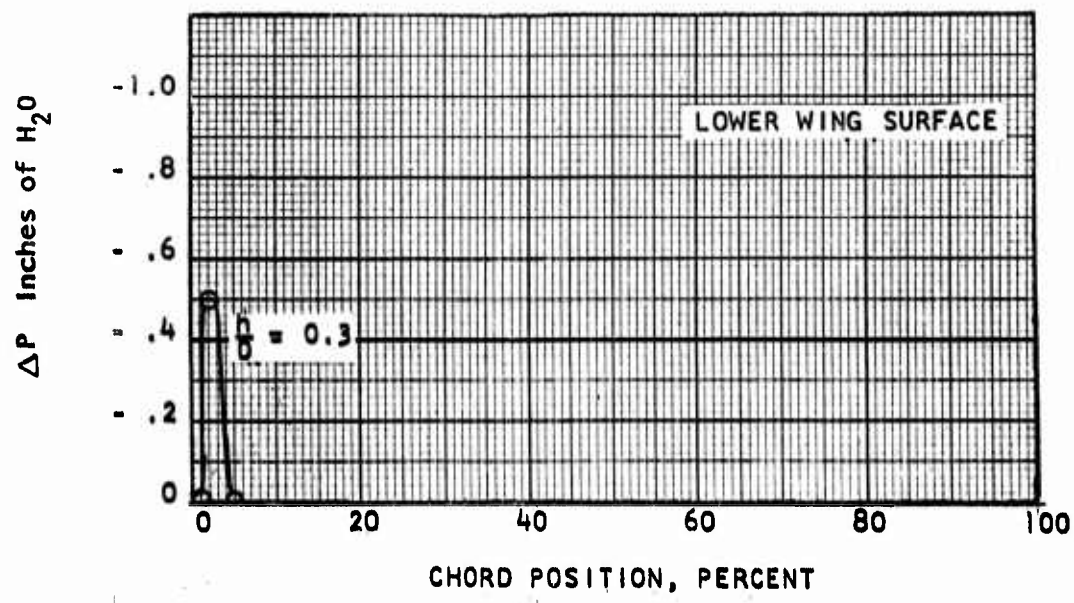


FIGURE 36

VERTODYNE MODEL TEST
WING SURFACE PRESSURES AS
A FUNCTION OF GROUND HEIGHT
MODEL STATIC ~ V = 0
FAN CENTERLINE PRESSURE STATION
MEDIUM PITCH FAN 10000 RPM Ø root = 39.7°

PRESSURES NOT INDICATED ARE ZERO
PRESSURES ARE IN RELATION TO AMBIENT STATIC PRESSURE

LEGEND

———————— h/D = ∞

– – – – – – – – h/D = 0.3

UPPER WING SURFACE

ALL LOWER SURFACE PRESSURES ARE ZERO

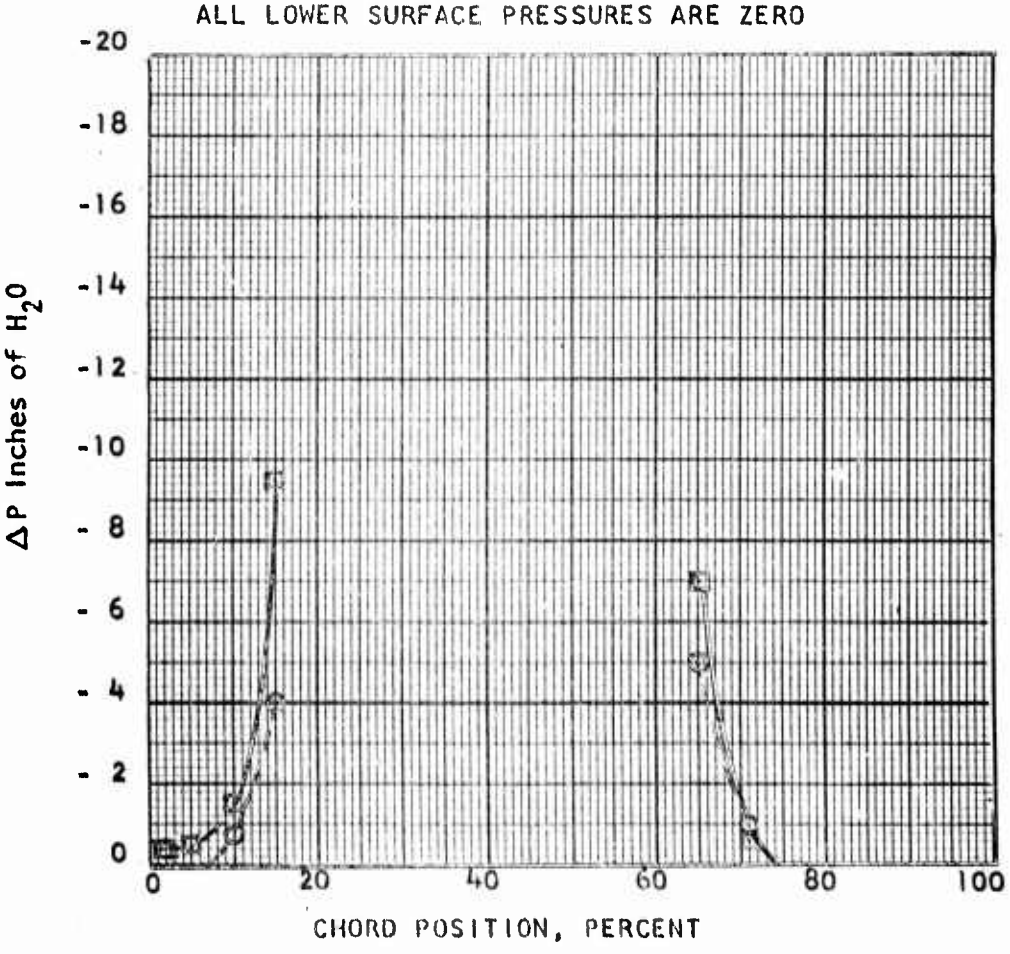


FIGURE 37

VERTODYNE MODEL TEST
WING SURFACE PRESSURES AS
A FUNCTION OF GROUND HEIGHT
MODEL STATIC $\sim$ V = 0
OUTBOARD PRESSURE STATION
MEDIUM PITCH FAN 10000 RPM Ø root = 39.7°

PRESSURES NOT INDICATED ARE ZERO
PRESSURES ARE IN RELATION TO AMBIENT STATIC PRESSURE.

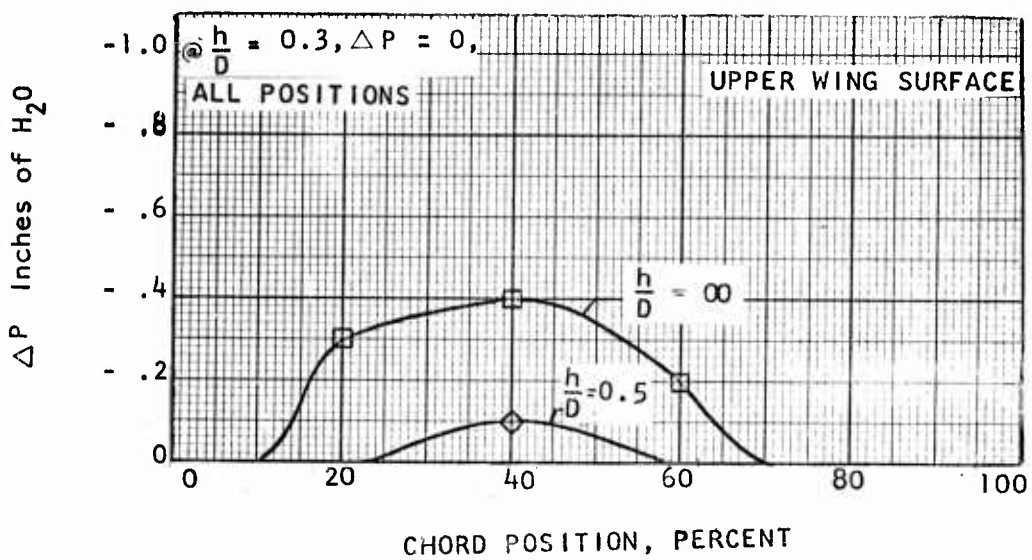


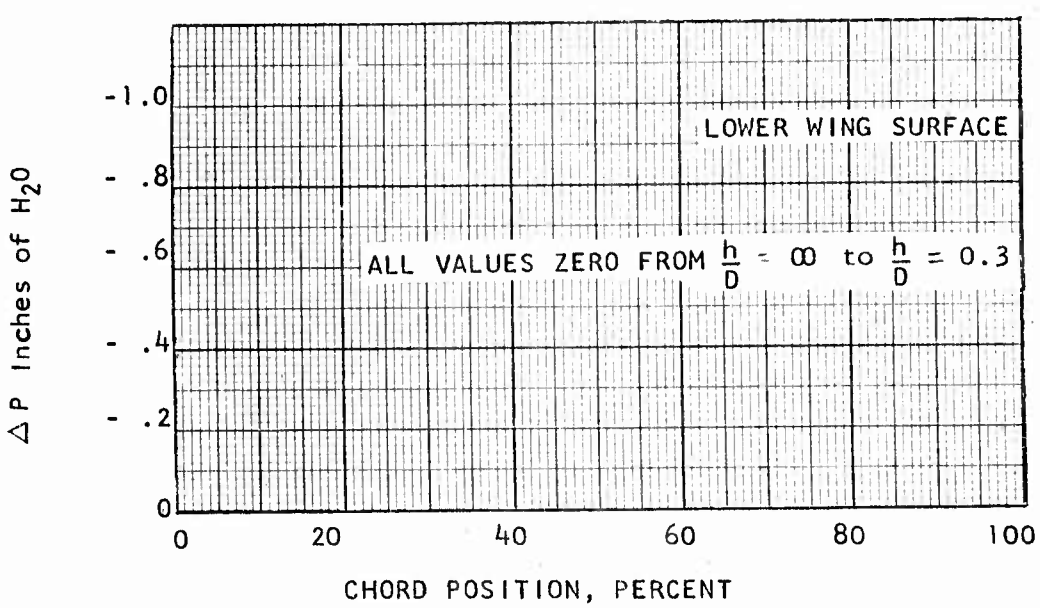


FIGURE 38

VERTODYNE MODEL TEST
FAN SHROUD PRESSURES AS
A FUNCTION OF GROUND HEIGHT
MODEL STATIC $\sim$ V = 0
MEDIUM PITCH FAN 10000 RPM $\phi$ root = 39.7°
FAN ROTATION COUNTERCLOCKWISE FROM ABOVE

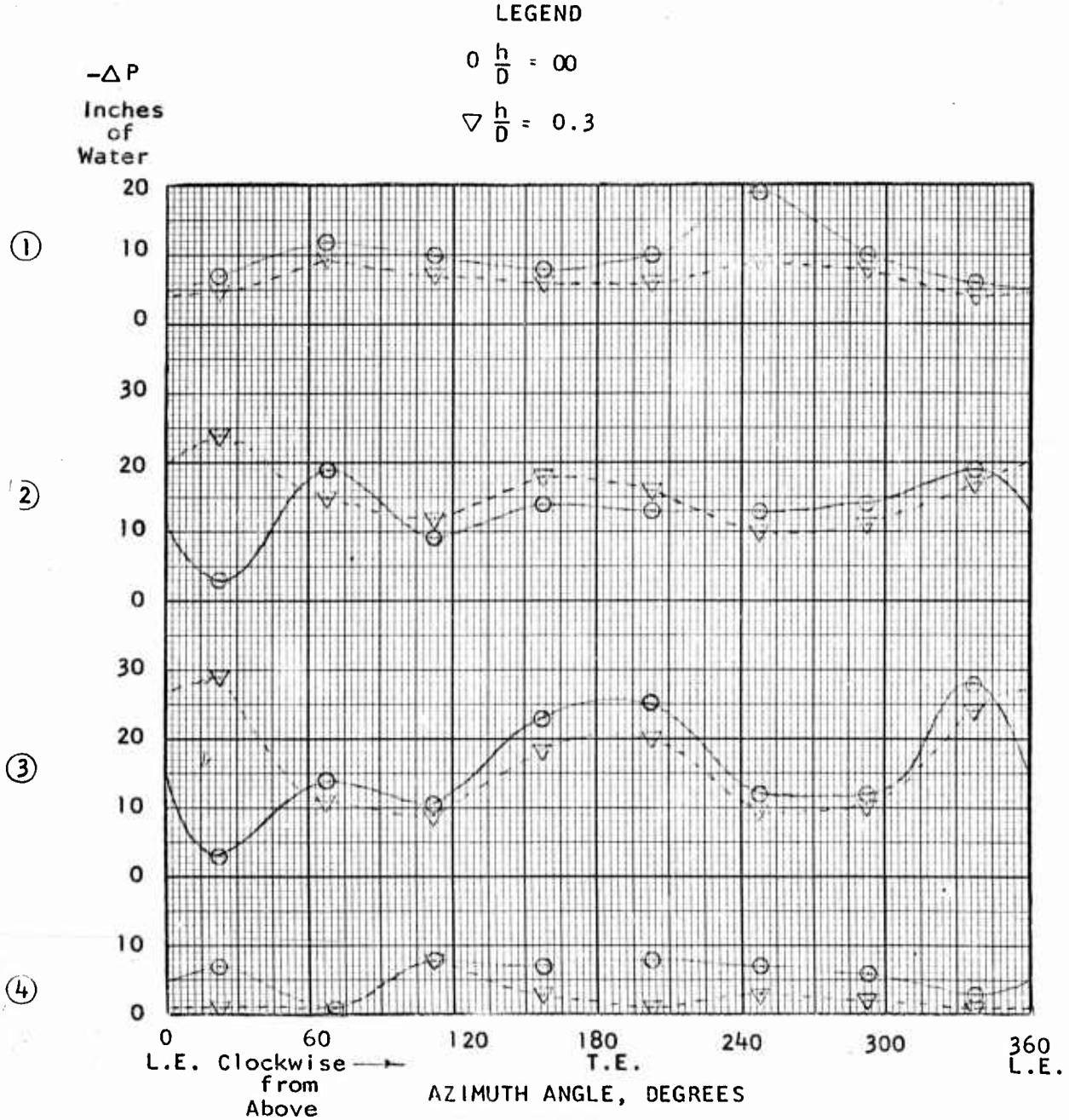


FIGURE 39

VERTODYNE PROGRAM

PRESSURE DISTRIBUTION

HOLE COVERED

V = 100 MPH

OUTBOARD PRESSURE STATION

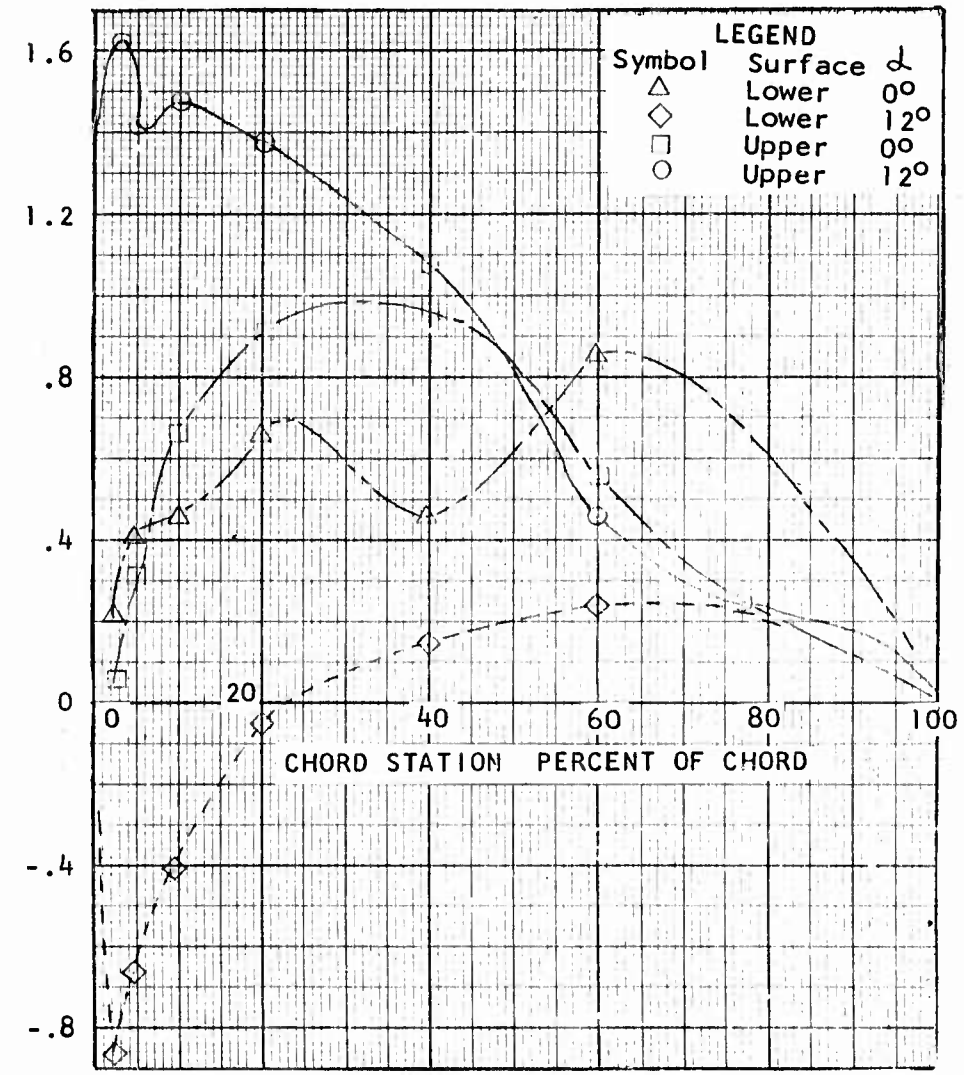


FIGURE 40

VERTODYNE PROGRAM

PRESSURE DISTRIBUTION

HOLE COVERED

OUTBOARD PRESSURE STATION

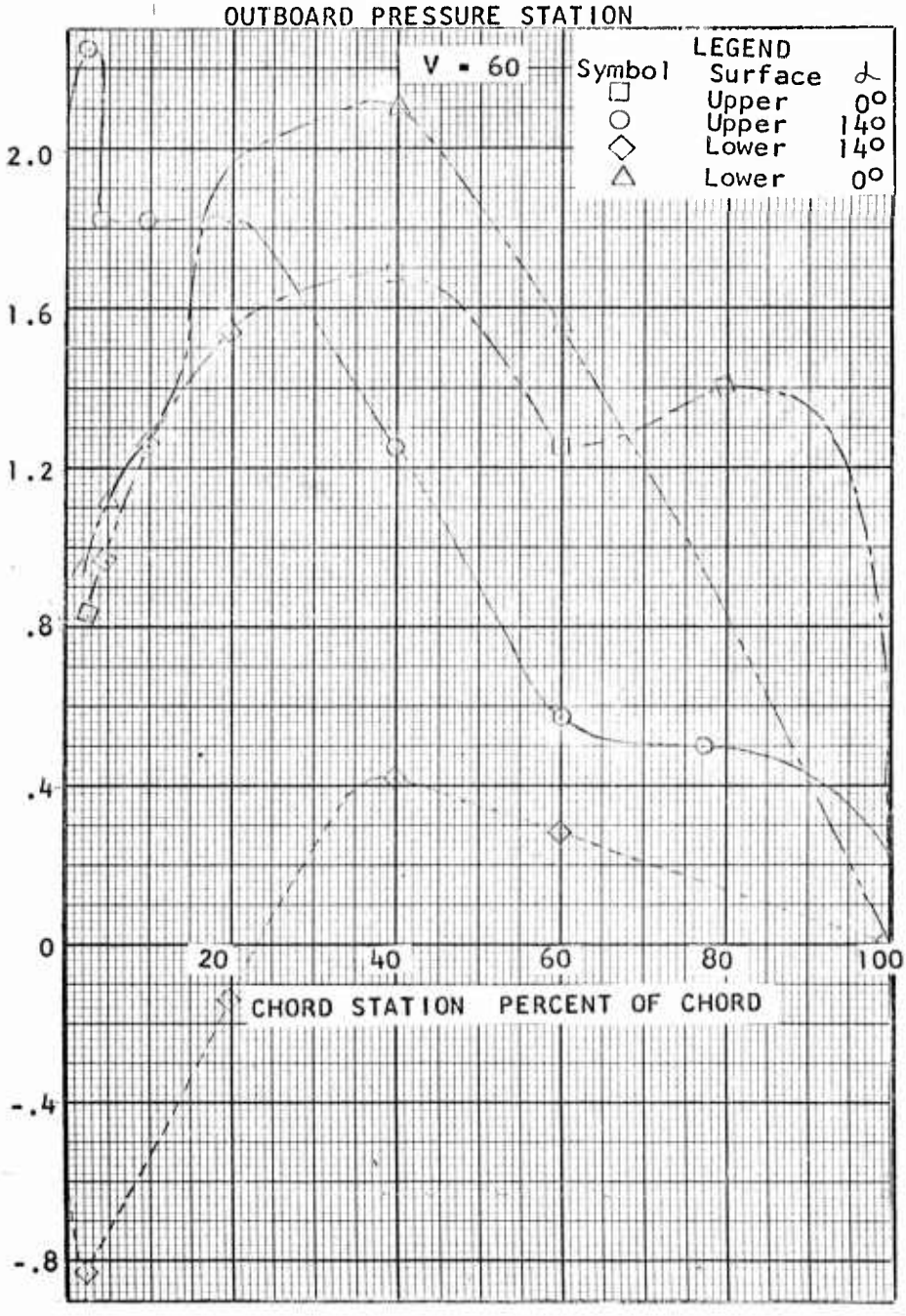


FIGURE 41

VERTODYNE PROGRAM

PRESSURE DISTRIBUTION

LOCKED ROTOR
NO POWER

V = 100 MPH

FAN CENTER PRESSURE STATION

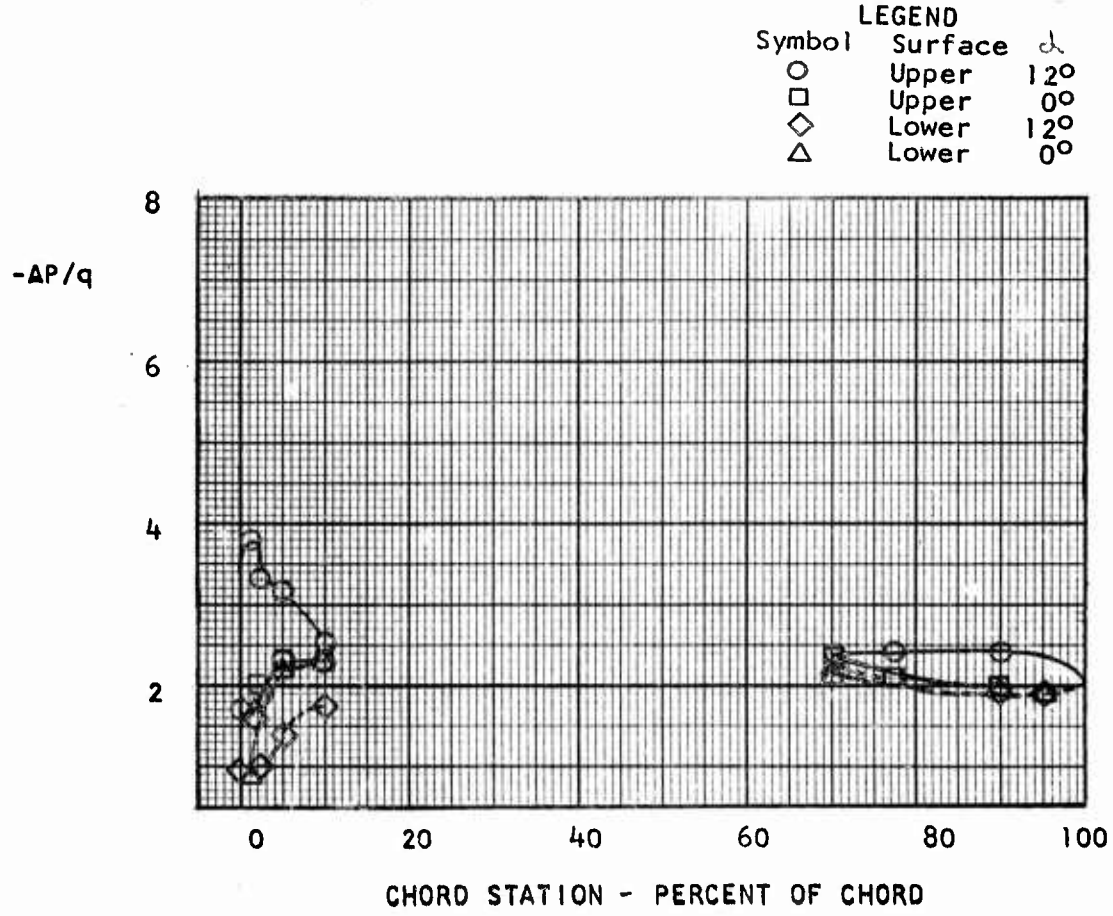


FIGURE 42

VERTODYNE PROGRAM

PRESSURE DISTRIBUTION

FAN CENTER PRESSURE STATION
HIGH PITCH FAN
9060 RPM $\phi_{Root} = 55.9^{o}$
V = 120

LEGEND

| Symbol | Surface | $\alpha$ |
|---|---|---|
| □ | Upper | 2° |
| ○ | Upper | 14° |
| ◇ | Lower | 14° |
| △ | Lower | 2° |

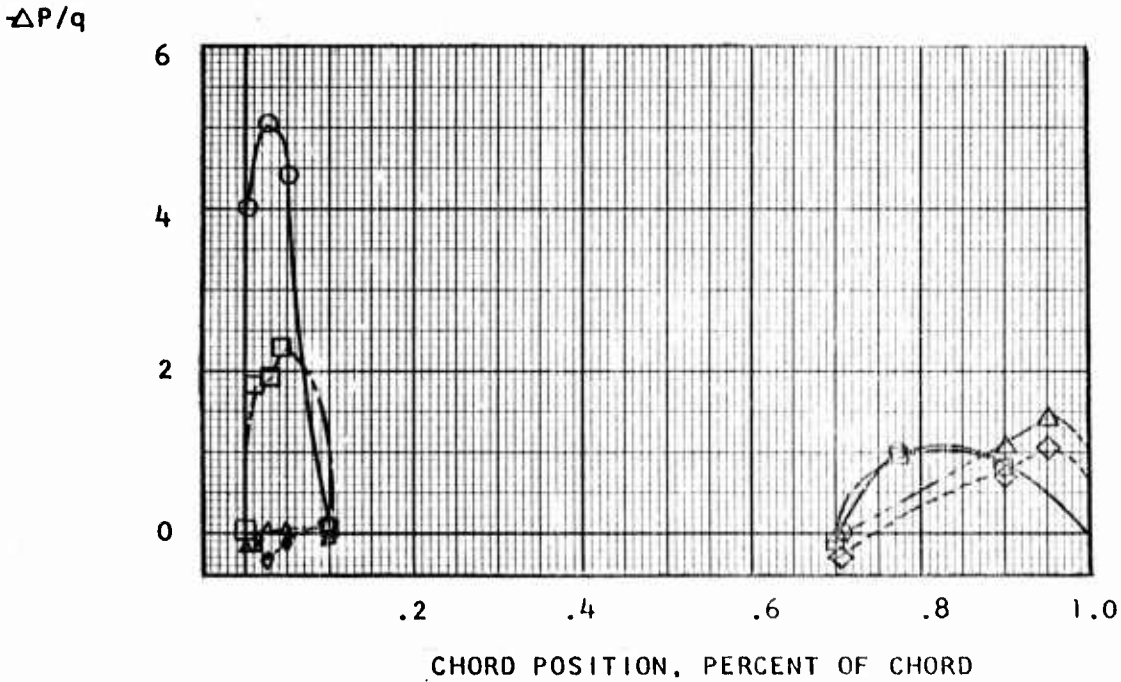


FIGURE 43

VERTODYNE PROGRAM

PRESSURE DISTRIBUTION

HIGH PITCH FAN 9060 RPM

$\phi_{Root} = 39.7^{\circ}$

V = 100 MPH

FAN CENTER PRESSURE STATION

| LEGEND | | |
|---|---|---|
| Symbol | Surface | $\alpha$ |
| □ | Upper | 0° |
| ○ | Upper | 14° |
| ◇ | Lower | 14° |
| △ | Lower | 0° |

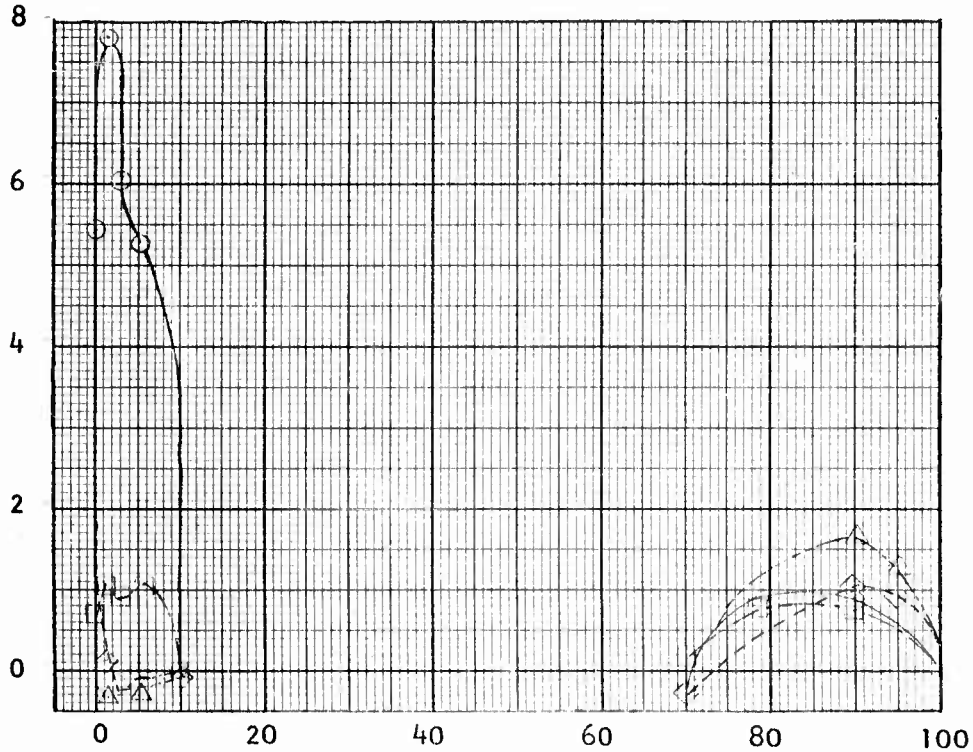


FIGURE 44

VERTODYNE PROGRAM
PRESSURE DISTRIBUTION
FAN CENTER PRESSURE STATION
HIGH PITCH FAN
9060 RPM $\phi_{Root} = 55.9^{o}$
V = 60

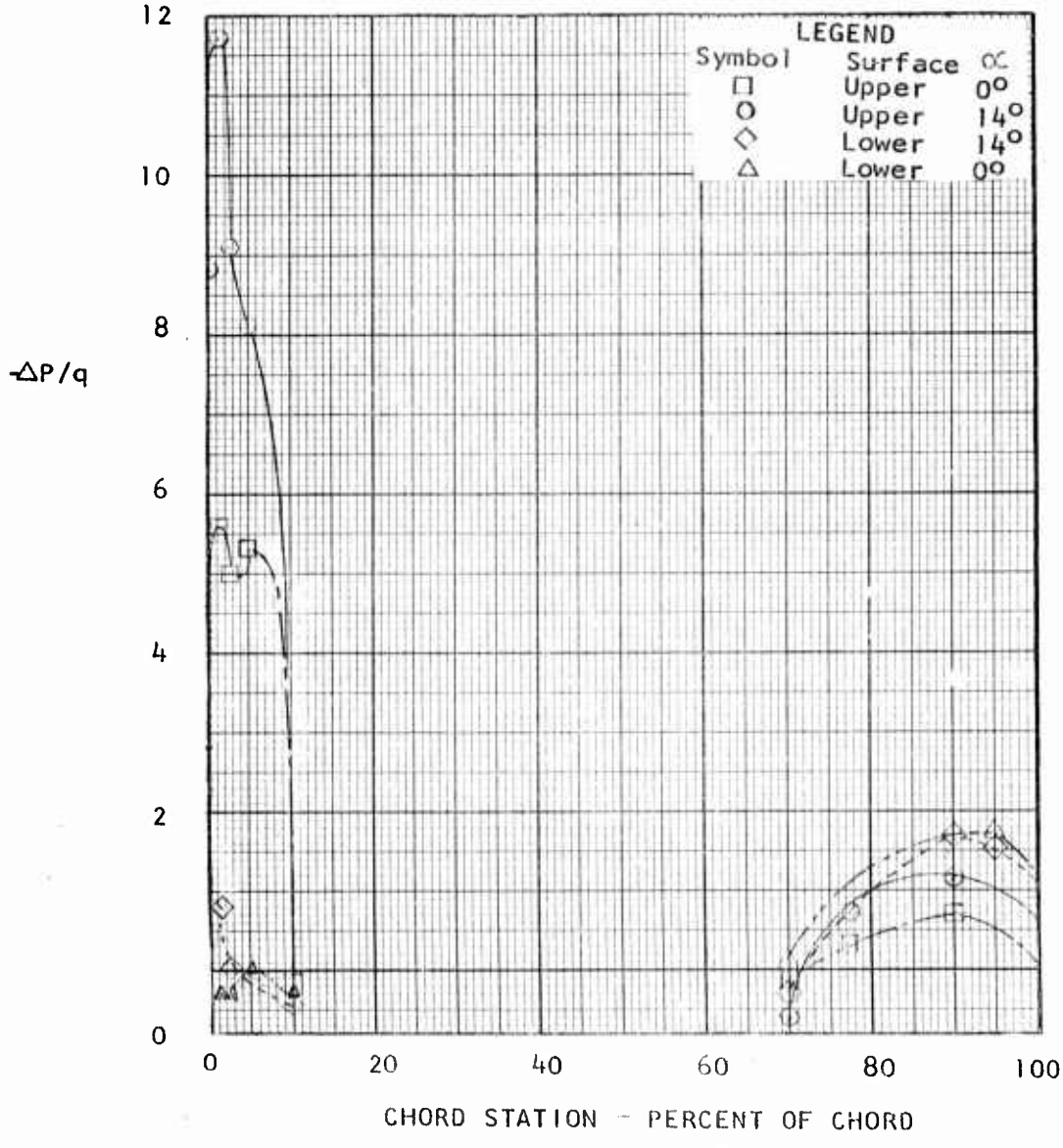


FIGURE 45

VERTODYNE PROGRAM

PRESSURE DISTRIBUTION

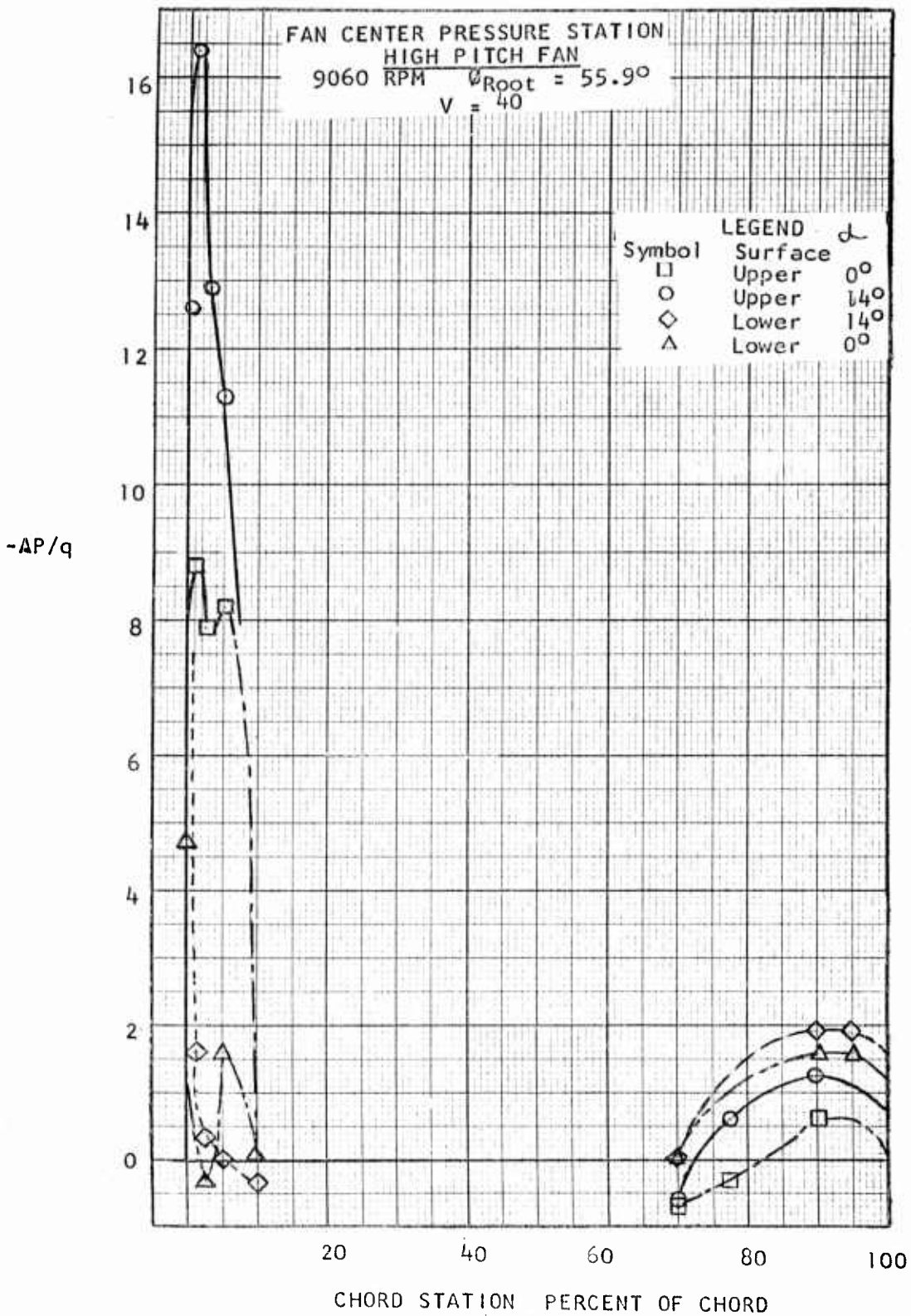


FIGURE 46

VERTODYNE PROGRAM
SHROUD PRESSURE DISTRIBUTION
HIGH PITCH FAN 9060 RPM
RUN 13 V = 100 $\phi_{Root}$ = 55.9°

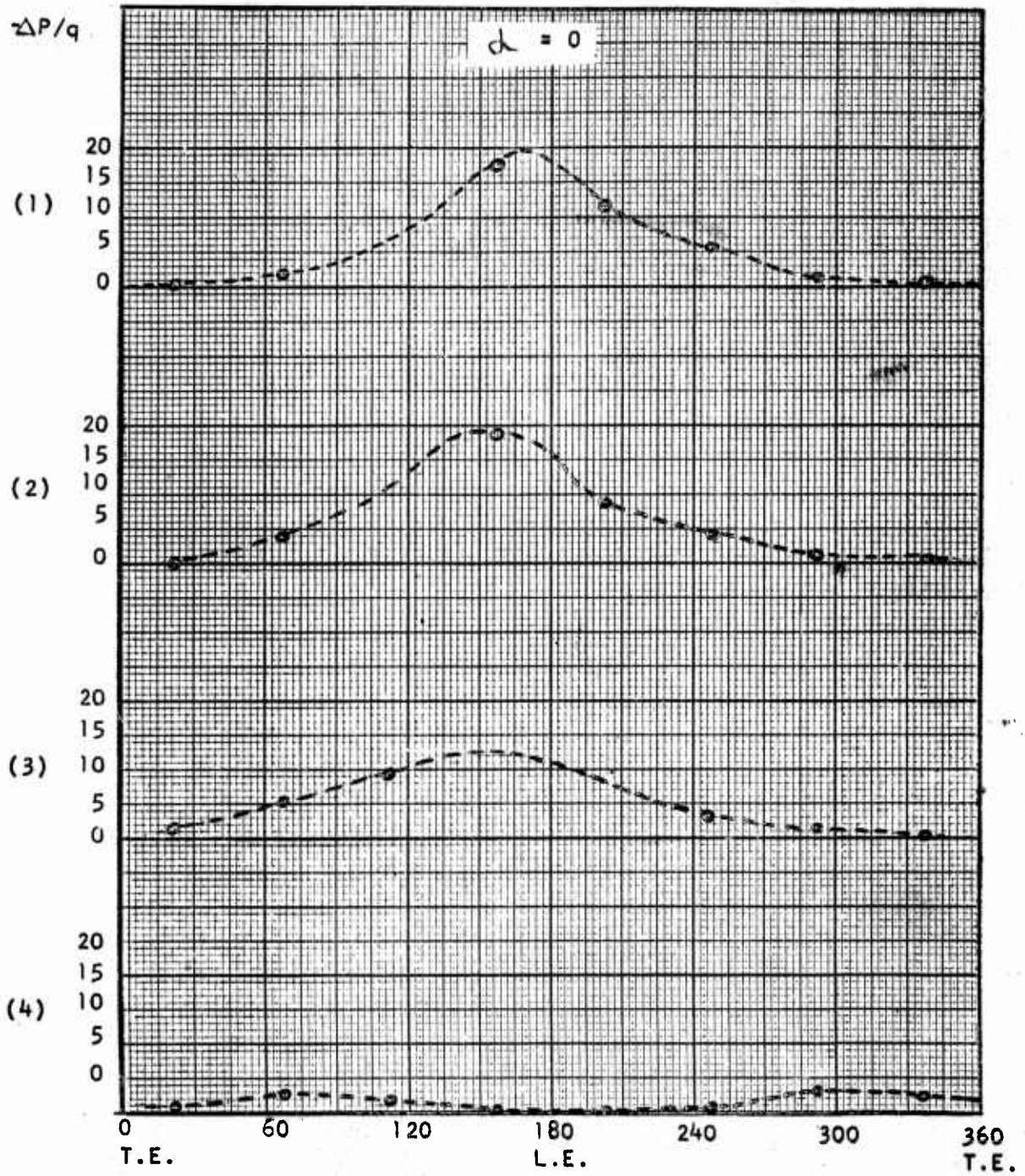


FIGURE 47

VERTODYNE PROGRAM
PRESSURE DISTRIBUTION
FAN CENTER PRESSURE STATION
HIGH PITCH FAN
9060 RPM $\phi_{Root} = 55.9^{\circ}$
V = 100

$\delta_{f_w} = 20^{\circ}$

| Symbol | Surface | $\alpha$ |
|---|---|---|
| □ | Upper | 2° |
| ○ | Upper | 14° |
| ◇ | Lower | 14° |
| △ | Lower | 2° |

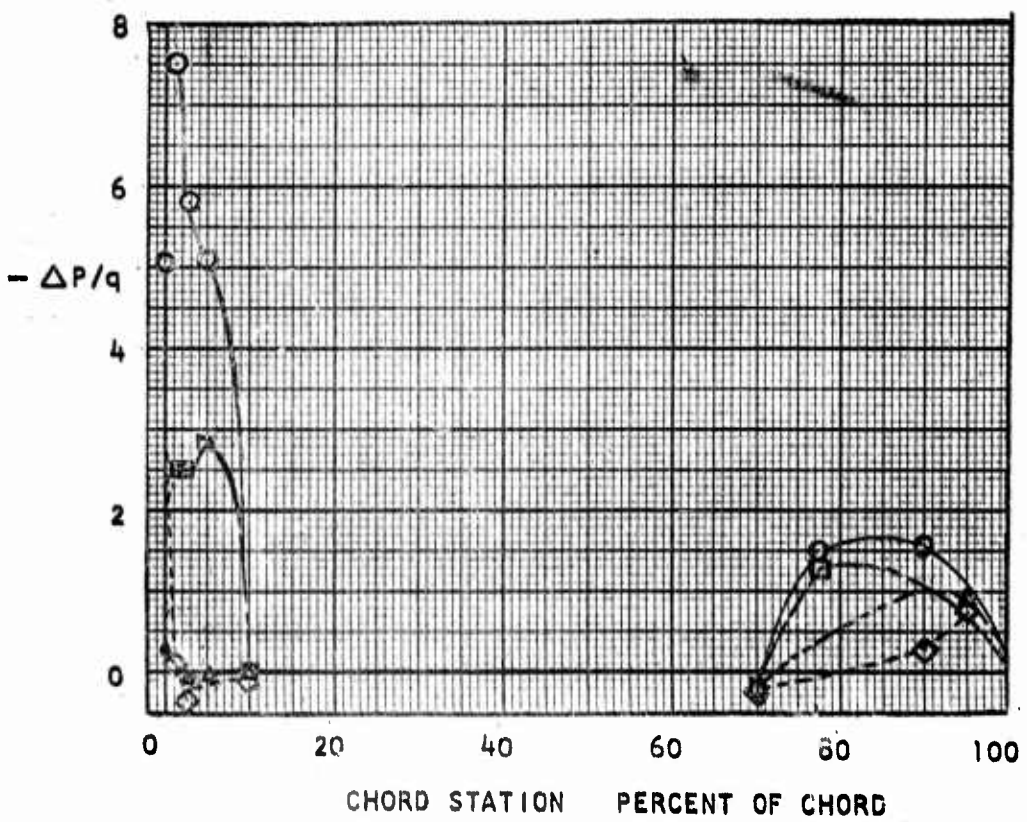


FIGURE 48

VERTODYNE PROGRAM

PRESSURE DISTRIBUTION

FAN CENTER PRESSURE STATION

HIGH PITCH FAN

9060 RPM $\quad \phi_{Root} = 55.9^{\circ}$

V = 100

$\delta_{f_f} = 40^{\circ}$

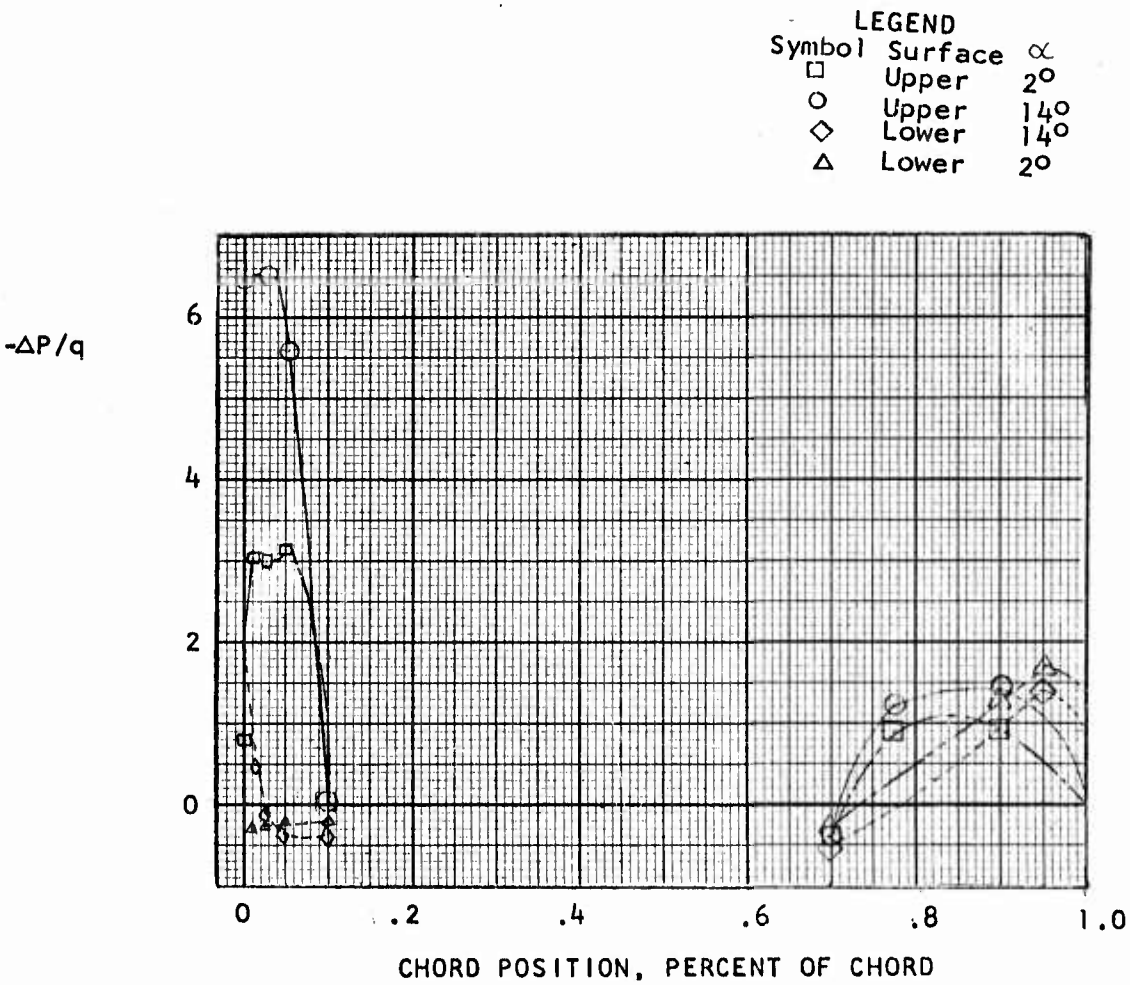


FIGURE 49

VERTODYNE PROGRAM

PRESSURE DISTRIBUTION

MEDIUM PITCH FAN

10000 RPM

$\phi_{Root} = 39.7^{\circ}$

V = 100 MPH

FAN CENTER PRESSURE STATION

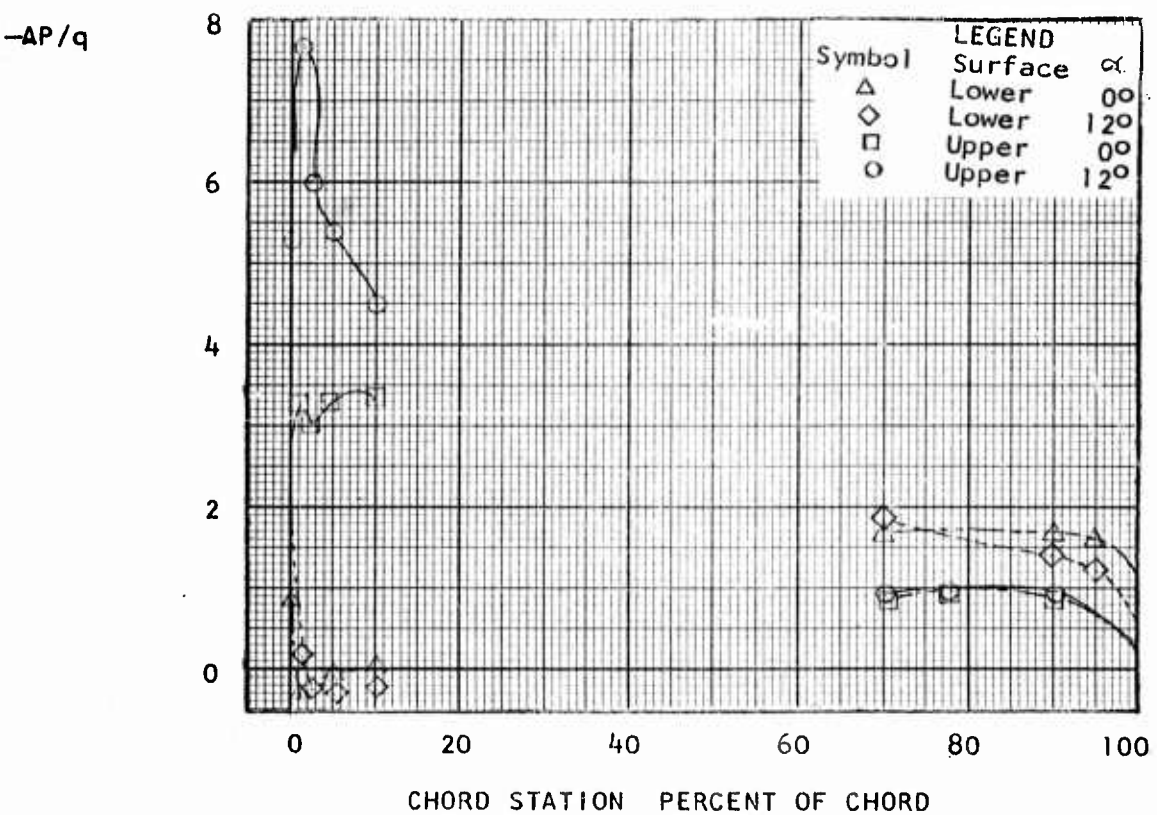


FIGURE 50

VERTODYNE PROGRAM

PRESSURE DISTRIBUTION

MEDIUM PITCH FAN

10000 RPM $\phi_{Root} = 39.7^{\circ}$

FAN CENTER PRESSURE STATION

V = 80

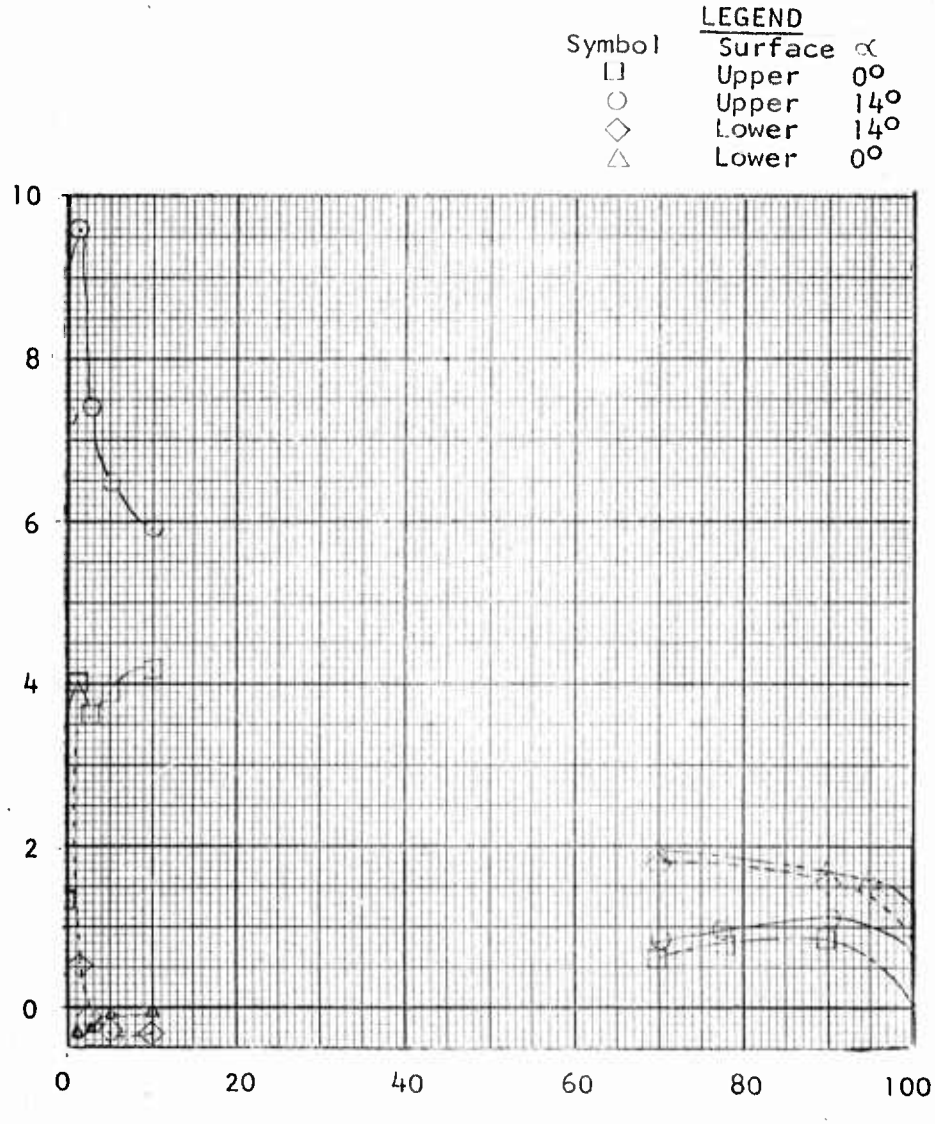


FIGURE 51

VERTODYNE PROGRAM

PRESSURE DISTRIBUTION

FAN CENTER PRESSURE STATION
MEDIUM PITCH FAN
10000 RPM $\phi_{Root} = 39.7^{\circ}$
V = 60 MPH

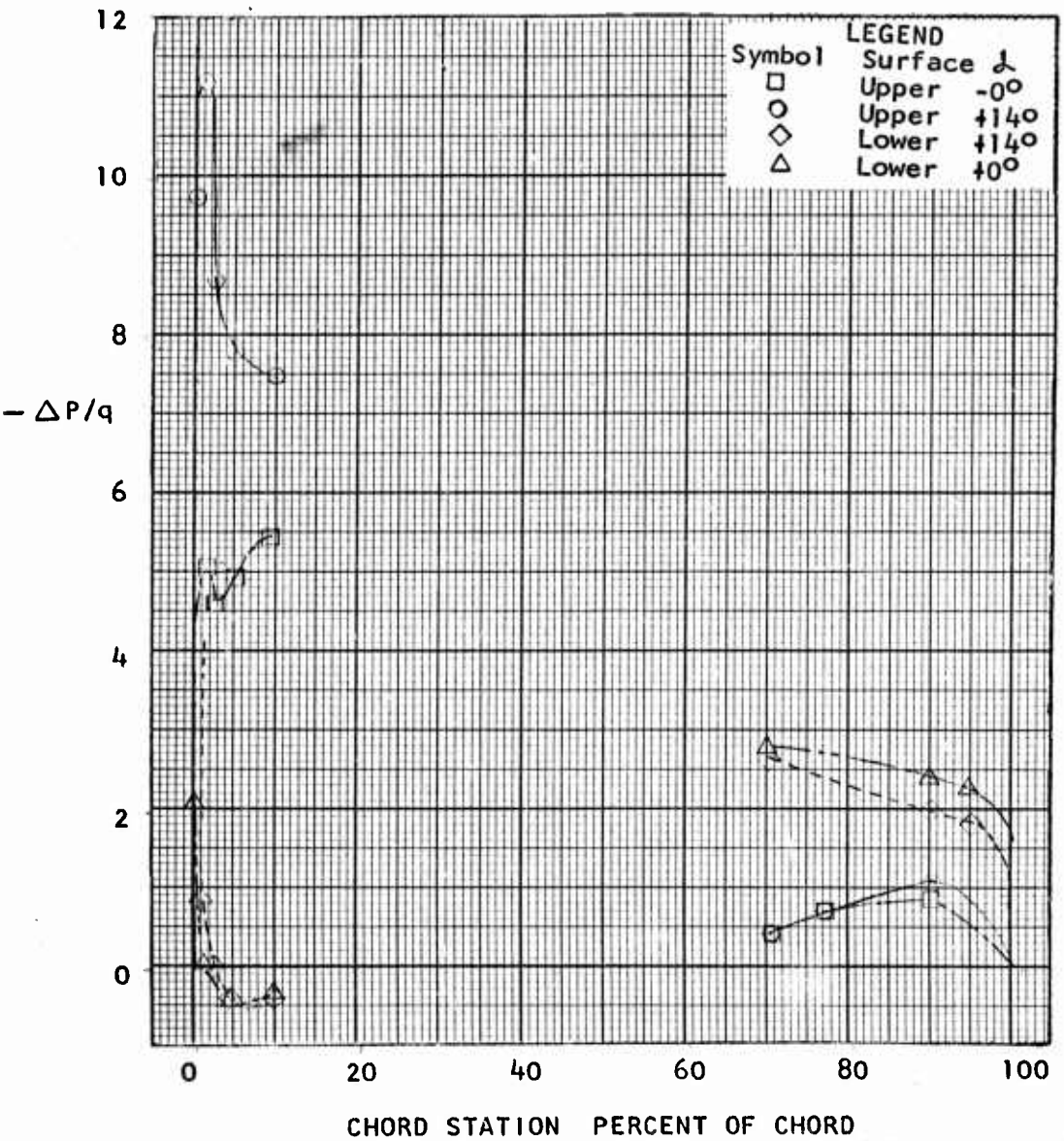


FIGURE 52

VERTODYNE PROGRAM
PRESSURE DISTRIBUTION
MEDIUM PITCH FAN
10,000 RPM $\phi_{Root}$ = 39.7°
FAN CENTER PRESSURE STATION
V = 40

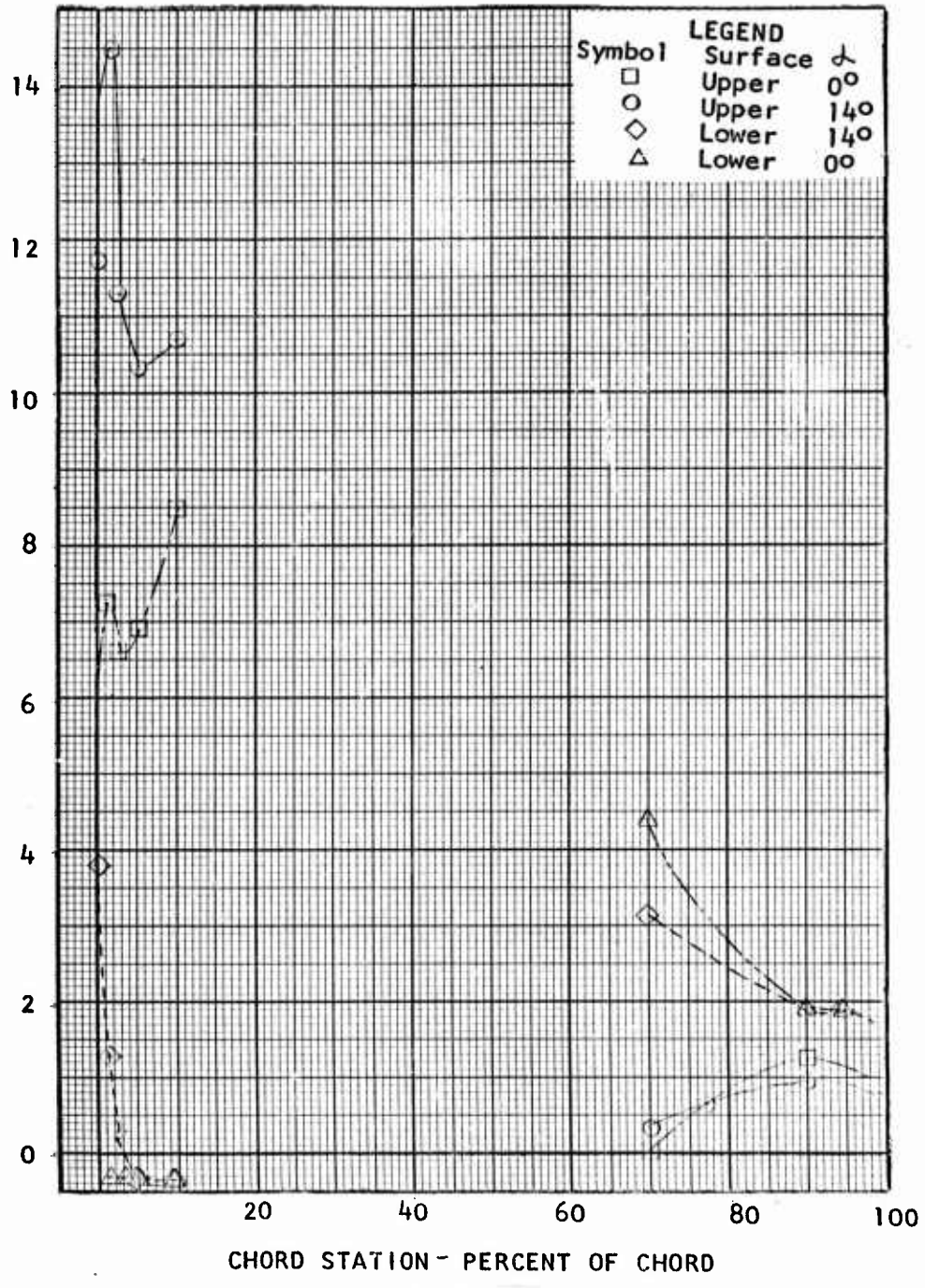


FIGURE 53

VERTODYNE PROGRAM
SHROUD PRESSURE DISTRIBUTION
MEDIUM PITCH FAN 10000 RPM $\phi_{Root} = 39.7^{\circ}$
RUN 10, V = 60

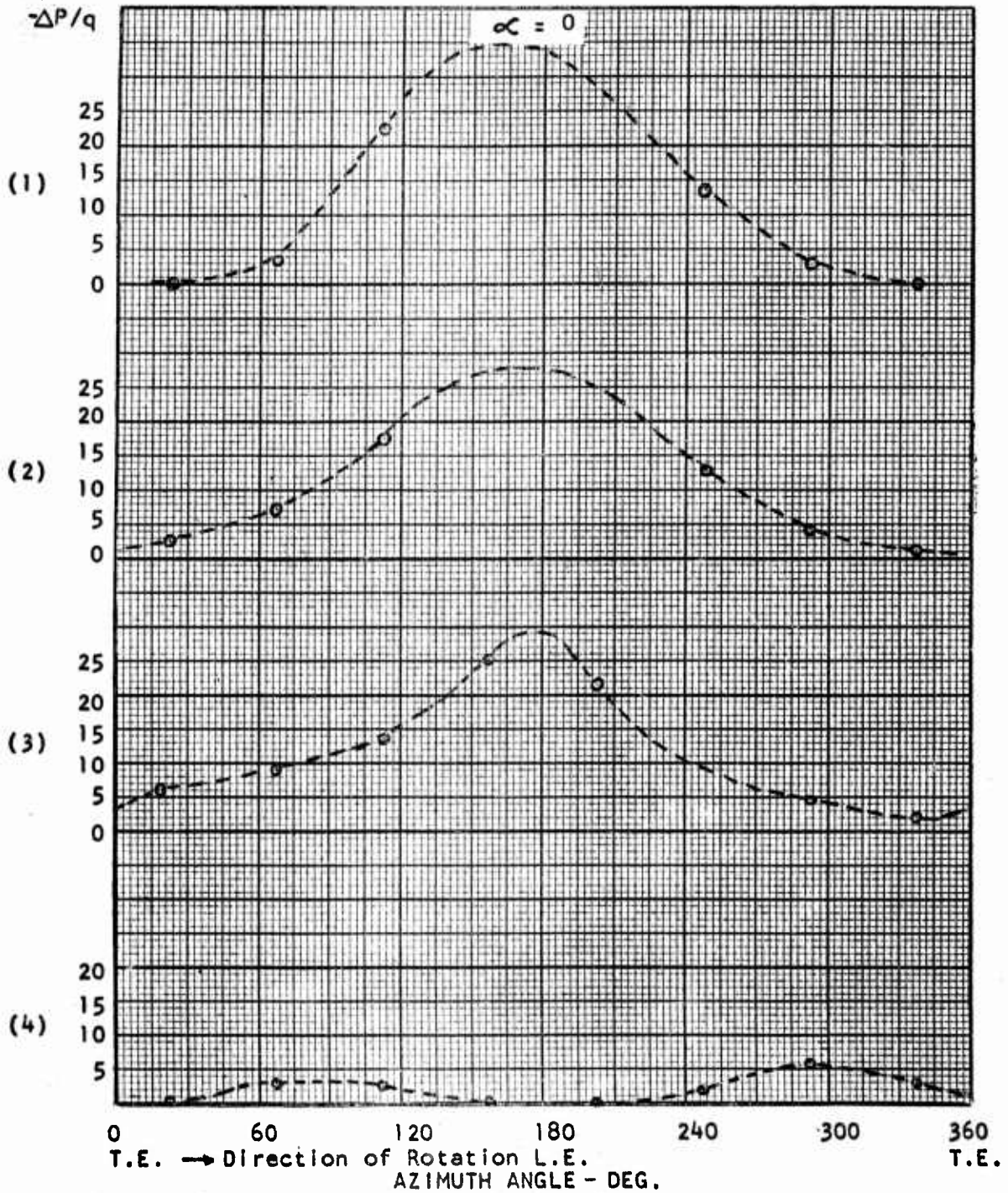


FIGURE 54

VERTODYNE PROGRAM

PRESSURE DISTRIBUTION

FAN CENTER PRESSURE STATION

$V = 100$

$\delta_{F_F} = 40^\circ$

MEDIUM PITCH FAN

10000 RPM $\quad \phi_{Root} = 39.7^\circ$

LEGEND

| Symbol | Surface | $\alpha$ |
|---|---|---|
| □ | Upper | 0° |
| ○ | Upper | 14° |
| ◇ | Lower | 14° |
| △ | Lower | 0° |

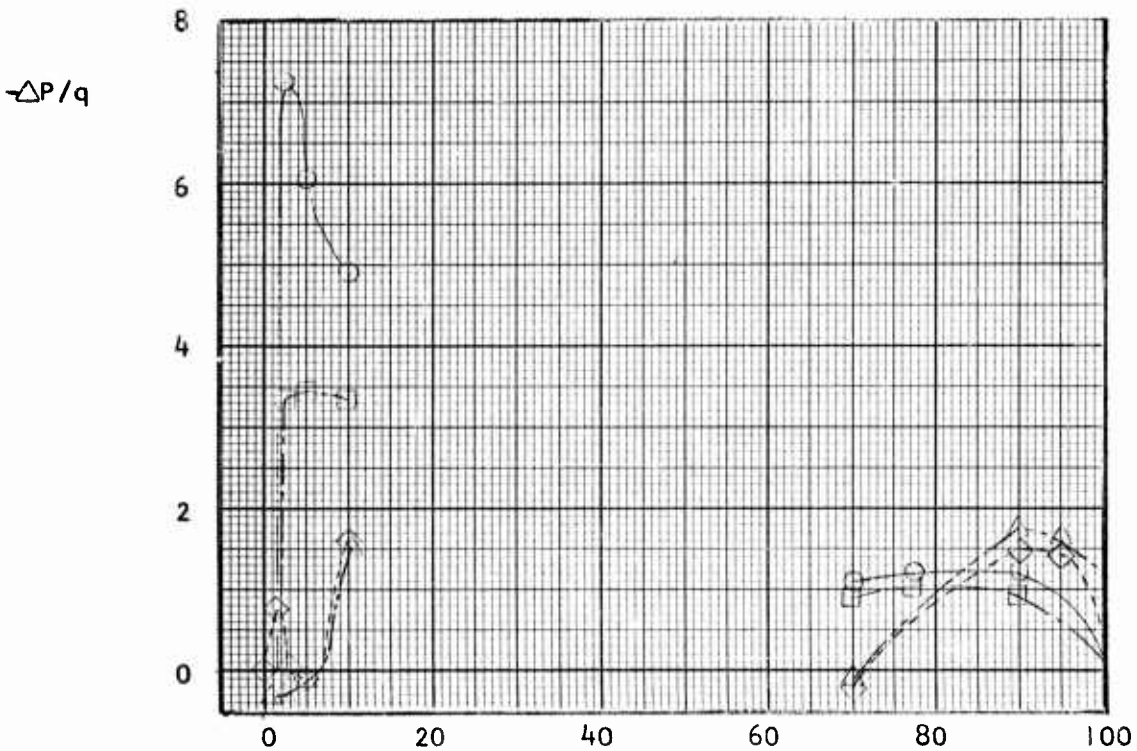


FIGURE 55

# APPENDIX A

# WIND TUNNEL PROGRAM AND LOG OF TEST RUNS

1. Wind Tunnel Program
2. Wind Tunnel Test Log
3. Static Test Log

# APPENDIX A

Test log data is presented in this appendix. Section 1, Vertodyne Tunnel Program, was the proposed test schedule. Section 2, Wind Tunnel Test Log, covers the actual series of tests run in the University of Detroit Wind Tunnel. Reference is made to Section 1 when discussing specific runs. It was necessary to modify the test schedule following the failure of the low pitch fan, and the subsequent appearance of discrepancies in the medium and high pitch fans. Section 3 covers the later series of static tests conducted in the test laboratory of the University of Detroit.

## 1. VERTODYNE TUNNEL PROGRAM

University of Detroit

Run #1 Duct covered
$V_o$ = 60 MPH
whence: $V_o$ = Tunnel velocity
Vary $\alpha$ from $\alpha_{negative\ stall}$ to $\alpha_{positive\ stall}$

Record: Model
Lift
Drag
Pitching Moment
Pressure Distribution

Run #2 Repeat #1 at $V_o$ = 100 MPH ($q = 25.6\ \#/ft^2$)

Run #3 Repeat #1 at $V_o$ = 140 MPH

Run #4 Duct covered, flap deflected 20°
$V_o$ = 100 MPH

Run #5 Fan unpowered
$V_o$ = 100 MPH
Vary $\alpha$ from $\alpha_{negative\ stall}$ to $\alpha_{positive\ stall}$

Record: Model
Lift
Drag
Pitching Moment
Pressure Distribution

Run #6 Fan unpowered, flap deflected 20°
Same as Run #5

Run #7 Fan powered ($\phi_R = 25.0°$), low pitch
$\phi_R$ = Fan blade root angle setting
$V_o$ = 30, 40, 50, 60 @ (8000 RPM)
Vary $\alpha$ from $\alpha_{zero\ lift}$ to $\alpha_{stall}$, $\Delta\alpha = 2°$

Run #7 (Continued)

Record:

| Model | Fan |
|---|---|
| Lift | Thrust |
| Drag | Torque |
| Pitching Moment | Pitching Moment |
| Pressure Distr. | RPM |

Run #8 Fan powered, fan exit flap 20°
Procedure same as Run #7

Run #9 Fan powered, fan exit flap 40°
Procedure same as Run #7

Run #10 Fan powered, ($\phi_R$ = 39.7°), medium pitch
$V_o$ = 30, 50, 75, 100 MPH
Vary $\alpha$ from $\alpha$ zero lift to $\alpha$ stall, $\Delta\alpha$ = 2°

Record: Model: Lift ↓ Fan: Thrust ↓

Run #11 Fan powered, fan exit flap 20°
Procedure same as Run #10

Run #12 Fan powered, fan exit flap 40°
Procedure same as Run #10

Run #13 Fan powered, ($\phi_R$ = 55.9°), high pitch
$V_o$ = 40, 60, 100, 140 MPH
Vary $\alpha$ from $\alpha$ zero lift to $\alpha$ stall, $\Delta\alpha$ = 2°

Record:

| Model | Fan |
|---|---|
| Lift | Thrust |
| Drag | Torque |
| Pitching Moment | Pitching Moment |
| Pressure Distribution | RPM |

Run #14 Fan powered, fan exit flap 20°
Procedure same as Run #13

Run #15 Fan powered, fan exit flap 40°
Procedure same as Rung #13

Run #16 Fan powered, low pitch fan, outer panel removed
$V_o$ = 40, 60, 80 MPH
Vary $\alpha$ from $\alpha_{\text{zero lift}}$ to $\alpha_{\text{stall}}$, $\Delta\alpha = 2^o$

Record: Model ↓ Fan ↓

Run #17 Fan powered, low pitch, outer panel removed
Fan exit flap 20°
Procedure same as run #16

Run #18 Fan powered, low pitch, outer panel removed
Fan exit flap 40°
Procedure same as Run #16

Run #19 Fan powered, medium pitch, outer panel removed
$V_o$ = 40, 60, 80, 100 MPH
Vary $\alpha$ from $\alpha_{\text{zero lift}}$ to $\alpha_{\text{stall}}$, $\Delta\alpha = 2^o$

| Record: Model | Fan |
|---|---|
| Lift | Thrust |
| Drag | Torque |
| Pitching Moment | Pitching Moment |
| Pressure Distribution | RPM |

Run #20 Fan powered, medium pitch, outer panel removed
Fan exit flap 20°
Procedure same as Run #19

Run #21 Fan powered, medium pitch, outer panel removed
Fan exit flap 40°
Procedure same as Run #19

Run #22 Fan powered, high pitch, outer panel removed
$V_o$ = 40, 60, 100, 140 MPH

Run #22 (Continued)

Vary $\alpha$ from $\alpha_{\text{zero lift}}$ to $\alpha_{\text{stall}}$, $\Delta\alpha = 2^{o}$

Record:

| Model | Fan |
|---|---|
| Lift | Thrust |
| Drag | Torque |
| Pitching Moment | Pitching Moment |
| Pressure Distrib. | RPM |

Run #23 Fan powered, high pitch, outer panel removed
Fan exit flap 20°
Procedure same as Run #22

Run #24 Fan powered, high pitch, outer panel removed
Fan exit flap 40°
Procedure same as Run #22.

## 2. WIND TUNNEL TEST LOG

### A. March 4 - March 19, 1958

March 4-10:

Finished installation of the Vertodyne model in the wind tunnel test section. The work involved installing the "ground plane," building and installing a fairing around the model motor enclosure to minimize tare drag reading into the balance system, connecting the 92 pressure pick-ups to the 100 tube manometer bank and calibrating the angle of attack indicator.

March 11:

Made first wind tunnel runs. Runs #1 and #2 were made as defined in the Vertodyne Wind Tunnel Program. Metal duct covers were used in place of cardboard covers in Runs #2, #3, and #4.

March 12:

Runs #3, #4, #5, and #6 were completed. Runs #3 and #4 were with the duct covered; #5 and #6 were with the medium pitch fan installed and unpowered.

March 13:

Model was partially dismantled in order to free the fan shaft. Also, a fairing was made to eliminate the gap between the model and the ground plane.

March 14-17:

Runs #5 and #6 were repeated in order to substantiate the non-linearity of the lift curve at small angles of attack found in the earlier runs. These repeats, Runs #5a and #6a, gave data at two degree increments, and checked very well with the earlier runs.

March 18-19:

The generator supplying power for the Vertodyne model was dismantled and sent to Spaulding Corp. of Detroit to be balanced and checked in preparation for the "powered" phase of the Vertodyne program.

## B. March 25 - April 3

March 25:

Started Run #7, V = 40 mph. Pronounced shaking in the strain gage recorders prevented testing angles of attack above 28°.

Run #7, V = 60 mph was stopped at 26° angle of attack, due to loss of low pitch fan. No damage to model, hub badly damaged - all blades destroyed. One blade among 13 could not be located.

March 26:

Repaired tunnel and had special washers made to prevent a recurrence of fan leaving the model. Checked tunnel and model, using medium pitch fan. Took "zero readings" for Run #10, V = 40 mph, but during the run-up of fan, #2 strain gage recorder went erratic. #2 thrust gage in model was replaced.

March 27:

Calibrated new thrust gage. Proceeded with Run #10, V = 40 mph. Encountered loud "screech" noise at 14° angle of attack. The same noise could be reproduced at all positive angles of attack at very low tunnel speeds. The noise was seemingly aerodynamic rather than mechanical.

March 28:

Proceeded with Run #10, V = 60, 80 and 100 mph, limiting the angles of attack to 16° in order to avoid conditions which apparently cause

the "screech" noise. An additional run was added to the program, testing the Vertodyne model at 80 mph with wing flap deflected 20°.

March 29:

Runs #11 and #12 were started and completed with no difficulties occurring.

March 31:

The high pitch fan was installed and run up to 9500 rpm. The model motor, however, could not be cooled enough to continue; therefore, the fan was shut down and the model was disassembled in order to check water leaks.

April 1:

After re-assembling the model, and running the fan at 9060 rpm, the model motor temperatures were checked and found to be within the motor limits. Thus, the high pitch fan runs were conducted at 9060 rpm rather than the design speed of 10,000 rpm. Run #13, V = 40 mph was started and completed.

April 2:

Run #13, V = 60, 100, 140 and 120 mph were completed. Run #13, V = 100 mph, flap angle at 20 degrees, was completed. Run #15, V = 40, 60, 100 and 120 mph were completed.

While inspecting the fan, some small cracks were found in the fan blades. The medium and high pitch fans were then packed and prepared for a "Zyglo" inspection process.

April 3:

The Zyglo process indicated that cracks had developed in both fans, thus the wind tunnel program was terminated. These indications later proved to be erroneous.

## 3. LOG OF STATIC TEST RUNS

### VERTODYNE STATIC TEST PROGRAM

### University of Detroit

### August 26-28, 1958

| DATE | RUN NO. | FAN $\emptyset_{Root}{}^{o}$ | RPM | h/D |
|---|---|---|---|---|
| Aug. 26 | 1a | 39.7 | 6000 | ∞ |
| | 1a | 39.7 | 7200 | |
| | 1a | 39.7 | 8000 | |
| | 1a | 39.7 | 9000 | |
| | 2a | 39.7 | 10030 | |
| | 3a | 55.9 | 6000 | |
| | 3a | 55.9 | 8000 | |
| | 3a | 55.9 | 9060 | |
| | 3a | 55.9 | 8490 | |
| | 3a | 55.9 | 8280 | |
| | 3a | 55.9 | 8760 | |
| | 3a | 55.9 | 8960 | |
| Aug. 27 | 3b | 55.9 | 9030 | 4.0 |
| | 1b | 39.7 | 6060 | 4.0 |
| | 2b | 39.7 | 10000 | 4.0 |
| | 1c | 39.7 | 6000 | 2.0 |
| | 2c | 39.7 | 10000 | 2.0 |
| | 3c | 55.9 | 9060 | 2.0 |
| | 3c' | 55.9 | 9120 | 2.0 |
| | 3d | 55.9 | 9060 | 1.0 |
| | 1d | 39.7 | 6000 | 1.0 |
| | 2d | 39.7 | 10030 | 1.0 |

| DATE | RUN NO. | FAN $\phi_{Root}$° | RPM | h/D |
|---|---|---|---|---|
| Aug. 27 (cont'd) | | | | |
| | 1e | 39.7 | 6030 | 0.75 |
| | 2e | 39.7 | 10000 | 0.75 |
| | 3e | 55.9 | 9030 | 0.75 |
| | 3f | 55.9 | 9060 | 0.5 |
| | 1f | 39.7 | 6030 | 0.5 |
| | 2f | 39.7 | 10000 | 0.5 |
| | 1a' | 39.7 | 6060 | ∞ |
| | 2a' | 39.7 | 10000 | ↓ |
| | 3a' | 55.9 | 9000 | |
| | 1a" | 39.7 | 6000 | |
| | 2a" | 39.7 | 10000 | |
| | 3a" | 55.9 | 9000 | |
| | 3f' | 55.9 | 9000 | 0.5 |
| | 3g | 55.9 | 9060 | 0.3 |
| | 1g | 39.7 | 6060 | 0.3 |
| | 2g | 39.7 | 9930 | 0.3 |
| Aug. 28 | 2f' | 39.7 | 6000 | 0.5 |
| | 1c' | 39.7 | 6000 | 2.0 |
| | 2c' | 39.7 | 9960 | 2.0 |
| | 3c' | 55.9 | 9090 | 2.0 |
| | 3a''' | 55.9 | 9600 | ∞ |
| | 3a''' | 55.9 | 9450 | ↓ |
| | 3a''' | 55.9 | 9180 | |
| | 3a''' | 55.9 | 9000 | |

# APPENDIX B

# WIND TUNNEL BALANCE SYSTEM

# DATA PLOTS

# APPENDIX B

Forward flight test data plots obtained from the University of Detroit are presented in this appendix. The symbols used differ slightly from those used in the main body of the report. A list of symbols for Appendix B has been included.

## APPENDIX B

## LIST OF FIGURES

(All are plots of lift, drag, and pitching moment coefficients vs. wing angle of attack)

## SYMBOLS USED IN APPENDIX B

1. BASIC WING DATA - FAN NOT ROTATING

Coefficient of Lift, $C'_L = \frac{\text{Lift Force}}{qs}$

Coefficient of Drag, $C'_D = \frac{\text{Drag Force}}{qs}$

Coefficient of Pitching Moment, $C'_{mt} = \frac{\text{Pitching Moment}}{qsc}$,

with the center of moment the fan axis

2. FAN POWERED

Coefficient of Lift, $C'_L = \frac{\text{Lift Force}}{(\rho/2)S(\omega r)^2}$

Coefficient of Drag, $C_D = C'_D + \Delta C_{D_L}$

$= \frac{\text{Net Drag Force}}{\frac{\rho}{2} S(\omega r)^2} + 0.01599 (C'_{Lw})^2 \times \frac{q^2}{\left[\frac{\rho}{2}(\omega r)^2\right]^2}$

Coefficient of Pitching Moment,

$C'_{mt} = \frac{\text{Pitching Moment}}{\frac{\rho}{2} Sc(\omega r)^2}$

3. GENERAL

$q$ Forward speed velocity pressure

$S$ Wing area, square feet

$C$ Wing chord length, feet

$\rho$ Air density, slugs per cubic foot

$\omega$ Fan rotatinal velocity, radius per second

$r$ Fan rotor radius, feet

$\delta_{f_w}$ Wing flap deflection, degrees

$\delta_{f_f}$ Fan exit turning angle, degrees

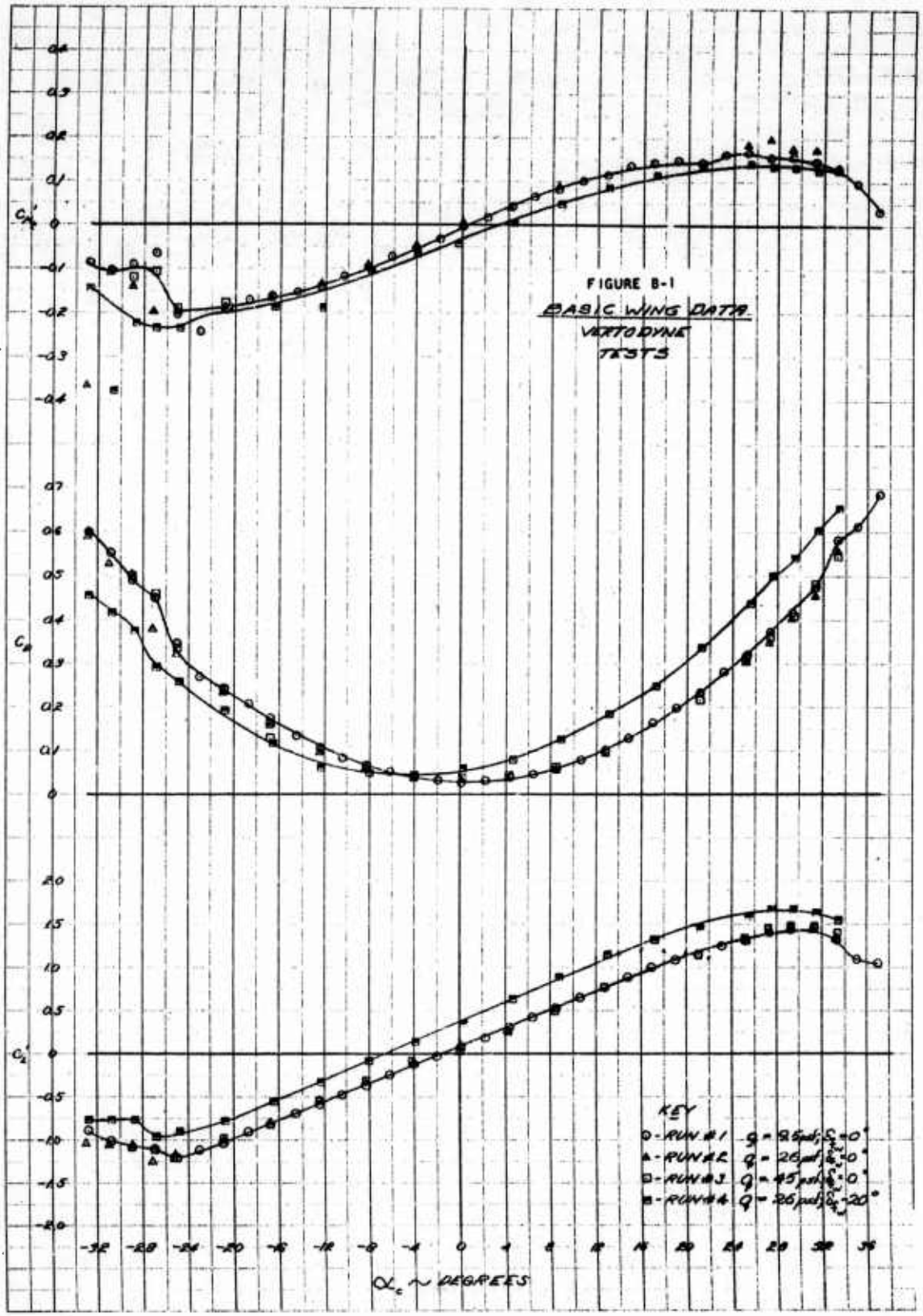
FIGURE B-1
BASIC WING DATA
VERTODYNE
TESTS
KEY
○ - RUN #1 q = 9.5 psf; $\delta_{e_{TE}}$ = 0°
▲ - RUN #2 q = 26 psf; $\delta_{e_{TE}}$ = 0°
□ - RUN #3 q = 45 psf; $\delta_{e_{TE}}$ = 0°
■ - RUN #4 q = 26 psf; $\delta_{e_{TE}}$ = -20°
$\alpha_c$ ~ DEGREES

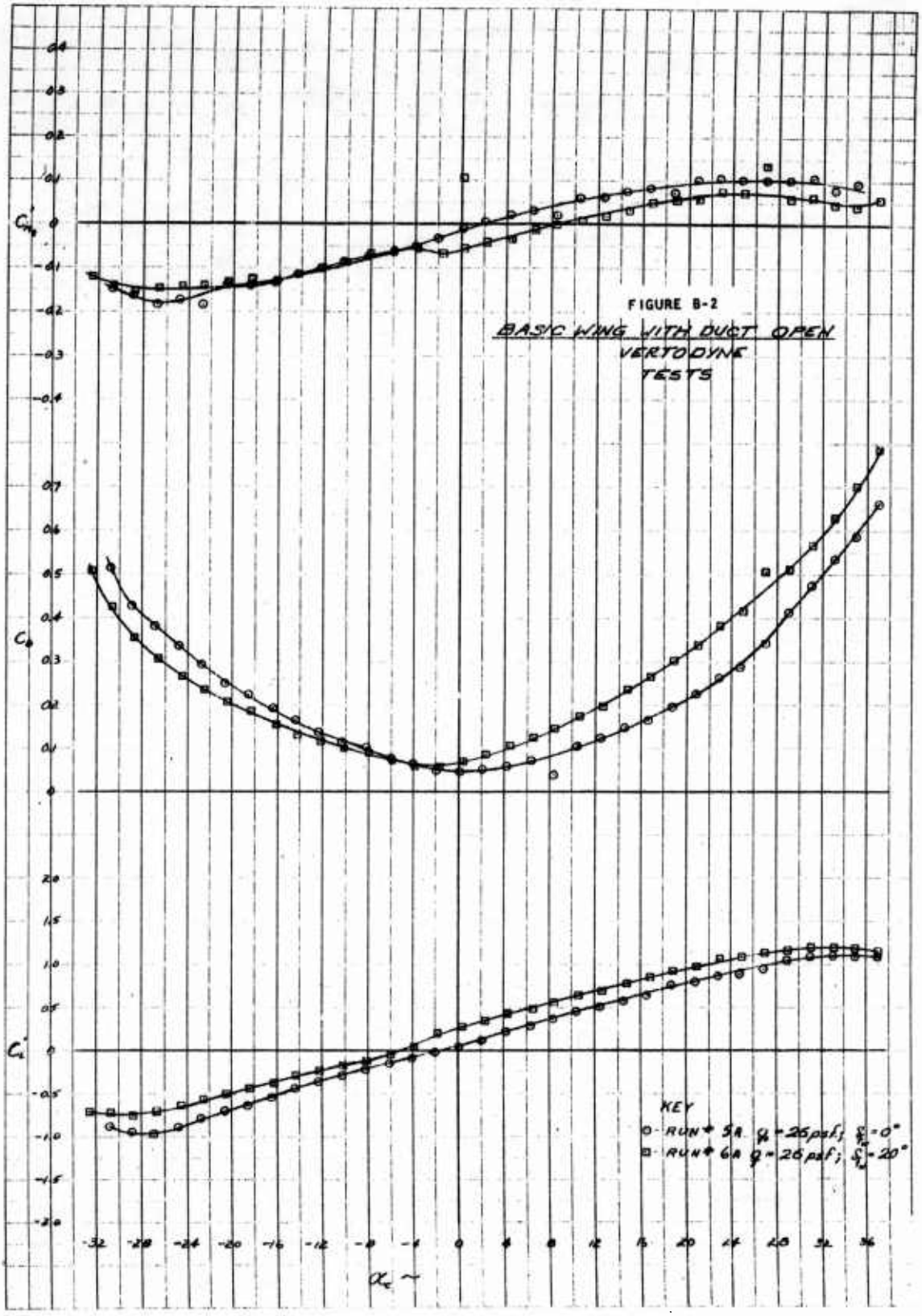
FIGURE B-2
BASIC WING WITH DUCT OPEN
VERTODYNE
TESTS
KEY
○ - RUN # 5A q = 26 psf; ξ = 0°
□ - RUN # 6A q = 26 psf; ξ = 20°

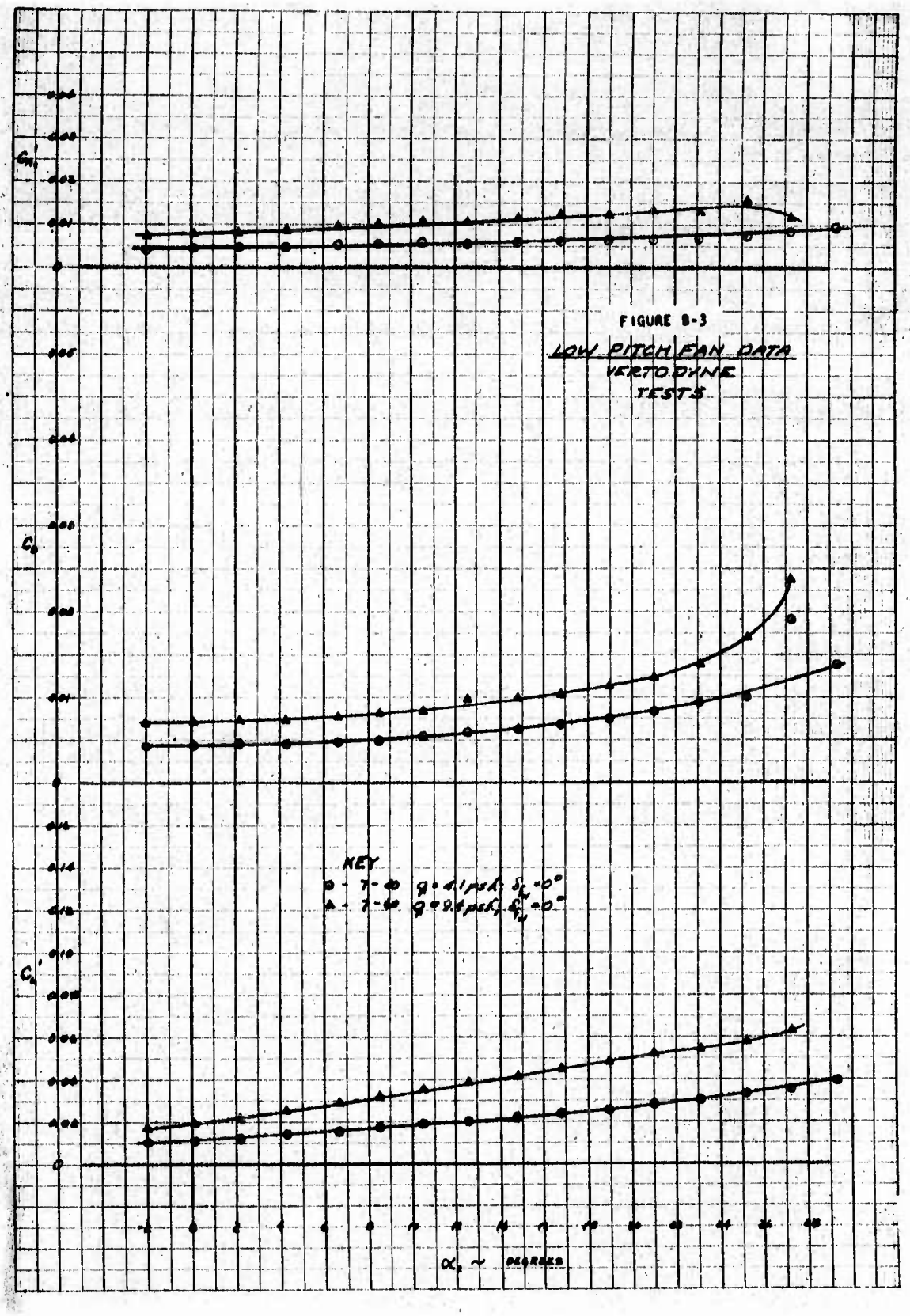


FIGURE B-3

LOW PITCH FAN DATA
VERTODYNE
TESTS

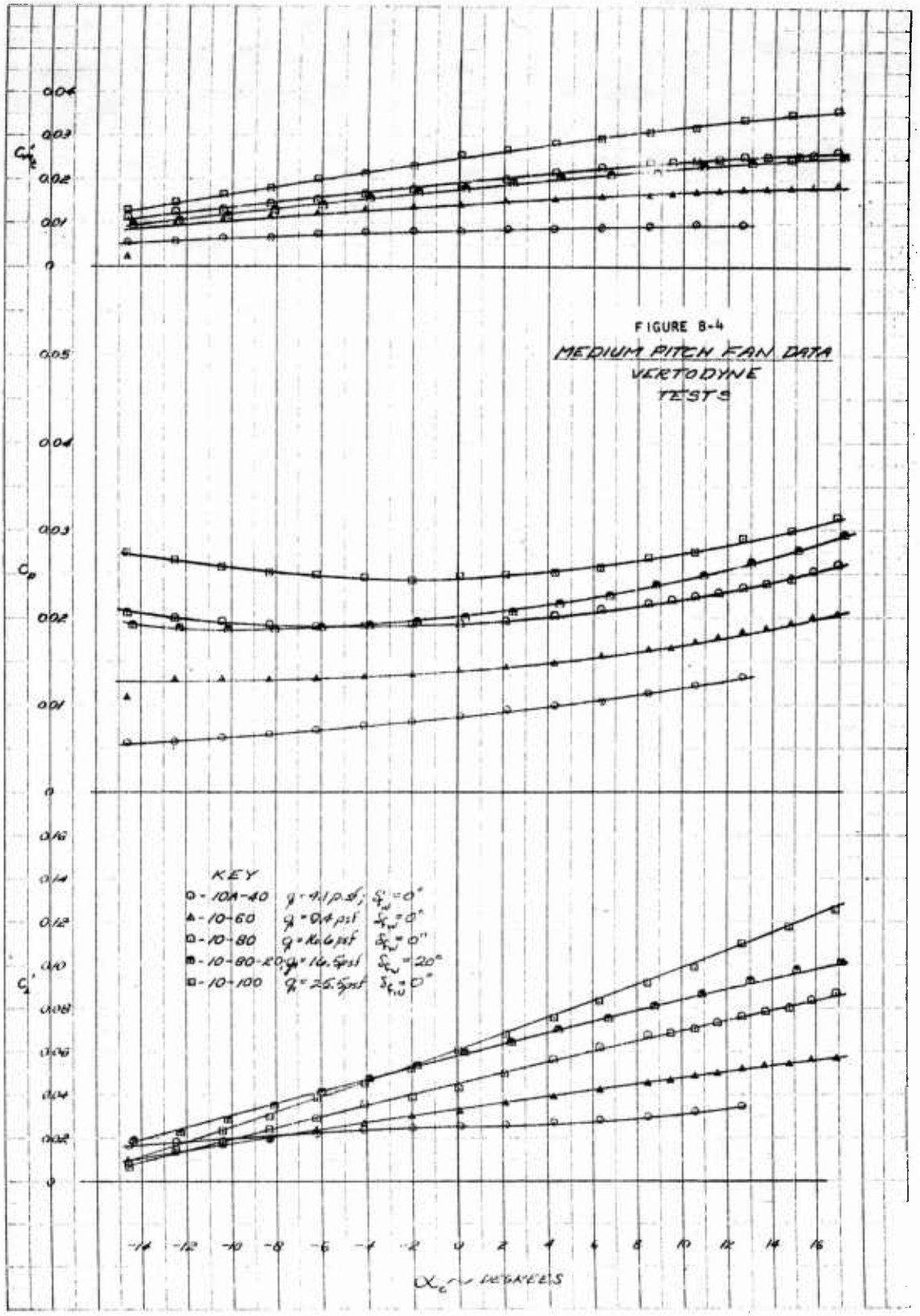


FIGURE 8-4

MEDIUM PITCH FAN DATA
VERTODYNE
TESTS

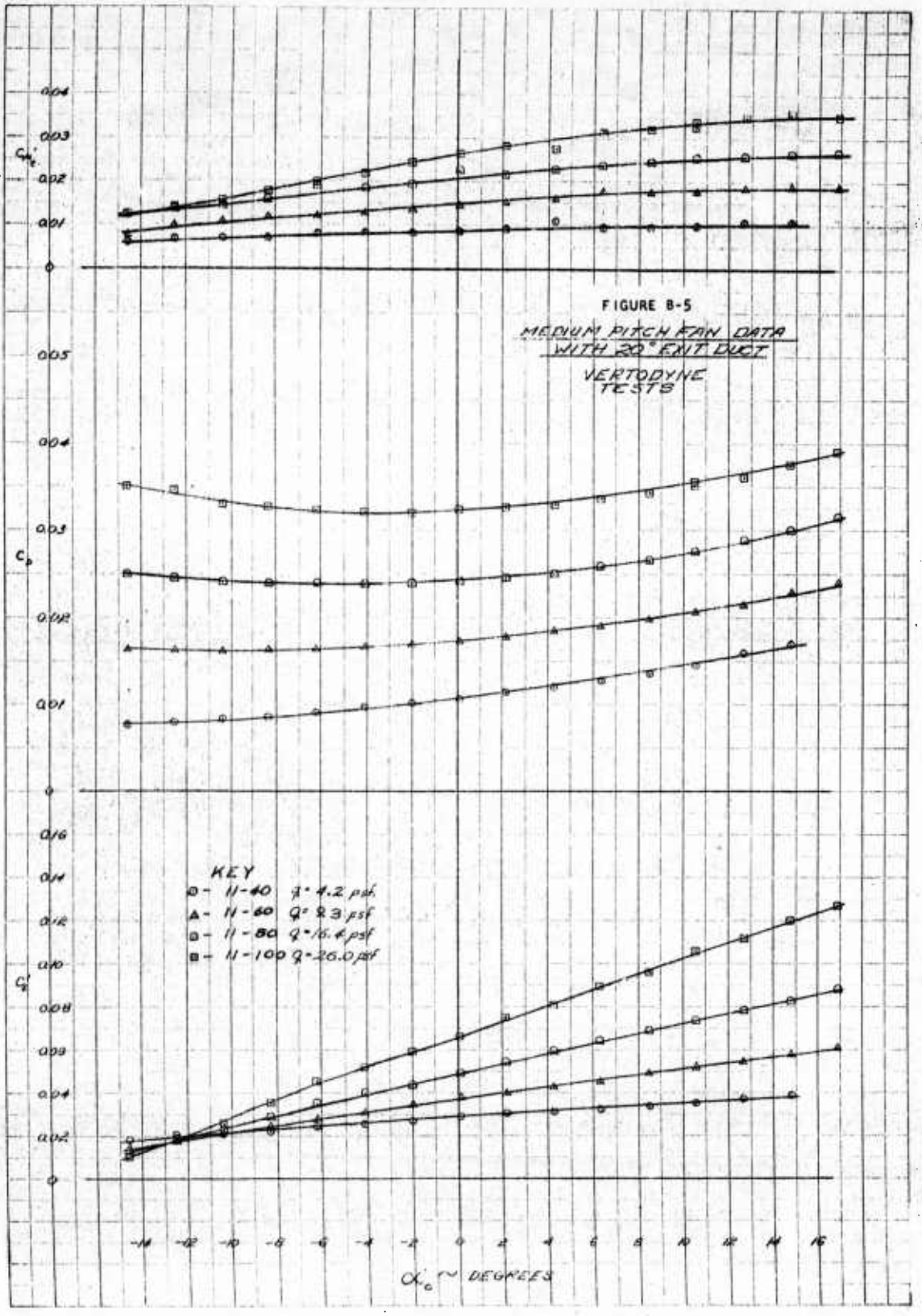


FIGURE B-5

MEDIUM PITCH FAN DATA WITH 20° EXIT DUCT

VERTODYNE TESTS

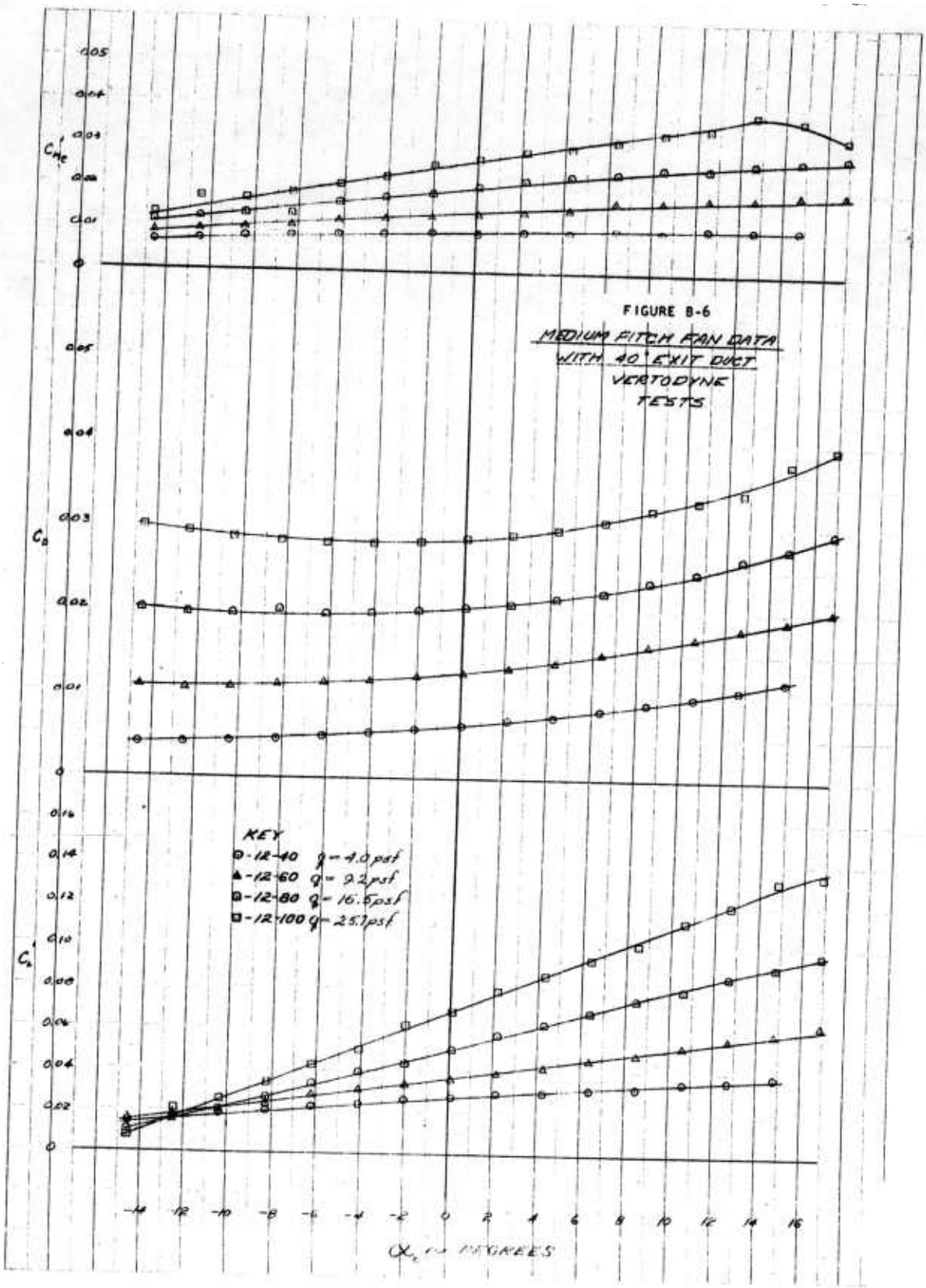


FIGURE B-6

MEDIUM PITCH FAN DATA WITH 40° EXIT DUCT VERTODYNE TESTS

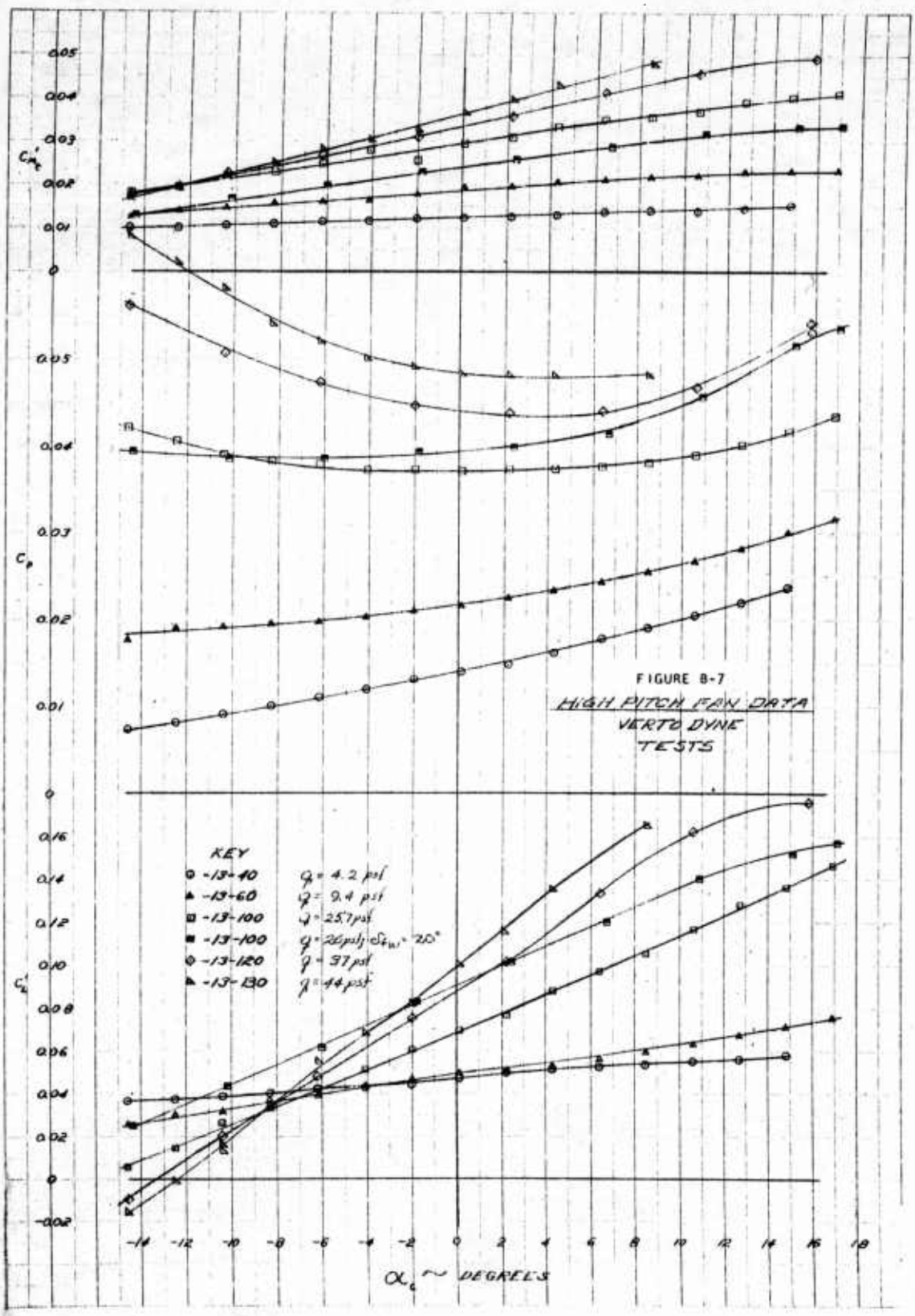


FIGURE B-7
HIGH PITCH FAN DATA
VERTODYNE
TESTS

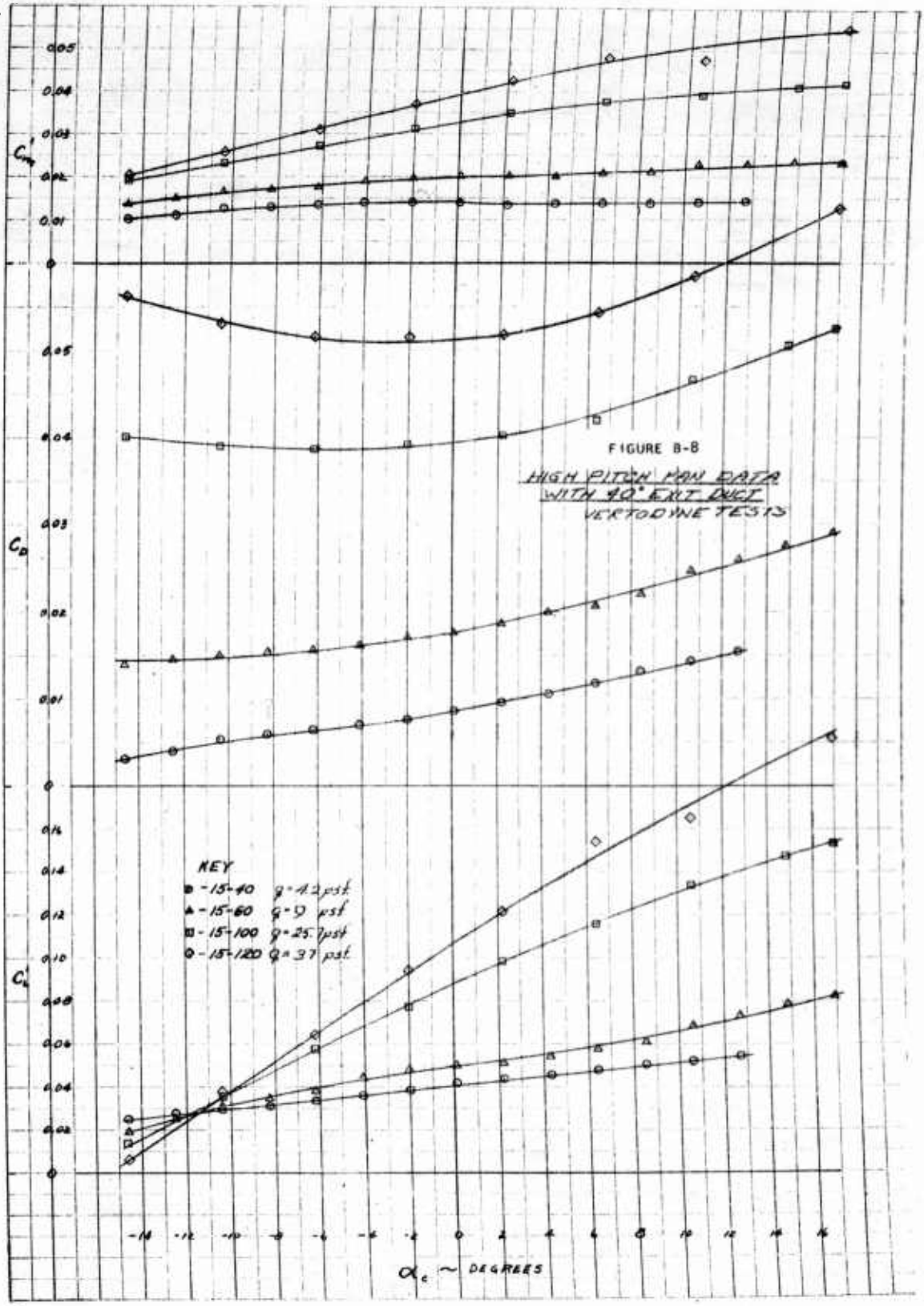


FIGURE B-8

HIGH PITCH MOM DATA
WITH 40° EXT. DUCT
VERTODYNE TESTS

UNCLASSIFIED